

INFORMATION TO USERS

This manuscript has been reproduced from the microfilm master. UMI films the text directly from the original or copy submitted. Thus, some thesis and dissertation copies are in typewriter face, while others may be from any type of computer printer.

The quality of this reproduction is dependent upon the quality of the copy submitted. Broken or indistinct print, colored or poor quality illustrations and photographs, print bleedthrough, substandard margins, and improper alignment can adversely affect reproduction.

In the unlikely event that the author did not send UMI a complete manuscript and there are missing pages, these will be noted. Also, if unauthorized copyright material had to be removed, a note will indicate the deletion.

Oversize materials (e.g., maps, drawings, charts) are reproduced by sectioning the original, beginning at the upper left-hand corner and continuing from left to right in equal sections with small overlaps. Each original is also photographed in one exposure and is included in reduced form at the back of the book.

Photographs included in the original manuscript have been reproduced xerographically in this copy. Higher quality 6" x 9" black and white photographic prints are available for any photographs or illustrations appearing in this copy for an additional charge. Contact UMI directly to order.

UMI

A Bell & Howell Information Company
300 North Zeeb Road, Ann Arbor MI 48106-1346 USA
313/761-4700 800/521-0600

CARDIAC ALLOGRAFT VASCULOPATHY IN HUMAN AND MOUSE

DISSERTATION

Presented in Partial Fulfillment of the Requirements for
the Degree Doctor of Philosophy in the Graduate
School of The Ohio State University

By

Arthur T. Armstrong, Jr., B.S.

* * * * *

The Ohio State University
1996

Dissertation Committee:

Dr. Arthur Strauch, Adviser

Dr. Randall Starling

Dr. Kenneth Jones

Approved by



Adviser

Graduate Program in Anatomy

UMI Number: 9630846

**UMI Microform 9630846
Copyright 1996, by UMI Company. All rights reserved.**

**This microform edition is protected against unauthorized
copying under Title 17, United States Code.**

UMI
300 North Zeeb Road
Ann Arbor, MI 48103

ABSTRACT

Cardiac allograft vasculopathy (CAV) has been characterized in the epicardial coronary arteries of human transplanted hearts and is the major limitation in long-term graft survival. The etiology of CAV is unknown and most likely multi-functional. Previous studies have reported the pathological features and clinical complications associated with CAV. These findings include a concentric intimal lesion seen throughout the length of the epicardial coronary arteries of the transplanted heart. The objectives of this thesis were three fold. First, we developed and validated a technique for quantifying CAV lesions using a computerized image analysis system. Then, we used this method in analyzing arterioles within endomyocardial biopsies from human transplanted hearts. Finally, we analyzed a mouse allograft model to augment our human studies.

An investigation was performed to establish a reproducible method for quantifying the morphological compartments of cross-sectioned arterioles with automated, color-recognition, image analysis software. Arterioles were digitized and measured independently by 3 investigators to determine inter-observer variability. The vascular compartments including the lumen, the internal elastic lamina and the outer wall were measured with image analysis software. Excellent reproducibility was demonstrated when statistically analyzed using analysis of variance. Images of known areas were also

measured and the accuracy of our methodology was validated. This method of morphometric analysis demonstrates the accuracy and precision necessary for quantitative analysis of CAV.

The quantitative method was used to analyze coronary arterioles (<100 μm in diameter) within endomyocardial biopsies from heart transplant recipients for the presence of CAV. The morphological compartments of trichrome stained vessels were quantified using the computer imaging method to measure the percent stenosis of 164 arterioles from 30 transplant recipients over time. The arterioles were divided into 3 groups based on their biopsy date post-transplant: Early (0-6 mo.), Middle (6-18 mo.) and Late (18-36 mo.). The percent stenosis of arterioles from a control group of non-diseased hearts was compared with the grafts. Also, arterioles from heart transplant recipients were immunohistochemically labeled with an antibody specific for proliferating cell nuclear antigen (PCNA). The arterioles were immunocytochemically labeled with an antibody specific for vascular smooth muscle α -actin and the fluorescent signal was analyzed. The results showed that the percent stenosis was not significantly different between the Early, Middle, Late and Control groups. Vessels from the Early, Middle and Late groups did not show binding of the PCNA antibody. The antibody signal intensity and amount of α -actin within each vessel was significantly higher in the Late groups as compared to the Early and Middle groups. We concluded that the coronary microvasculature of human transplanted hearts does not exhibit intimal thickening nor cellular proliferation within 3 years post-transplant. However, as

demonstrated by an increase of smooth muscle α -actin over time, vascular remodeling may occur in response to cytokines released due to injury.

A mouse allograft model was used to address limitations observed in the human biopsy study. The mouse model allowed us to observe coronary arteries throughout the entire heart. Vascular lesions were developed in the mouse through transplanting a donor heart from the DBA/2(H-2^d) strain into the abdomen of the c57Bl/6(H-2^b) strain. A time-dependent study was performed with grafts extracted from 30, 60, and 90 days following transplantation. The coronary branches $>85\mu\text{m}$ in diameter were quantitated and given a ranking corresponding to lesion severity: mild, moderate, and severe. The results showed that advanced lesions occurred at 60 days post-transplant as compared to controls of non-transplanted donor hearts. A regional difference was also observed within the heart grafts as to where lesions occurred. In conjunction with the biopsy study, immunohistochemical analyses were performed on the mouse grafts using PCNA and vascular smooth muscle α -actin antibodies. PCNA was observed only in the interstitium of the early grafts and not in the vasculature. Positive labeling for α -actin was prevalent in a variety of forms dependent on the development of the lesion. The mouse allograft model showed the heterogeneous nature of CAV throughout the entire heart and length of the vessel.

Dedicated to the recipients of heart transplants

ACKNOWLEDGMENTS

I wish to thank my parents and family for their love and support over the years.

I wish to thank my adviser, Art Strauch, for the support, knowledge, and time he has given me.

I also would like to thank Randy Starling who has been a mentor and a role model.

I thank Ken Jones for encouraging me to push back the frontiers of science.

I am grateful to my fellow graduate students for their friendship.

I also wish to thank Charlie Orosz, Elaine Wakely, and Shelly Klenstic for their invaluable work with the mouse heart grafts.

I also wish to thank David Hall and Bob Voight at Resolution Technology for all their help and expertise with the imaging system.

I thank the people in Cardiology who have assisted me on a daily basis including Gretchen Whitby, Ginny Highfill, Carl Leier, Ruth Ann Kennedy, Annie Arrigo, Doug Brown and Maria Saavedra.

A special thank you to Julie Gon for making life bearable.

VITA

November 28, 1967.....Born - Columbus, Ohio
1990.....B.S. Biology, Muskingum College.
1992 - present.....Graduate Research and Teaching Assistant,
The Ohio State University

PUBLICATIONS

1. A.T. Armstrong, A.R. Strauch, A. Kardan and R.C. Starling, "Morphometric and immunocytochemical analysis of coronary arterioles in human transplanted hearts." *J. Heart Lung Transplant*. In Press.

FIELDS OF STUDY

Major Field: Anatomy,
with studies in Pathobiology

TABLE OF CONTENTS

Abstract.....	ii
Dedication.....	v
Acknowledgments.....	vi
Vita.....	vii
List of Tables.....	x
List of Figures.....	xi
Chapters:	
1. Historical overview and background.....	1
1.1 Overview.....	1
1.2 Histological characteristics of CAV.....	3
1.3 Clinical diagnostic tests for CAV.....	6
1.4 Pathogenesis of CAV and associated risk factors.....	9
1.5 Atherosclerosis and vascular injury.....	14
1.6 Modulation of vascular smooth muscle cells.....	19
1.7 Therapies for CAV.....	24
1.8 List of references.....	27
2. Validation of morphometric methodology.....	34
2.1 Introduction.....	34
2.2 Methods and materials.....	36
2.2.1 Tissue and slide preparation.....	36
2.2.2 Imaging.....	37
2.2.3 Morphometric analysis.....	39
2.2.4 Statistical analysis.....	40
2.3 Results.....	41
2.3.1 Validation of accuracy.....	41
2.3.2 Inter-observer variable analysis.....	41
2.3.3 Intra-observer variable analysis.....	42

2.4	Discussion.....	42
2.5	List of references.....	46
3.	Quantitative morphometric and immunocytochemical analysis of coronary arterioles from human transplanted hearts.....	52
3.1	Introduction.....	52
3.2	Methods and materials	54
3.2.1	Endomyocardial biopsies.....	54
3.2.2	Histologic morphometric analysis	55
3.2.3	Epicardial coronary analysis	57
3.2.4	Immunohistochemistry procedure using PCNA antibody.....	57
3.2.5	Immunocytochemistry procedure using smooth muscle α -actin antibody.....	58
3.3	Results.....	60
3.3.1	Histological analysis.....	60
3.3.2	Comparison of biopsies with corresponding angiograms.....	60
3.3.3	Immunohistochemical analysis using PCNA antibody.....	61
3.3.4	Immunocytochemical analysis using α -actin antibody.....	61
3.4	Discussion.....	62
3.4.1	Study limitations.....	65
3.4.2	Conclusion.....	66
3.5	List of references.....	68
4.	Mouse heart allograft model.....	77
4.1	Introduction.....	77
4.2	Methods.....	82
4.2.1	Mouse strains used for the transplant procedures.....	82
4.2.2	Surgical procedures.....	82
4.2.3	Immunosuppression.....	83
4.2.4	Histological procedure.....	84
4.2.5	Morphometric analysis of allografts.....	85
4.2.6	Comparison of perfused vessels.....	86
4.2.7	Immunohistochemistry procedure using PCNA antibody.....	87
4.3	Results.....	88
4.3.1	Coronary vessel perfusion.....	88
4.3.2	Morphometric analysis	89
4.3.3	Regional analysis	91
4.3.4	PCNA analysis.....	92
4.3.5	Smooth muscle α -actin analysis.....	93
4.4	Discussion.....	94
4.5	List of References.....	98
	Bibliograpy.....	121

LIST OF TABLES

<u>Table</u>		<u>Page</u>
1	Comparison of atherosclerotic and CAV lesions.....	15
2	Area measurements collected by investigators.....	48
3	Quantitative morphometric data from coronary arterioles.....	70
4	Immunocytochemical analyses of arterioles labeled with smooth muscle α -actin antibody.....	71
5	Comparison of perfused vessels.....	89
6	Quantitative data from mouse graft coronary arteries.....	90
7	Analysis of variance comparing allografts and controls.....	91

LIST OF FIGURES

Figure		Page
1	Histological section of lesioned coronary artery.....	32
2	Phenotypic modulation of smooth muscle α -actin.....	33
3	Morphological compartments of coronary arteriole.....	49
4	Linear regression between two sets of measure.....	50
5	Graph comparing repeated measures.....	51
6	Histologic section of endomyocardial biopsy.....	72
7	Human tonsil section with positive PCNA labeling.....	74
8	Intramyocardial arteriole with negative PCNA labeling.....	75
9	Arterioles fluorescently labeled with actin antibody.....	76
10	Histological cross section of mouse heart allograft.....	101
11	Examples of no lesion and mild lesion.....	102
12	Examples of moderate and severe lesions.....	103
13	Lesion distribution in 30 day grafts.....	105
14	Lesion distribution in 60 day grafts.....	103
15	Lesion distribution in 90 day grafts.....	106
16	PCNA labeled vessels from control group and 30 day grafts.....	110
17	PCNA labeled vessels from 60 and 90 day grafts.....	111

18	PCNA labeled cells with 30 day graft.....	113
19	PCNA labeled control tissue.....	114
20	α -Actin labeled control hearts.....	114
21	α -Actin labeled 30 day graft arteries.....	115
22	α -Actin staining of vessels in lesioned 30 day grafts.....	116
23	α -Actin staining of vessels in 60 and 90 day grafts.....	117
24	α -Actin staining of controls.....	118
25	α -Actin staining of myocardium.....	119
26	Comparison of lesion development in mouse and human.....	120

CHAPTER 1

HISTORICAL OVERVIEW AND BACKGROUND

Introduction

The first human cardiac transplantation procedure was performed in 1967 by Christiaan Barnard, M.D. at Groote Schuur Hospital in Cape Town, South Africa [1] which was followed closely in 1968 by the first heart transplant in the U.S. at the Stanford University Medical Center. Since that time more than 30,000 heart transplantations have been performed worldwide [1]. In the early years of heart transplantation (HTX), the statistics for one year survival was 22% [2]. The predominate immunosuppressant drugs used to treat HTX recipients were azathioprine and corticosteroids. Since infection and acute rejection were the most common causes of death, a better form of immunosuppression was needed. Cyclosporine became available as an immunosuppressant in 1983 and dramatically reduced the acute rejection seen during the first year following transplantation [3]. The advent of cyclosporine in

conjunction with improved organ procurement procedures and histocompatibility typing has helped HTX to become an acceptable form of therapy for heart failure. One-year survival rates now approach 85% nationally [4].

Currently, the major limitation of long-term cardiac allograft survival is the development of occlusive vascular disease resulting in graft ischemia and myocardial infarction. This form of graft coronary disease varies in its onset which can be anywhere from 3 months to 22 years post-transplantation [5]. Coronary disease was indicated as the cause of death of the first long-term HTX survivor and also of the longest living HTX recipient who died recently after 22 years with the same transplanted heart. There is no official name for this vascular condition despite its well documented clinical and pathobiological characteristics. This disease has been referred to over the past twenty years as transplant coronary artery disease, graft arteriosclerosis, chronic rejection, transplant vascular sclerosis and accelerated graft atherosclerosis. In this thesis, this disease will be referred to as cardiac allograft vasculopathy (CAV). The term “cardiac allograft” is used to distinguish this disease from related conditions reported in every other type of solid organ graft [6]. In the kidney, vascular disease is the leading cause of chronic renal allograft failure. This type of vasculopathy also has been described, to a lesser extent, in liver and lung allografts [6]. The term “vasculopathy” is preferred over arteriosclerosis because, although this disease occurs predominately in the coronary arteries, it has also been observed in the adjacent coronary veins [4].

CAV is a major cause of death in long-term heart transplant recipients who live beyond one year post-transplant. The goal of this chapter is to provide an overview of the morphological lesions and pathogenesis of CAV. Previous studies of CAV will be presented to provide a background into the many potential mechanisms for this disease. The chapters that follow will detail the research performed in our laboratory to study CAV morphometrically in the human coronary microvasculature and the mouse allograft model.

Histological Characteristics of CAV

CAV was first observed in the dog orthotopic HTX model by Kosek et al. in 1968 [7]. Bieber et al. were the first to report CAV in humans in 1970 [8]. CAV most generally is presented as a concentric intimal lesion in the coronary arteries that encroaches from all sides into the lumen. In 1970 Kosek et al. observed in human autopsies that this lesion consisted of intimal fibrosis and accumulation of monocytes [9]. These investigators also noted that CAV occurred in the absence of acute rejection. Acute rejection typically occurs early after transplantation and is characterized by cellular infiltration within the myocardium. In 1984, Cornelius et al. histologically examined coronary arteries from transplanted hearts at autopsy and determined that severe intimal thickening due to myointimal cellular proliferation and fibrosis was present [10]. In 1987, Billingham looked at 106 autopsies and explanted heart grafts and

distinguished two types of lesions [11]. The first type was a focal intimal plaque similar to typical atherosclerotic lesions as will be discussed later in this chapter. This observation has been confirmed by others and it is unclear whether this focal lesion is typical atherosclerosis, possibly residing in the donor heart, or whether it is a variant form of CAV [3,12]. The second, more predominant lesion observed by Billingham was a concentric diffuse lesion that involved both the primary and secondary branches of the epicardial coronary arteries [11].

There are general features of CAV lesions that emerge from histologically-stained sections of coronary arteries (Figure 1). The internal elastic lamina (IEL) often remains intact until late in the disease process when large lesions disrupt this structure [3]. The thickened intima consists of T cells, macrophages and modulated smooth muscle cells as confirmed by Billingham et al. using monoclonal antibodies specific for each cell type [5]. B cells were not found in the thickened intimas. The smooth muscle cells within the tunica media did not usually appear affected and were not hypertrophied [5]. Migrating smooth muscle cells were seen emerging from the tunica media through fenestrations in the mostly intact IEL [5,9]. Modulated smooth muscle cells and macrophages within the intima occasionally contained lipid droplets (foam cells) [5]. Cellular infiltrates resulting from acute rejection usually were not present. Calcification of the lesion was rare and was seen only in very late survivors who were 6 years or more beyond their transplant anniversary date [5].

The type and size of vessels affected by CAV and the position of lesions are still in question. CAV lesions have been confirmed in both large caliber and medium-sized vessels [10]. Lin et al. compared percent stenosis in coronary artery cross-sections from 25 cardiac allografts at autopsy or in explants to determine if disease severity was either distal or proximal [13]. They observed that the lesions were uniform throughout the vessel and thus concluded there was no regional difference. Geographically-uniform lesions would occlude the distal branches first and give a tapering appearance when visualized angiographically. However, their study only included sections of main coronary branches >5mm in diameter, leaving the effects of CAV on smaller vessels unknown.

Studies that specifically focused on small caliber coronary branches and arterioles have yielded varying results. Palmer et al. reported on one orthotopic allogenic HTX in which they saw arteriolar occlusion in an endomyocardial biopsy taken 10 months post-transplantation [14]. Demetris and colleagues described the morphology of arterioles from 12 human HTX at autopsy [15]. They found that small vessels (<50 μm in diameter) did not exhibit intimal thickening and that CAV lesions were only present in large and medium-sized intramural arteries. Large vessels such as the aorta and pulmonary arteries also were found to have intimal thickening, although lesions within these vessels appeared to have little effect on patient well-being compared to the diseased coronary arteries [16].

Clinical Diagnostic Tests for CAV

Angina pectoris usually does not develop in HTX recipients as indicative of coronary occlusion due to CAV because of the afferent autonomic denervation related to the HTX procedure. The only clinical warnings for the HTX patient are a decrease in ventricular performance or acute myocardial infarction which can lead to sudden cardiac death [4]. For these reasons, a reliable technique for diagnosing occluded coronary vessels at an early stage of CAV would be beneficial. The three most widely implemented diagnostic techniques are coronary angiography, intravascular coronary ultrasound, and endomyocardial biopsy analyses.

Gao et al. analyzed angiograms from 81 HTX patients and grouped the lesions into three categories [17]. Type A lesions showed discrete, tubular or multiple stenosis at proximal, middle or distal branches. Type B lesions showed diffuse concentric narrowings at the middle or distal segments. Type C lesions showed abrupt narrowing of the distal branches that differed from the gradual tapering seen in Type B lesions. Gao then compared angiograms from CAV lesioned-transplanted hearts with non-transplanted hearts that exhibited native coronary artery disease. The non-transplanted hearts all exhibited type A lesions which mostly occurred proximally along the vessel axis. Gao concluded that transplanted hearts with CAV have a mixture of all three types of lesions [17].

Angiograms have been regularly taken from HTX recipients in most hospitals over the past decade and until recently have been considered the most useful measurement tool for diagnosing CAV. Johnson et al. compared angiograms from ten HTX patients to assess the accuracy of this technique in diagnosing CAV [18]. Their study concluded that angiography significantly underestimates CAV in its early stages. Vessels that measured normal on angiograms were found to be diseased at autopsy when analyzed histologically. The study stressed the importance of doing angiograms immediately after transplantation to serve as a baseline for determining minimal intimal thickening. The results of this study emphasize that a more sensitive test is needed to diagnose CAV in its early stages.

Intravascular coronary ultrasound (IVCU) appears to be able to overcome the limitations in sensitivity of angiography because IVCU can show the vessel wall morphology *in situ* [12]. IVCU is performed using a catheter-mounted transducer that sends and receives ultrasound signals that enable a visual image of the vessel wall to be created. Angiography can only “see” the lumen filled region and not the vascular wall. St. Goar et al. compared ultrasounds with angiograms from HTX patients and concluded that IVCU was more sensitive in diagnosing CAV than angiography [19]. The IVCU technology has not been widely implemented and its potential utility in CAV diagnosis is still in question. However, Rickenbacher et al. did a prospective study using IVCU and found an increase in intimal thickening over time with the most dramatic change in the first 2 years after transplant [20]. Unfortunately, IVCU is limited in that it can only

analyze vessels ≥ 2 mm in diameter [3]. Other techniques are required to examine the smaller coronary vessels.

Endomyocardial biopsies are regularly taken from HTX recipients to monitor acute rejection. These same biopsies have been studied for their potential in diagnosing CAV. Neisch et al. looked for ischemic damage to cardiomyocytes within biopsies as a possible predictor of CAV [21]. They based ischemic injury on myocyte vacuolization, coagulative necrosis, and myocardial scar tissue. No significant correlation between myocyte ischemic injury and CAV was found. However, in a more recent study by Gaudin et al., ischemic injury to myocytes within early biopsies was significantly correlated to the incidence of CAV in angiograms [22]. They believe that early myocyte injury occurs as a result of the ischemic period associated with organ procurement and surgical procedures and not, as Neisch speculates, from late stage CAV lesions. Instead Gaudin believes that the ischemic period prior to transplantation may initiate or accelerate CAV. This hypothesis will be addressed later in the chapter. However, the value of using ischemic injury within biopsies to diagnose CAV is still undetermined.

Additional biopsy-based studies included analyzing the appearance of intramyocardial arterioles found in these specimens. Palmer et al. observed arteriolar intimal thickening within biopsies obtained from a single heart and speculated that changing morphology of these arterioles could be an early predictor of CAV [14]. This was the basis for our analysis of arterioles within endomyocardial biopsies from HTX recipients at various times after transplant as presented in Chapter 3.

Finally, several noninvasive tests for CAV diagnostics were evaluated by Smart et al. [12]. They examined 2D echocardiography, bicycle exercise gated-wall motion, 48-hour Holter recording, and thallium 201 single photon emission computerized tomography (SPECT) imaging [12]. Although they concluded that the Holter recording had the only significant relation with CAV prediction, Holter monitoring is not commonly used to screen for CAV.

Pathogenesis of CAV and Associated Risk Factors

The etiology of CAV is unknown. Due to the diffuse nature of the disease, many investigators believe CAV is caused by immune injury to the endothelium. However, not all of the vessels are equally affected, and some are completely spared, which leads many to believe CAV does not arise solely from immune injury. Indeed, CAV was originally referred to as chronic rejection, but this term is rather vague and does not address possible non-immunogenic conditions that could contribute to CAV.

The fact that the only vessels affected in the recipient's body are those in the transplanted organ initially leads one to suspect immune injury [23]. Obviously, the other vessels throughout the recipient also experience immunosuppression, ischemic periods, and viral infection which are some of the suggested non-immune injuries. Most likely the immune injury would involve histocompatibility antigens which are not normally expressed by the endothelial cells. The coronary artery endothelial cells can

express Class I and II histocompatibility antigens and human leukocyte antigens (HLA) under pathological conditions relevant to transplantation [23-25]. These antigens can elicit a cellular immune response involving an accumulation of activated T cells that release cytokines which in turn recruit macrophages to the graft coronary arteries. Antibodies to endothelial antigens have been found in the serum of both renal and cardiac transplant recipients [12]. In addition, HTX recipients with CAV have a higher plasma level of soluble interleukin-2 receptors which are one of many cytokine markers of an immune response and possibly could be used to predict CAV [12,25].

Hammond et al studied 268 patient biopsies to classify rejection patterns as cellular, vascular or mixed [26]. They defined vascular rejection as endothelial cell swelling and intimal deposition of immunoglobulin and complement as assayed by immunofluorescence. These investigators found that the vascular pattern of rejection correlated with decreased survival due to CAV [26]. Also, Pollock et al. observed that CAV is more likely to develop when there is an HLA mismatch between donor and recipient [25]. In addition, Uretsky et al. reported that patients with two or more rejection episodes requiring therapy within the first 2 post-transplant years are at a greater risk for CAV [25]. However, these results are controversial.

In support of non-immune injury hypotheses, several studies suggest that there is no direct relationship between histocompatibility and CAV. CAV has been shown to occur in animal transplant models that are either HLA compatible or incompatible [27]. The target leading to an immune response in these animals may not be HLA endothelial

antigens. Rather, it is possible that cell surface adhesion molecules, such as intercellular cell adhesion molecule-1 (ICAM-1) and vascular cell adhesion molecule (VCAM-1), are expressed and then bind lymphocytes to the endothelium [27]. Studies of HTX biopsies have shown that both VCAM-1 and ICAM-1 are expressed during rejection and most likely upregulated by cytokines that accumulate during the rejection process [28].

Another possible source of non-immune injury is hyperlipidemia within the recipient. There is a high correlation with CAV and hyperlipidemia as suggested by several studies. Gao et al. looked for correlations between risk factors and CAV and considered such variables as recipient age, HLA type mismatches, incidence of post-transplant rejection, lipid levels and plasma triglycerides. They found significant correlation only with plasma triglycerides. Winters et al. compared coronary artery percent stenosis at autopsy of fifteen HTX recipients with their cholesterol levels and body mass indices [29]. They found increased cholesterol levels and obesity to correlate with incidence of CAV. Grady et al. observed cholesterol and triglyceride levels of fifty-four HTX recipients both before and after transplant [30]. Their results showed a significant increase in cholesterol levels at one year post-transplant, but these levels declined after three years post-transplant. Triglyceride levels also increased but remained high at three years post-transplant. The cause of hyperlipidemia in HTX patients is unknown but may result from the immunosuppression therapy following transplantation. Both cyclosporine and prednisone have been suggested to cause hyperlipidemia in both heart and renal transplant patients [31]. However, Billingham et

al. compared the immunosuppressant therapies azathioprine and cyclosporine and concluded that there was no difference in relation to CAV incidence [11]. What makes evaluation of the hyperlipidemia connection more frustrating is that dietary changes have little affect on lowering cholesterol or triglyceride levels in HTX patients [31]. Moreover, lipid lowering drugs may interact with the immunosuppressive drugs and cause other clinical problems [31].

The ischemic period, low temperature conditions required for organ procurement and preservation, and reperfusion injury may be additional sources of non-immune allograft injury. Rowen et al. looked at myocyte hypertrophy and fibrosis in biopsies from ninety-five HTX recipients up to three years post-transplant and compared them according to whether they received locally or distally procured donor hearts [32]. They concluded that donor hearts procured distal from the geographical site of transplant had no effect on cardiomyocyte hypertrophy and fibrosis that typically develops after HTX [32]. As previously mentioned, the biopsy studies reported by Neisch et al [21] and Gaudin et al [22] were conflicting in regard to whether there was a correlation between ischemic injury and CAV. Perhaps ischemic injury predisposes the vasculature to other CAV mechanisms.

Cytomegalovirus (CMV) infection has been suggested as a possible risk factor for CAV. CMV is a herpes virus that has a latency within an unknown host cell although lymphocytes are strongly suspected as hosts [33]. CMV also is thought to be transferred from donor hearts raising the possibility that cardiomyocytes may be a host [33].

Marek's disease is an avian herpes virus which is known to induce atherosclerosis in chickens [33]. This study in conjunction with the work of Melnick et al., who reported CMV antigens in human arterioles [33], is consistent with the idea that CMV may play a role in CAV. CMV infection of endothelial cells results in cell destruction within 24 hours after infection which can elicit an immune response. Moreover, CMV infection can augment the immune response by stimulating the secretion of cytokines such as interleukin-1 (IL-1) and tumor necrosis factor- α (TNF- α) in infected cells and by mimicking the HLA-DR and MHC Class I antigen genes.

One other non-immune risk factor related to CAV may be the donor heart itself. Tuzcu et al. assessed coronary arteries using angiography and ultrasound for lesions early after transplant [34]. They concluded that native coronary artery disease is frequently transmitted from the donor to the recipient.

The original question posed in this Introduction was whether CAV is chronic rejection. Is CAV a continuation of acute rejection, not related to rejection, or in part associated with rejection? Izutani et al. used a return transplantation technique in rats to address this question [35]. They returned grafted hearts to their original donor strain at different time intervals post-transplant. CAV could be prevented if the graft was returned back to the donor strain within 5 days after transplantation. However, after 5 days the heart developed CAV despite placement back into the donor strain. So other mechanisms must be involved after the initial immune injury occurs that accelerates CAV to such an extent that there is no recovery. These other mechanisms may be similar

to those seen in other forms of vascular injury and no doubt depend on cellular and molecular conditions that normally prevail in any potential host. Most studies show no relationship between CAV and typical atherosclerotic risk factors such as smoking, diabetes, age and sex [33]. However, there may be a link between CAV and hyperlipidemia and obesity.

To summarize, our knowledge of the basic mechanisms of CAV are not well understood. End stage disease markers are all we have to study, so identification of the most significant and damaging risk factors may not be precise. Ideally, studies of the early stages of CAV would permit better assessment of the risks involved. In theory, each risk may trigger a different response that is mediated by unique combinations of cellular signaling molecules which in turn reveal themselves through expression of CAV-specific markers or pathobiologic conditions.

Atherosclerosis and Induced Vascular Injury: Comparative Aspects

Atherosclerosis is an occlusive vascular disease often resulting in myocardial infarction and is the leading cause of death in the United States. The clinical effects are evident primarily in medium-sized arteries throughout the body including coronary, carotid, basilar, vertebral, superficial femoral, and iliac arteries [36]. Atherosclerosis has no strict relation to high or low hemodynamic shear stress, but is more likely due to unusual forces such as eddy currents and backflow [36]. The disease is characterized by

asymmetric, lipid-filled, fibrocellular lesions caused by vascular injury. Atherosclerosis has many similarities to CAV and for that reason many of the experimental approaches used to study atherosclerosis also have been applied to assess the pathobiology of CAV as well. However, there are definite histological differences between atherosclerotic lesions and CAV lesions as compared in Table 1. The term “atherosclerosis” implies a significant lipid involvement compared to the more general term “arteriosclerosis” which indicates a more cellular form or proliferative disease such as that seen in CAV.

Atherosclerotic Lesion	CAV Lesion
asymmetric, eccentric	symmetric, concentric
focal	diffuse
IEL disruption	IEL intact
calcification	calcification rare
abundant foam cells	foam cells can occur

Table 1: Comparison of Atherosclerotic and CAV Lesions

Atherosclerosis is thought to occur in response to a vascular injury. The “response to injury” hypothesis was first suggested by Virchow in 1856 [37]. The current version of the hypothesis has been extensively modified and refined largely through the work of Russell Ross and colleagues at the University of Washington who present it as a cascade of cellular and molecular events [36,37]. The hypothesis proposes that there is an initial injury to the endothelial cell lining of the arterial wall. This injury may be due to mechanical forces or various risk factors including hypercholesterolemia,

smoking, diabetes, or infectious agents. In response to endothelial injury, monocytes and T lymphocytes adhere to the injured endothelium via primarily cell surface selectin- and integrin-type receptors and migrate across into the intima. The migrated monocytes differentiate into macrophages that are capable of accumulating lipid material and becoming foam cells. Various growth factors and cytokines are released by the activated leukocytes resulting in smooth muscle cell (SMC) proliferation and migration from the media. These intimal smooth muscle cells exhibit a “modulated phenotype” and produce interstitial extracellular matrix components along with proteolytic enzymes and various cytokines, and growth factors. A fibroproliferative lesion develops in the intima which ultimately is composed of dense connective tissue with embedded SMCs, macrophages, T cells, lipids, necrotic cells and calcification products.

Vascular injury can involve both endothelium denudation and non-denudation types of events. Denudation of the endothelium produces severe structural damage and can be caused by either mechanical or immune injury [37]. Balloon catheters have been used in experimental animal studies to instigate complete endothelial denudation and IEL and medial injury [37]. This extensive trauma to the vessel lining causes immediate platelet aggregation and thrombus formation and the response to injury model quickly develops. Clowes et al. suggest that there is a correlation between the degree of endothelial denudation/medial injury and the extent of myointimal thickening [38]. Nylon catheters can induce less injury such that just the endothelium is ruptured while sparing the IEL and media [38]. There is a moderate degree of platelet aggregation and

leukocyte adherence but regeneration of the endothelium does occur. More importantly, there is no smooth muscle cell proliferation in this particular injury model. Apparently, the regenerated endothelium suppresses the SMC proliferation response through unknown mediators although there is speculation in the literature that anti-proliferative heparin sulfate macromolecules may be involved [39,40].

Milder forms of vascular injury that do not denude the endothelium include hypercholesterolemia and viral infection. Faggiotto et al. induced hypercholesterolemia in monkeys and observed lesions in the aorta and iliac arteries despite the fact that the endothelial cells were morphologically normal [37]. However, 12 days following the administration of a high cholesterol diet, they saw accumulations of leukocytes, lipids and modulated SMCs. Also, the adhesion of monocytes to endothelial cells has been shown *in vitro* to increase in the presence of low density lipoproteins (LDL) [37].

Viruses such as cytomegalovirus (CMV) have also been shown to induce endothelial cell injury without denudation. Such non-denudation models of vascular wall injury may be very useful in elucidating the causes of CAV which likewise involves the sparing of the intima.

Native atherosclerosis takes many years to develop. In contrast there are forms of accelerated arteriosclerosis, which include cardiac allograft vasculopathy (CAV), that can develop relatively rapidly over a 3-5 year period. Forms of accelerated arteriosclerosis include coronary vein graft bypass surgery and coronary artery balloon angioplasty. Both procedures involve mechanical injury and partial to complete endothelial

denudation with occasional medial injury as well. Restenosis can occur after balloon angioplasty which complicates 30-50% of the cases [41]. It is puzzling why 50-70% of the cases do not restenose after undergoing the same mechanical injury. Perhaps the lesion in non-affected individuals is merely compressed and not eroded which could involve the particular physical characteristics of the specific lesion. A hypothesis by Glagov states that the vascular wall remodels through intimal thickening to adapt in such a way as to maintain stability with respect to flow and tensile stress [41]. Once the baseline stress level is achieved, restenotic hyperplasia stops [41]. In general, the development of lesions characteristic of the above clinical conditions is rapid and severe, but vary amongst each other even though they all probably arise as a consequence of vascular wall injury.

The growth factors and cytokines involved in vascular response to injury participate in and promote a complex network of cellular interactions and responses. Platelet derived growth factor (PDGF), basic fibroblast growth factor (bFGF), and insulin-like growth factor-1 (IGF-1) have all been shown to induce proliferation of SMCs and act as a chemoattractant for them as well [36,42]. These growth factors are produced by endothelial cells (EC), macrophages, platelets and even by SMCs themselves resulting in the establishment of autocrine regulatory loops. Colony stimulatory factors (CSF) are produced by T-cells, SMCs and ECs and promote macrophage stability and replication [36]. Transforming growth factor- β 1 (TGF- β 1) is produced by macrophages, ECs, platelets and T-cells. TGF- β 1 strongly stimulates synthesis of extracellular matrix

molecules by SMCs [36]. TGF- β 1 has also been shown to both inhibit and stimulate SMC proliferation, most likely through modulation of PDGF receptor levels in these cells [4,36, 42,]. TGF- β 1 also transiently induces expression of vascular smooth muscle α -actin in certain cell types, the significance of which will be discussed later [43]. IL-1 and TNF- α have also been shown to induce autoproliiferation of SMCs via PDGF production [4,36,42,]. In addition, IL-1 and TNF- α induce ECs to express cell surface adhesion molecules which bind and recruit monocytes and lymphocytes [28]. Monocyte chemotactic protein-1 (MCP-1) is generated by macrophages and SMCs [36]. MCP-1, as its name implies, is a chemoattractant for monocytes. These are just the cytokines thought to be most influentially involved with vascular injury, but none of them individually are solely responsible.

Modulation of Vascular Smooth Muscle Cells

The modulation of vascular smooth muscle cells is a central feature of the pathogenic events leading to arteriosclerosis and CAV. SMC modulation is considered by many to represent a regression to a fetal developmental state [42,43]. In normal development, vessels begin as endothelial channels which become surrounded by day eight in the mouse by mesenchymal cells. Subsequently, the ECs signal the

mesenchymal cells through unknown pathways, probably involving changing patterns of blood flow, to differentiate into SMCs. These same pathways, in reverse, may be involved in the modulation of smooth muscle cells during vascular injury.

SMCs exhibit two distinct phenotypic states: synthetic and contractile [37,42,44,45]. The synthetic phenotype prevails in the embryo, neonatal smooth muscle tissues, and atherosclerotic lesions. Synthetic-state SMCs contain a euchromatic nucleus and have a prominent endoplasmic reticulum and Golgi complex. Major functions of synthetic SMCs are proliferation and the synthesis and secretion of extracellular matrix components. In contrast, contractile phenotype SMCs reside in mature blood vessels in fully developed vertebrates. They contain a heterochromatic nucleus and abundant cytoplasmic actin and myosin filaments. A well developed contractile apparatus allows these cells to function by contracting in response to chemical and mechanical stimuli. The contractile responsiveness of SMCs within the media of a normal vessel is important for normal cardiovascular function. In response to vascular injury, the medial SMCs modulate from the contractile to the synthetic phenotype. Actin isoforms within SMCs can be used as markers to distinguish the cellular phenotypic state of the SMCs. The contractile phenotype is characterized by an abundance of the α isoform of actin whereas the modulated synthetic form replaces α -actin with β and γ isoforms of actin [42].

Studies on cultured smooth muscle cells have provided much information as to the dynamic phenotypic dynamic properties of SMCs. When contractile SMCs are seeded below a critical cell density they often will undergo a change in phenotype within

one week [44]. Cultured SMCs lose contractile capabilities, proliferate, and synthesize 4 to 5 times the normal amounts of extracellular matrix components including interstitial collagens and fibronectin. Occasionally, the mature contractile phenotype can be preserved if cells are maintained at high density on certain extracellular matrix materials [43]. With multiple passages or if sparsely seeded for too long a period, SMCs cannot revert back to the contractile phenotype. “Modulation” is proposed as a more appropriate term compared to “de-differentiation” because the former implies that SMCs remain differentiated while expressing a different phenotype [42,45]. The idea that SMCs exhibit developmental plasticity unlike striated muscle cells is becoming more appreciated in the literature. It has been proposed that some SMCs remain partially or completely undifferentiated in the intima during development and that these cells are the first to proliferate in later developing lesions [44]. These undifferentiated cells are referred to as intimal cushions and have been proposed by some to seed the initial points of atherosclerotic lesions [44].

Radioactively-labeled thymidine incorporation has been used to measure DNA synthesis in animal models in conjunction with balloon catheter injury experiments to provide an indication of SMC proliferation in lesions [37,45]. Initially, balloon injury results in complete endothelial denudation along with a varying amount of medial injury. Immediate platelet aggregation and thrombus formation follows that could persist up to 24 hours after injury. Leukocyte adherence to the damaged area also has been noted within a few hours after injury. During the first 48 hours following injury there was a

recovery period with very little proliferation evident, even though PDGF was being released by the aggregated platelets. The inner layer of medial smooth muscle cells began to proliferate at 2- 4 days after injury. However, the greatest increase in proliferation activity in the media occurred during the period when SMCs began migration into the intima. Within the intima, SMC proliferation started later and lasted longer with maximal labeling around 4 days post injury. Recovery of the medial cells occurred 2-3 weeks after injury whereas, the recovery of intimal SMCs required 12 weeks. Age also was found to be a predisposing factor in SMC proliferation rate. Clowes and Schwartz determined that only half of the SMCs that migrated from the media to the intima divided within 2 weeks post-injury and that these cells form 90% of the cells within the lesion [46,47]. It is interesting to speculate that the 50% portion of SMCs that did not proliferate were instead remodeled such that their normal contractile function was significantly compromised. Indeed, recent studies of restenosis in human coronary arteries suggest that the proliferation rate of affected SMCs is actually rather low compared to animal injury models [47].

Aside from being a phenotypic marker of SMC modulation, previous studies have shown vascular smooth muscle α -actin to be important in proliferation, cell shape, and differentiation. VSM α -actin mRNA and protein synthesis are suppressed during phenotypic modulation and in actively proliferating SMC cultures [45]. Using an animal-balloon injury model, Clowes et al. observed that α -actin mRNA declined and that cytoplasmic β and γ actin mRNAs increased within 8 hours after injury [48].

Clowes et al. also inhibited SMC proliferation *in vitro* using heparin and observed that the actin isoform switched from α to β and γ still occurred. However, the heparin-treated cells eventually reinduced α -actin mRNA. Their study suggests that expression of actin isoforms is somewhat independent of proliferation [48].

VSM α -actin seems important in maintaining the cytoskeleton and stabilizing cell shape [49]. Expression of α -actin is influenced by the density and growth state of the cultured SMCs [37]. In culture, freshly isolated SMCs reorganize their cytoskeleton with the result that myofilament bundles are disassembled while actin stress fibers become more common. The cells change from a contractile state, characterized by a fusiform shape, to a broader, flatter shape with the new β - and γ -actin isoforms predominating. α -Actin is thought to have a direct effect on the morphological differentiation of fetal SMCs. Qu et al. blocked α -actin polypeptide expression in cultured myoblasts which prevented their ability to differentiate despite the ability to express other actin isoforms [49]. In particular, the cells failed to acquire the elongated morphology characteristic of mature myocytes.

Distinct vascular actin (VAC) promoter binding proteins are thought to regulate expression of the VSM α -actin gene in a cell growth-state dependent manner. Cogan et al. demonstrated that the VAC protein, TEF-1, was enriched in proliferating, undifferentiated myoblasts but absent in mature quiescent myocytes [50]. These results suggest that TEF-1 levels in proliferating myoblasts apparently diminish as the cells mature. A second unknown transcription factor is required for promoter-function in

mature cells but its promoter binding site has not yet been identified. The developmentally-regulated usage of binding elements within the promoter to drive α -actin gene activation during periods of cell growth may be governed by mechanisms that are distinctly different from those that operate during the differentiation process.

Figure 2 summarizes the involvement of α -actin expression in the phenotypic modulation of SMCs. Once the expression of the α -actin gene is better understood, perhaps SMC modulation can be controlled following vascular injury.

Therapies for CAV

Due to the diffuse nature of the lesion, conventional therapies for atherosclerosis such as coronary vein graft bypass and angioplasty are not practical options. However, when the lesion is proximal and discrete, these particular therapies have worked successfully [51]. In most cases the only effective therapy is re-transplantation. However, the one year survival rates are low for second heart transplants [52]. Another problem with re-transplantation is the organ donor shortage which makes this a controversial option.

Since CAV is a proliferative disease, anti-proliferative agents such as heparin and rapamycin have been studied for therapeutic use. Heparin inhibits SMC proliferation, retards SMC migration, and causes SMCs to assemble a natural extracellular matrix and therefore seems to be an attractive therapy for CAV [53]. Since heparin has such strong

effects even when delivered in small amounts, Clowes recommends giving it for a brief period of 1-2 weeks along with a long-term angiotensin-converting enzyme inhibitor [53]. However, results of heparin treatments with regard to CAV are undetermined. Rapamycin is an immunosuppressant being used in animal allograft models. Several studies have shown that rapamycin has the ability to inhibit smooth muscle cell proliferation through blocking the effects of growth factors [54,55]. Gregory et al. determined that rapamycin reduced intimal thickening produced by mechanical injury in rat carotid arteries [56]. In addition, Schmid et al. observed a decrease of CAV within rapamycin-treated rat allografts [57]. Further studies of antiproliferative drugs should prove to be beneficial for CAV patients.

Other therapies currently being studied are based on cellular mechanisms involved with vascular injury. For example, platelets are thought to be involved with endothelial injury and anti-platelet treatments have been used although with inconclusive results [3]. Another animal study was performed using dehydroepiandrosterone, ω 3 fatty acids and angiopeptin [12]. The study showed that these agents may retard CAV, but their benefits have not yet been demonstrated conclusively in humans. Presently, most hospitals take preventative measures for CAV that are based on known atherosclerotic risk factors. These include controlling lipid intake, weight, smoking and hypertension. Unfortunately, these controls appear to have little effect in the prevention of CAV.

CAV is a multi-factorial disease involving many variables and multiple mechanisms. The most promising future therapies will need to interrupt several of these

mechanisms on a cellular or molecular level to be effective. Cytokines, growth factors, and cell adhesion molecules appear to be the mediators involved and a better understanding of their roles in the etiology of CAV is needed. Cell-targeted therapies, especially those directed toward SMCs, appear to be most promising particularly if the introduction of recombinant DNA molecules or drugs into modulated cells can be shown to influence metabolic properties or biosynthetic activity and effectively convert synthetic into contractile SMCs.

LIST OF REFERENCES

1. Hosenpud J, Novick R, Breen T, et al. The registry of the international society for heart and lung transplantation: twelfth official report-1995. *J Heart Lung Transplant* 1995; 14: 805-15.
2. Gao SZ, Schroeder JS, Alderman EL, et al. Clinical and laboratory correlation of accelerated coronary artery disease in the cardiac transplant patient. *Circ* 1987; 76(Supp V): v56-v61.
3. Jamieson SW. Investigation of heart transplantation coronary atherosclerosis. *Circ* 1992; 85(3): 1211-1213.
4. Hosenpud JD, Shipley GD, and Wagner CR. Cardiac allograft vasculopathy: current concepts, recent developments, and future directions. *J Heart Lung Transplant* 1992; 11: 9-23.
5. Billingham ME. Histopathology of graft coronary disease. *J Heart Lung Transplant* 1992; 11: 538-44.
6. Miller LW. Allograft vascular disease: a disease not limited to hearts. *J Heart Lung Transplant* 1992; 11(3): s32-s37.
7. Kosek JC, Hurley EJ, and Lower RW. Histopathology of orthotopic canine cardiac homografts. *Lab Invest* 1968; 19: 97-103.
8. Bieber CP, Stinson EB, Shumway NE, et al. Cardiac transplantation in man: VII: cardiac allograft pathology. *Circ* 1970; 41: 753-762.
9. Kosek JC, Bieber C, and Lower RR. Heart graft arteriosclerosis. *Transplantation Proc* 1971; 3(1): 512-514.
10. Uys CJ and Rose AC. Pathologic findings in long-term cardiac transplants. *Arch Pathol Lab Med* 1984; 108: 112-16.

11. Billingham ME. Cardiac transplant atherosclerosis. *Transplantation Proc* 1987; 19(4): 19-25.
12. Ventura HO, Mehra MR, Smart RW. Cardiac allograft vasculopathy: current concepts. *American Heart J* 1995; 129: 791-99.
13. Lin H, Wilson JE, Kendall TJ, et al. Comparable Proximal and distal severity of intimal thickening and size of epicardial coronary arteries in transplant arteriopathy of human cardiac allograft. *J Heart Lung Transplant* 1994; 13: 824-33.
14. Palmer DC, Tsai CC, Roodman ST, et al. Heart graft arteriosclerosis. *Transplantation* 1985; 39: 385-88.
15. Demetis AJ, Zerbe T and Banner B. Morphology of solid organ allograft arteriopathy: identification of proliferating intimal cell population. *Transplantation Proceedings* 1989; 21: 3667-69.
16. Russel ME, Fujita M, Masek M, et al. Cardiac graft vascular disease. *Transplantation* 1993; 56: 1599-1601.
17. Gao SZ, Schroeder JS, Alderman EL, et al. Clinical and laboratory correlation of accelerated coronary artery disease in the cardiac transplant patient. *Circ* 1987; 76(Suppl. V): v56-v61.
18. Johnson DE, Alderman EL, Schroeder JS, et al. Transplant coronary artery disease: histopathologic correlations with angiographic morphology. *J Am Coll Cardiol* 1991; 17: 449-57.
19. Valentine H, Pinto FJ, St.Goar FG, et al. Cytomegalovirus and other herpes viruses: do they have a role in the development of accelerated coronary arterial disease in human heart allografts. *J Heart Lung Transplant* 1992; 11: s14-s20.
20. Rickenbacher PR, Pinto FJ, Chenybrawn A, et al. Incidence and severity of transplant coronary artery disease early and up to 15 years after transplantation as detected by intravascular ultrasound. *J Am Coll Cardiol* 1995; 25: 171-7.
21. Neish AS, Loh E, and Schoen FJ. Myocardial changes in cardiac transplant-associated coronary arteriosclerosis: Potential for timely diagnosis. *J Am Coll Cardiol* 1992; 19: 586-92.
22. Gaudin PB, Rayburn BK, Hutchins GM. Peritransplant injury to the myocardium associated with the development of accelerated arteriosclerosis in heart transplant

- recipients. *Am J Surg Pathol* 1994; 18: 338-46.
23. Libby P. Immunopathology of coronary arteriosclerosis in transplanted hearts. *J Heart Lung Transplant* 1992; 11(3): s32-s37.
 24. Yeung AC, Anderson T, Meredith I, et al. Endothelial dysfunction in the development and detection of transplant coronary disease. *J Heart Lung Transplant* 1992; 11: s69-s72.
 25. Young JB. Cardiac allograft arteriopathy: an ischemic burden of a different sort. *Am J Cardiol* 1992; 70: 9F-13F.
 26. Hammond EH, Yowell RL, Price GD, et al. Vascular rejection and its relationship to allograft coronary artery disease. *J Heart Lung Transplant* 1992; 11: 5111-9.
 27. Costanzo-Nordin MR. Cardiac allograft vasculopathy: relationship with acute cellular rejection and histocompatibility. *J Heart Lung Transplant* 1992; 11: s90-s103.
 28. Allen MD, McDonald T, Carlos T, et al. Endothelial adhesion molecules in heart transplantation. *J Heart Lung Transplant* 1992; 11: s8-s13.
 29. Winters GL, Kendall TS, Radio SJ, et al. Post transplant obesity and hyperlipidemia: major predictors of severity of coronary arteriopathy in failed human heart allografts. *J Heart Lung Transplant* 1992; 11: s69-s72.
 30. Grady KL, Costanzo-Nordin MR, Herold LS, et al. Obesity and hyperlipidemia after heart transplantation. *J Heart Lung Transplant* 1991; 10: 449-54.
 31. Johnson MR. Transplant coronary disease: Nonimmunologic risk factors. *J Heart Lung Transplant* 1992; 11: s124-s132.
 32. Rowan RA and Billingham ME. Pathologic changes in the long-term transplant heart: a morphometric study of myocardial hypertrophy, vascularity, and fibrosis. *Human Pathol* 1990; 21: 767-772.
 33. Kendall TJ, Wilson JE, Radio SJ, et al. Cytomegalovirus and other herpes viruses: do they have a role in the development of accelerated coronary arterial disease in human heart allografts. *J Heart Lung Transplant* 1992; 11: s14-s20.
 34. Tuzcu E, Hobbs RE, Rincon G, et al. Occult and frequent transmission of atherosclerotic coronary disease with cardiac transplantation. *Circ* 1995; 91: 1706-1713.

35. Izutani H, Shirakura R, Miyagawa S, et al. Essential immune attack in graft coronary arteriosclerosis induction detected by return transplantation technique in rat. *Transplant Proceed* 1995; 27: 579-81.
36. Ross R. Atherosclerosis: a defense mechanism gone awry. *Am J Path* 1993; 143(4): 987-1002.
37. Ip JH, Fuster V, Badimon L, et al. Syndromes of accelerated atherosclerosis: role of vascular injury and smooth muscle cell proliferation. *J Am Coll Cardiol* 1990; 15: 1667-87.
38. Ross R. The pathogenesis of atherosclerosis. *New England J Med* 1986; 314(8): 488-497.
39. Brennen MJ, Millis AJ, Mann D, et al. Structural alterations in fibronectin correlated with morphological changes in smooth muscle cells. *Dev Biol* 1983; 97: 391-397.
40. Castellot JJ, Wright TC and Karnovsky MJ. Regulation of vascular smooth muscle cell growth by heparin sulfate. *Sem Thromb Hemostasis* 1987; 13: 489-503.
41. Glagov S. Intimal hyperplasia, vascular modeling and the restenosis problem. *Circ* 1994; 89: 2888-91.
42. Thyberg J, Hedin U, Sjölund M, et al. Regulation of differentiated properties and proliferation of arterial smooth muscle cells. *Arteriosclerosis* 1990; 10: 966-990.
43. Björkuud S. Effects of TGF- β on human arterial smooth muscle cells in vitro. *Arteriosclerosis and Thrombosis* 1991; 11: 892-902.
44. Schwartz S, Campbell GR, and Campbell SH. Replication of smooth muscle cells in vascular disease. *Circ Res* 1986; 58: 427-444.
45. Dilley RJ, McGeachi JK, and Prendergast FJ, A review of the proliferative behavior, morphology and phenotypes of vascular smooth muscle. *Atherosclerosis* 1987; 63: 99-107.
46. Clowes AW, Clowes MM, Fingerle J, et al. Kinetics of cellular proliferation after arterial injury versus role of acute distension in the induction of smooth muscle proliferation. *Laboratory Investigation* 1989; 60: 360-364.
47. Schwartz RS, Murphy JG, Edwards WD, et al. Restenosis after balloon angioplasty. *Circ* 1990; 82: 2190-2200.

48. Clowes AW, Clowes MM, Kocher O, et al. Arterial smooth muscle cells in vivo: relationship between actin isoform expression and mitogenesis and their modulation by heparin. *J Cell Biol* 1988; 107: 1939-45.
49. Qu G. Modulation of vascular alpha actin. Thesis. 1995.
50. Cogan J. Vascular alpha actin gene sequence and transcription factor binding site. Thesis. 1995.
51. Halle III AA, DiSciascio G, Massin EK, et al. Coronary angioplasty, atherectomy and bypass surgery in cardiac transplant recipients. *J Am Coll Cardiol* 1995; 26(1): 120-8.
52. Smith JA, Ribakove GH, Hunt SA, et al. Heart retransplantation: The 25 year experience at a single institution. *J Heart Lung Transplant* 1995; 26(1): 120-8.
53. Clowes AW. Control of intimal hyperplasia by heparin. *J Heart Lung Transplant* 1992; 11: s21.
54. Cao W, Mohacsi P, Shorthouse R, et al. Effects of rapamycin on growth factor-stimulated vascular smooth muscle cell DNA synthesis. *Transplantation* 1995; 59: 390-5.
55. Marx SO, Jayaraman T, Go LO, et al. Rapamycin-FKBP inhibits cell cycle regulation of proliferation in vascular smooth muscle cells. *Circ Research* 1995; 76(3): 412-7.
56. Gregory CR, Huang X, Pratt RE, et al. Treatment with rapamycin and mycophenolic acid reduces arterial intimal thickening produced by mechanical injury and allows endothelial replacement. *Transplantation* 1995; 59: 655-61.
57. Schmid C, Heeman U, Azuma H, et al. Rapamycin inhibits transplant vasculopathy in long-surviving rat heart allografts. *Transplantation* 1995; 60: 729-33.

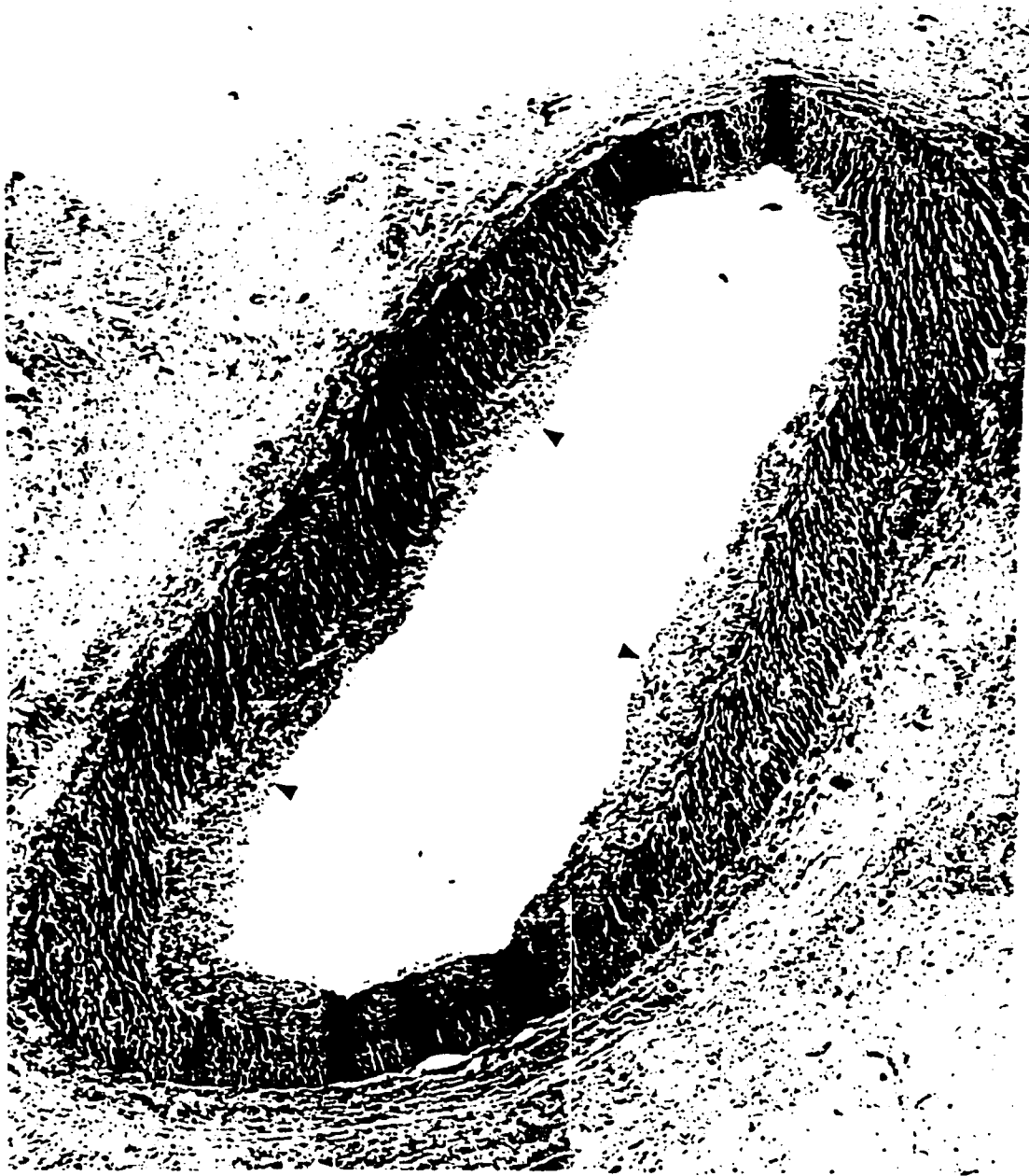


Figure 1: Human coronary artery from a transplanted heart. Arrows indicate the characteristic intimal lesion associated with CAV. (Masson's Trichrome, x80.)

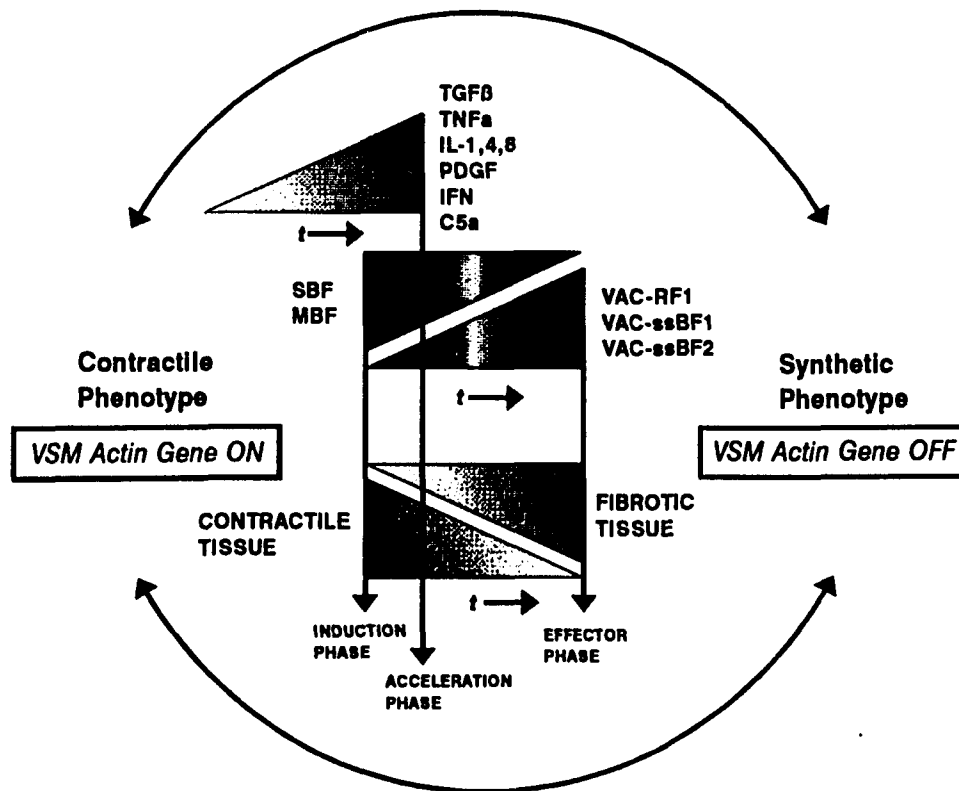


Figure 2: The diagram shows the phenotypic modulation of smooth muscle cells in relation to α -actin expression. Vascular injury introduces cytokines, as listed at the top of the diagram, in the vessel wall which silence vascular smooth muscle (VSM) α -actin gene expression in allografts. Other studies in our laboratory have identified DNA binding proteins that can either promote (SBF, MBF) or repress (RF1, BF1, BF2) the promoter. Wedges depict concentration gradients over time. The hypothesized points of induction, acceleration, and effector phases of CAV are noted on the time line. Loss of gene activity facilitates the replacement of normal smooth muscle contractile tissue with fibrotic intimal lesions.

CHAPTER 2

VALIDATION OF MORPHOMETRIC METHODS

Introduction

The advent of molecular biology techniques and microcomputer-based quantitative image analysis systems has facilitated the investigation of the microvasculature.

Historically investigators have utilized various quantitative techniques to characterize and evaluate large vessel anatomy and pathology. Quantitative morphometric analysis of pathological specimens has been used to study the coronary microvasculature in hypertensive humans utilizing endomyocardial biopsies, the small coronary vessels within human autopsied hearts, and the coronary vessels in animal models [1-5].

Validated quantitative techniques are lacking to measure the morphometric compartments of small vessels under 100 microns in diameter.

Histologic features previously used by researchers to define vessel wall architecture and obtain quantitative area measurements include the vessel lumen, intima, internal elastic lamina, tunica media, and outer vessel border. Perimeter and area determinations have relied on methods that involve manual tracing of borders in digitized

images with the aid of computer software [2,3] or by means of a light pen [4]. Other methods determine the given area from calculations applied to the manual counting of calibrated points on an overlying microscopic grid [5]. Recent technological advances now permit the acquisition of full-color, digitized images at high magnification from histologic sections. Individual pixels can be acquired and analyzed based on computer-assisted color recognition to define borders and calculate the areas within them.

Objective quantification using color thresholding was confirmed by Fermin et al. after measuring a variety of histological samples that did not include arteries [6]. Color recognition strategies may provide much clearer differentiation of structural zones within vascular elements and potentially eliminate the individual operator's subjective visual assessment of the boundaries surrounding vessel wall compartments. Based on our research interests in the microvasculature, we arbitrarily chose to examine small vessels from endomyocardial biopsies to develop and validate our methods.

The purpose of this investigation was to validate the accuracy and reproducibility of an automated, color-recognition imaging methodology. Once validated, this technique was used to analyze human arterioles and mouse vasculature as presented in Chapters 3 and 4 respectively. Histologic sections of endomyocardial biopsies from human transplant recipients are routinely analyzed to evaluate the extent of cardiac rejection [7].

Intramyocardial arterioles within these biopsies were used to validate the reproducibility of morphometric methods described in this chapter. However, small vessels from virtually any source could be analyzed using this approach.

Methods and Materials

Tissue and Slide Preparation

All pathologic specimens were obtained from human heart transplant recipients. Participating patients gave written informed consent and the investigational protocol was approved by the Ohio State University College of Medicine Human Subjects Institutional Review Board. Endomyocardial biopsy specimens are obtained 2-4 weeks after transplantation and at specified intervals for a five-year period. Right ventricular endomyocardial biopsies were obtained utilizing standard techniques [8]. A Cordis 54 cm 2.2 mm forceps disposable bioptome was used in the procedure. Two specimens were fixed in Zamboni's fixative and embedded in paraffin. Tissue sections were sliced 4 μm thick, mounted and subsequently stained with Masson's Trichrome.

Imaging

The image analysis system we used was customized for our needs and consisted of computer hardware and software from multiple sources. Intramyocardial vessel images were obtained via a three-chip color camera (model #Hv-C11, Hitachi, Woodbury, NY) connected to the video port of a light microscope (Zeiss, Thornwood, NY) fitted with a 40X Plan objective (N.A.=.65). The Hitachi camera and coupler magnified the image 38X beyond the magnification of the objective. Therefore, the image was visualized on the monitor at a final magnification of 1520X. The three-chip configuration provided ideal color fidelity to accurately reproduce the image as observed microscopically by the user. An acquisition microprocessor board (Coreco, Quebec, Canada) in the host computer received the video signal from the camera, displayed it on a high resolution color monitor (model #GVM-13UQ, Sony, Montvale, NJ) with 640x480 lines of resolution, and converted the signal into a digital format. The image was then captured and either immediately analyzed or stored on optical disk for later processing. The Optimas® image analysis software package (version 4.1, Optimas Inc., Edmonds, WA.) controls the acquisition functions described above and manages other system capabilities including the image processing, measurement, and output functions. Hard-copy image output was available from a grayscale laser printer and/or a color video printer. An IBM-compatible 486 DX 33 MHz tower with 16 MB of RAM and 340 MB hard drive was the host computer configuration. A rewritable optical disk drive

provided additional storage capacity for retrieved images that averaged 1.6 MB in size. The imaging system was calibrated using a photographically etched grid stage micrometer (Klarmann Rulings, Inc., Manchester, NH). The accuracy of the grid micrometer is traceable to the National Institute of Standards Technology (N.I.S.T.). In addition to the calibration, Optimas® used the grid micrometer to correct for differences in aspect ratios that occur between the horizontal and vertical axis on the monitor.

To address the accuracy of our proposed methods, we measured the areas of five variably-sized polygons with a Planix 7 planimeter (Tamaya). Using a high resolution 1200 DPI color scanner (model #12000C, Tamarack Telecom, Inc., Hsinchu, Taiwan) the same five shapes were digitized. The areas of the digitized polygons were measured with Optimas® and compared with the areas determined by planimetry.

To address the reproducibility of our proposed methods, ten individual vessels each from a different transplant recipient biopsy were selected as the study group and digitized for quantification. These vessels ranged in size from 20 to 50 μ m in diameter with a mean of 30 μ m. Moreover, the ten vessels were selected on the criteria of being circular cross sectioned vessels with neither oblique transection nor branching. Using the image analysis system, the three investigators measured the ten vessels independently while following the same protocol for morphometric analysis as described below.

Morphometric Analysis

The histology of microvessels reveals three distinct borders, that divide the vessel into morphological compartments of the lumen, intima and tunica media. The areas within these compartments were defined and quantified by the three investigators, as shown in Figure 3, using the image analysis software, Optimas® version 4.1. The image analysis software recognized color hues within pixels and automatically demarcated specified colors of interest in the image. This color specification technique, termed “thresholding”, automatically bordered the luminal area as well as the vessel outer wall that encompasses the entire vessel. The distal border of the internal elastic lamina (IEL) had to be defined using an automatic tracing technique within the Optimas® software package. The automatic trace differentiated between the subtle pixel color differences that defined the IEL border. This technique required user assistance in guiding the trace in areas of disrupted borders. The areas within these 3 bordered regions were then measured by Optimas®.

All area measurements within the 3 bordered compartments were calculated by Optimas® in μm^2 and sent directly to a spreadsheet in Microsoft® Excel version 5.0. The percent stenosis of the vessel was calculated from these area measurements with the formula: $\% \text{ Stenosis} = \text{Intima} / (\text{Intima} + \text{Lumen}) \times 100$. A blind study was conducted in which each of the three investigators (A, B and C) measured the 10 vessels

independently. In addition, to test intra-observer variability, two investigators (A and C) measured each of the 10 vessels on 2 separate occasions blinded to their previous measurements.

Statistical Analysis

Statistical analysis of inter-observer variability was performed using ANOVA (Statview, Abacus Concepts, Berkeley, CA) to compare measurements made by each of the three investigators. The measurements compared included the lumen area, IEL area, outer wall area, and percent stenosis. Statistical significance was defined as $p < 0.05$. Intra-observer reproducibility was determined for the two investigators who measured the ten vessels twice by comparing the difference from the mean of their repeated measurements. The statistical method of Bland and Altman was applied to assess agreement between two measures [9]. In comparing the percent stenosis, the difference of the percentage from the mean was plotted in a figure to show difference against mean for each vessel measured [9]. Reproducibility of measurement is valid when the difference from mean is less than two standard deviations [9]. In addition, both validation of accuracy and intra-observer variability were analyzed with simple linear regression (Statview, Abacus Concepts, Berkeley, CA).

Results

Validation of Accuracy

The area measurements for the five shapes using the planimeter were (a) 22.0cm², (b) 20.2cm², (c) 9.0cm², (d) 11.0cm² and (e) 38.7cm². The area measurements for the five shapes using digital analysis were (a) 22.0cm², (b) 19.7cm², (c) 9.0cm², (d) 10.9cm² and (e) 38.0cm². The accuracy of the two systems was compared using simple linear regression giving an r² value of .999 and a p value of .5083.

Inter-Observer Variable Analysis

All individual measurements and group means \pm standard deviation are presented in Table 2. Each investigator measured the lumen area, IEL (internal elastic lamina) area, and outer wall area of the 10 vessels (30 measurements). The percent stenosis was calculated as previously described using the raw data. The large standard deviations reflect the unusually large size of vessel 10. Analysis of variance amongst the three data sets demonstrated that the measurements performed by the three observers were highly reproducible.

Intra-Observer Variable Analysis

Two investigators repeated the measurements in two separate blind studies. This data is included in Table 2 (A2 and C2). Intra-observer variability was examined by two statistical analyses. Simple linear regression was used to determine the relationship between the two sets of measures from separate occasions. Figure 3 shows the relationship for percent stenosis, $y=1.033x - 2.166$, $r^2 = .974$ $p=.0001$. The r^2 values for lumen area (.998), IEL area (.999), and outer wall area (.999) were also highly significant. Comparison of 2 measures of a variable might best be represented by the plot of the differences in measures from the mean (y-axis) and the mean of the 2 measures (x-axis) [9]. Repeatability was considered valid when the difference from the mean was less than 2 standard deviations as defined by the British Standards Institution [9]. Figure 4 plots the values for the percent stenosis and documents that our intra-observer measures falls within these criteria.

Discussion

Recent studies have emphasized the relevance of studying intramyocardial vessel pathology in common human diseases such as hypertension, diabetes mellitus, hypertrophic cardiomyopathy, collagen vascular diseases, and transplant vascular sclerosis [1,4,5,10]. Intramyocardial or "small vessel" diseases have been defined

pathologically as affecting arterioles less than 100 μm in diameter [1,11,12]. Precise measurements are particularly important in small vessels where the internal elastic lamina may not be distinct and basement membrane thickening due to the deposition of extracellular matrix proteins is the characteristic pathologic change.

The goal of the studies described in this report was to develop an efficient, reproducible, quantitative method to analyze small vessel pathogenesis. We have demonstrated that color-recognition image analysis is a highly reproducible method that can be automated utilizing the macro language within the Optimas® software. An experienced operator can complete data collection for a typical intramyocardial vessel in 5 minutes.

Published investigations have used a variety of techniques to analyze intramyocardial vessels in both semi-quantitative and quantitative manners. Established methods of quantitation involving point counting on an ocular grid as described by Schwartzkopff et al. are in use [5]. However, with the increasing availability of computerized image analysis systems and software, established methods such as point counting on a grid are becoming less efficient and outmoded. This is especially the case in clinical pathology laboratories where the volume of histologic material that must be analyzed may be quite large. Researchers are beginning to use microcomputer imaging systems to measure the morphology of coronary branches, but no information has been presented in the literature that evaluates the reproducibility of any established measurement methodology. Eich et al. used a commercially available microcomputer

imaging system (Zeiss VideoPlan®) to analyze intramyocardial vessels, but this system has not been validated to our knowledge and requires manual identification of histologic features [2].

In a study of human intramyocardial arterioles Tanaka described an image analysis system in detail as well as their use of a light pen to trace morphological borders [4]. The methodology we have described using color recognition of digitized pixels to define borders not only is more efficient but also may be more accurate because the automated differentiation of zones within vessels is not subject to errors associated with the individual operators estimation of histologic borders. Tanaka addressed reproducibility between two investigators and reported that there was a small variance between them [4]. We validated the accuracy of measurements with our microcomputer based image analysis system using an accepted but archaic planimetry approach where the border is manually traced using an eyepiece and cross-hair. We believe the system we have described is theoretically more accurate because it eliminates much of the subjectivity in assessing potentially subtle histologic features.

The usefulness and application of this methodology is evident based on the acknowledged inconsistency of previously employed morphometric methods. Standardized quantitative morphometric techniques will facilitate a more thorough understanding of small vessel diseases. The development of molecular biological tools will further aid in the characterization of the subendothelial proliferative process as assessed by the color recognition imaging methodology since techniques such as

immunohistochemistry and *in situ* hybridization can be quantitated utilizing a color recognition image analysis system. In theory, the imaging technique described in this report can be applied to any small vessel system or anatomic structure(s) that can be demarcated using standard histological dyes.

List of References

1. van Hoeven KH and Factor SM. Endomyocardial biopsy diagnosis of small vessel disease: a clinicopathologic study. *Int. J. Cardiol.* 26:103-110; 1990.
2. Eich DM, Nestler JE, Johnson DE, et al. Inhibition of accelerated coronary atherosclerosis with dehydroepiandrosterone of cardiac transplantation. *Circulation* 87:261-269; 1993.
3. Segal SS, Kurjiaka DT and Caston A.L. Endurance training increases arterial wall thickness in rats. *J. Appl. Physiol.* 74(2):722-726; 1993.
4. Tanaka M, Fujiwara H, Onodera T, et al. Quantitative analysis of narrowing of intramyocardial small arteries in normal hearts, hypertensive hearts, and hearts with hypertrophic cardiomyopathy. *Circulation* 75(6):1130-1139; 1987.
5. Schwartzkopff B, Motz W, Frenzel H, et al. Structural and functional alterations of the intramyocardial coronary arterioles in patients with arterial hypertension. *Circulation* 88:993-1003; 1993.
6. Fermin CD, Gerber MA and Torre-Bueno. Colour thresholding and objective quantification in bioimaging. *J of Microscopy* 1992;44:114-24.
7. Billingham ME. Diagnosis of cardiac rejection by endomyocardial biopsy. *Heart Transplant* 1:25-30; 1981.
8. Starling RC, VanFossen DB, Hammer DF, et al. Morbidity of endomyocardial biopsy in cardiomyopathy. *Am. J. Cardio.* 68:133-136; 1991.
9. Bland JM, Altman DG. Statistical methods for assessing agreement between two methods of clinical measurement. *The Lancet* Feb 8:307-310; 1986.
10. Mosseri M, Schaper J, Yaron R, et al. Coronary capillaries in patients with congestive cardiomyopathy or angina pectoris with patent main coronary arteries. *Circulation* 84:203-210; 1991.

11. James TN. Small arteries of the heart. *Circulation* 56:2-14; 1977.
12. Geer JC, Bishop SP, and James TN. Pathology of small intramural coronary arteries. *Pathol. Ann.* 14:125-154; 1979.

INVESTIGATOR	Lumen Area μm^2					IEL Area μm^2				
	A	B	C	A2	C2	A	B	C	A2	C2
VESSEL 1	38.96	40.79	44.40	36.42	38.42	332.80	333.58	333.60	335.55	329.74
VESSEL 2	11.82	9.91	15.63	10.68	10.34	113.54	110.99	111.95	109.68	113.76
VESSEL 3	76.51	71.10	76.25	75.28	78.65	249.54	247.72	248.41	249.76	250.99
VESSEL 4	107.63	96.65	106.78	108.10	99.05	266.68	267.67	271.39	262.17	274.37
VESSEL 5	33.45	36.45	31.13	32.21	28.95	123.87	122.93	125.16	129.66	124.64
VESSEL 6	70.32	71.79	68.36	69.84	68.50	248.70	252.39	249.18	252.76	252.47
VESSEL 7	18.20	18.17	18.04	18.27	16.91	196.22	195.00	199.32	195.05	197.33
VESSEL 8	77.65	81.11	75.97	78.56	84.10	284.77	283.98	283.41	281.82	290.86
VESSEL 9	83.94	85.07	84.05	100.94	87.91	327.63	331.29	326.65	329.88	324.17
VESSEL 10	446.77	446.77	421.13	446.77	423.72	902.14	904.07	920.44	911.38	902.25
MEAN	96.52	94.17	95.78	97.70	93.65	304.58	306.95	304.96	305.77	306.05
STD. DEVIATION	126.92	118.74	126.77	127.16	120.19	222.93	228.20	223.89	225.67	222.40
ANOVA F/P	.001 / .9991					.0003 / .9997				

INVESTIGATOR	Outer Wall μm^2					Percent Stenosis %				
	A	B	C	A2	C2	A	B	C	A2	C2
VESSEL 1	735.30	766.41	772.84	738.85	758.05	88.29	87.77	86.69	89.15	88.35
VESSEL 2	289.94	299.73	295.21	305.28	287.76	89.59	91.07	86.04	90.26	90.91
VESSEL 3	372.10	362.19	364.26	361.18	368.35	69.34	71.30	69.31	69.86	68.66
VESSEL 4	557.25	552.38	565.00	547.16	573.55	59.64	63.89	60.65	58.77	63.90
VESSEL 5	202.12	210.48	216.96	201.49	218.06	73.00	70.35	75.13	75.16	76.77
VESSEL 6	483.66	485.61	488.67	484.00	495.69	71.72	71.55	72.56	72.37	72.87
VESSEL 7	496.51	490.40	488.41	485.11	486.22	90.72	90.68	90.95	90.63	91.43
VESSEL 8	516.46	539.09	537.49	508.31	552.10	72.73	71.44	73.19	72.12	71.09
VESSEL 9	528.04	531.41	545.10	532.28	540.98	74.38	74.32	74.27	69.40	72.88
VESSEL 10	1476.94	1499.7	1481.58	1498.0	1482.86	50.48	50.58	54.25	50.98	53.04
MEAN	565.83	575.55	573.74	566.17	576.36	73.98	74.30	74.29	73.87	74.99
STD. DEVIATION	352.80	354.22	359.72	358.93	353.73	12.97	11.48	12.65	13.24	12.35
ANOVA F/P	.002 / .9979					.002 / .9979				

Table 2: Vessel morphometric measurements performed by investigators A, B, and C are shown in the table along with an analysis of variance between the investigators. No significant difference was seen between measurements performed by the three investigators. Investigators A and C repeated the same measurements and their repeated measures are listed in the table under A2 and C2.



Figure 3: Human intramyocardial vessel measuring $50\mu\text{m}$ in diameter. Three distinct morphological borders were drawn for each vessel which effectively divided the vessel into compartments A (lumen), B (intima), and C (tunica media). Area measurements were derived by the color-recognition software for the three regions defined by these borders. The areas measured were as follows: Lumen Area = A, IEL Area = A+B, and Outer Wall Area = A+B+C. The percent stenosis was calculated using the equation $B / [A + B]$. (Masson's Trichrome, x1520.)

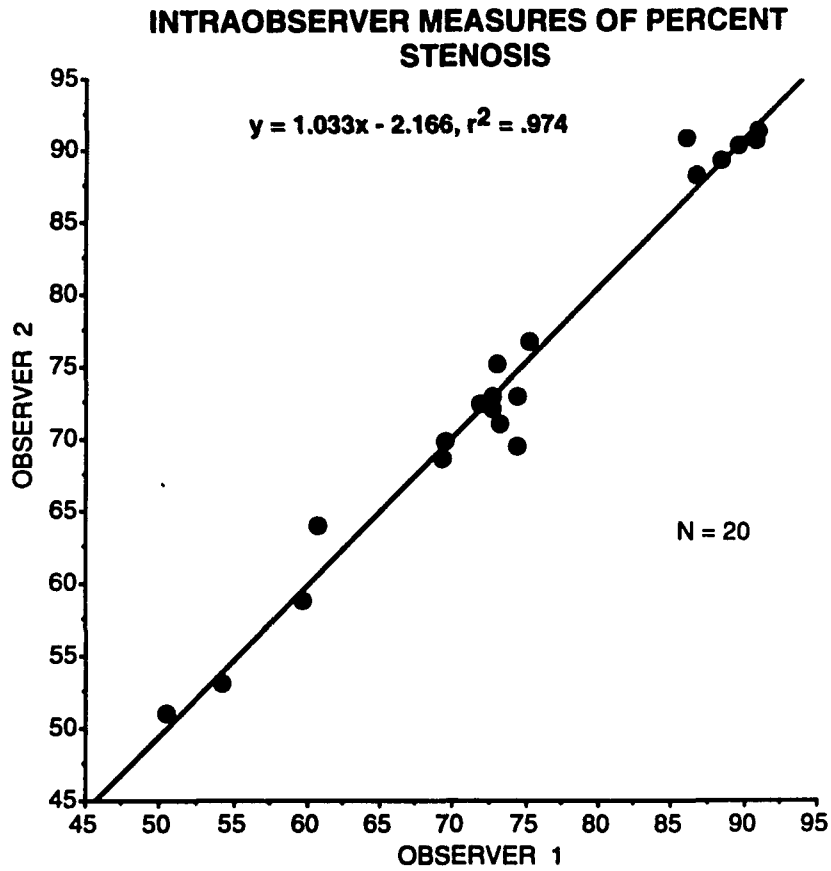


Figure 4: Linear regression expressing the relationship between two sets of repeated measures of percent stenosis from data collected by two observers.

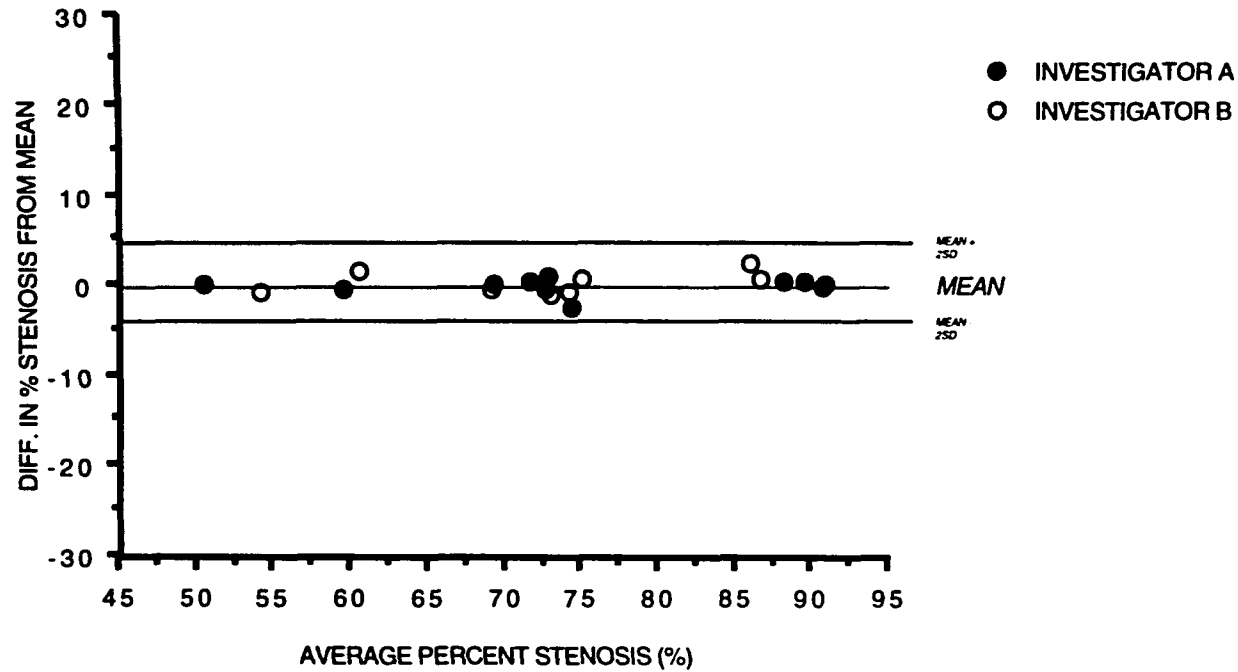


Figure 5: Comparison of differences in percent stenosis from the mean (y-axis) and the mean of the repeated measures of both investigators (x-axis). Repeatability is valid when the difference in percent stenosis from mean is less than 2 standard deviation (SD) units.

CHAPTER 3

QUANTITATIVE MORPHOMETRIC AND IMMUNOCYTOCHEMICAL ANALYSIS OF CORONARY ARTERIOLES FROM HUMAN TRANSPLANTED HEARTS

Introduction

Cardiac allograft vasculopathy (CAV) is the major limitation of long-term survival in heart transplant recipients. Although CAV is considered to be a form of accelerated coronary artery disease, its etiology is unknown and likely derived from several factors. Previous studies have reported the pathological features and clinical complications associated with CAV [1-5]. These findings include a concentric intimal lesion observed throughout the length of the epicardial coronary arteries of the transplanted heart. Coronary angiography has been considered the clinical standard to diagnose CAV in transplant recipients. Notable features include “distal pruning”, which occurs when distal vessels are occluded. Gao has described the 3 typical angiographic lesions observed [6]. Lin et al. have shown that intimal thickening is present in the proximal and distal segments of the epicardial coronary arteries [2]. Coronary angiography depicts the luminal characteristics but cannot define the intimal pathology. Consequently, coronary

angiography is being supplanted by intravascular ultrasound which allows the visualization and quantification of intimal thickening in vessels with a luminal diameter ≥ 2 mm.

If a diffuse endothelial injury is responsible for CAV, it is very likely that small vessels (<100 μm in diameter) could also be involved. Palmer proposed that “proliferative graft arteriosclerosis may appear as advanced small vessel disease before extensive large vessel involvement is detected by coronary angiogram” and that endomyocardial biopsy specimens might be utilized to detect cardiac allograft arteriosclerosis [7]. As a supplement to coronary angiography and ultrasound, a prospective analysis of the vasculature within endomyocardial biopsy specimens might provide an opportunity to study the temporal aspects of CAV *in vivo*. Previous qualitative, retrospective studies have looked for the presence of CAV in arterioles from transplanted human hearts. Demetris and colleagues reported on the morphology of arterioles from 12 transplanted human hearts [8]. Only large extraorgan arteries and medium-sized intraorgan muscular arteries ($>50\mu\text{m}$ external diameter) were found to exhibit intimal thickening. To our knowledge intimal thickening due to CAV has not been confirmed quantitatively in the small vessel branches (<100 μm in diameter).

The purpose of our investigation was to document the incidence of CAV in human heart transplant recipients through a prospective analysis of endomyocardial biopsies taken over a 3 year period following transplantation. We sought to characterize the microvascular anatomy using quantitative morphometrics and to gain insight into the

composition of the intimal components. To better understand the relationships between the cellular populations within coronary arterioles and the etiology of CAV, we used immunocytochemical methods to study vascular smooth muscle proliferation and phenotypic modulation in endomyocardial biopsy specimens. We hypothesized that an “immune mediated endothelial injury” would yield diffuse vascular disease in epicardial coronary arteries that would extend to arterioles less than 100 μ m in diameter. In accordance with the pathological features of CAV observed in epicardial coronary arteries, we also expected the small vessel branches to exhibit increased intimal hyperplasia over time following transplantation.

Methods and Materials

Endomyocardial Biopsies

All pathologic specimens were obtained from human heart transplant recipients. Participating patients provided informed written consent and the investigational protocol was approved by the Human Subjects Institutional Review Board of the Ohio State University College of Medicine. Endomyocardial biopsy specimens were obtained weekly after transplantation for 6 weeks and at specified intervals thereafter for a five-year period. Right ventricular endomyocardial biopsies were obtained utilizing standard

techniques [9]. A disposable Cordis 54 cm 2.2 mm forceps bioptome was used in the procedure. Two specimens were fixed in Zamboni's fixative, embedded in paraffin, sectioned 4 μm thick and mounted to glass slides.

Histologic Morphometric Analysis

Coronary arterioles within 148 biopsy sections from 30 transplant patients were visualized (Masson's trichrome stain) and analyzed using computer assisted morphometry. A representative biopsy specimen visualized at typical light microscopic viewing magnification (50X) is shown in Figure 6. The endomyocardial arterioles ranged in size from 20-85 μm in diameter and were selected based on the criteria of being circular cross-sectioned vessels with neither oblique transections nor branching. Vessels were not included when tangential sectioning planes were evident. Sampling is an issue that cannot be adequately addressed using human subjects. We are limited to study 4-6 biopsy specimens obtained at the time of each heart biopsy procedure. All specimens are paraffin embedded and 10 steps are made in each block and 8 sections, 4 μm in thickness, are made yielding over 60 sections. In about 20% of biopsy procedures we fail to locate any suitable vessels for analysis. Studies we have performed with animal models appear to circumvent this limitation. Vessels suitable for analysis were

digitized using a light microscope (Zeiss, Thornwood, NY) coupled to a 3-chip color camera (model #HV-C11, Hitachi, Woodbury, NY) that was interfaced to an IBM-compatible 486 host computer.

Arterioles stained with Masson's trichrome stain typically demonstrate well demarcated compartmental borders which facilitates quantitative morphometric analyses, as discussed in Chapter 2. Three distinct histologic borders enabled us to divide the vessel into morphological compartments that included the lumen, intima and tunica media. Using image analysis software (Optimas 4.1, Optimas Inc. Edmonds, WA), outer borders for each morphological compartment were defined automatically by color recognition. Manual tracing was occasionally required in regions where the IEL border was not distinct. The areas within the 3 bordered compartments were measured by the image analysis system which was calibrated using a stage micrometer (Klarmann Rulings, Manchester, NH) traceable to the National Institute of Standards Technology. The area measurements were then used to calculate the percent stenosis of small vessels with the formula $\% \text{ Stenosis} = \text{Intima area} / (\text{Intima area} + \text{Lumen area}) \times 100$. The morphological compartments are depicted on a representative intramyocardial arteriole in Figure 1 of Chapter 2. In addition to percent stenosis, ratios of the luminal area / medial area and luminal area / [luminal area + intimal area + medial area] also were derived.

The data collected from the transplant biopsies were grouped according to the post-transplant period when the biopsy was performed: Early (0-6 months), Middle (6-

18 months), and Late (18-36 months). A control group consisting of biopsies from 9 individuals without structural heart disease was used for statistical comparisons.

The methodology used to analyze the arterioles in this study was validated in Chapter 2. The accuracy and repeatability of the technique was statistically proven.

Epicardial Coronary Analysis

Fifty-one arterioles from biopsies were analyzed in conjunction with the corresponding coronary angiogram. Percent stenosis of the arterioles was compared to the angiographic findings in the epicardial coronaries. Coronary angiograms were visually classified by a blinded experienced interventional cardiologist as: normal n=37, proximal disease n=5, distal disease n=2 and mixed disease n=7. Angiograms were classified on the basis of single vessel disease or greater. Factorial ANOVA was used to compare the percent stenosis of the arterioles with the type of epicardial coronary disease (none, proximal, distal, mixed).

Immunohistochemistry Procedure Using PCNA Antibody

The mouse monoclonal antibody PC10 (DAKO, Carpentry, CA) a horseradish peroxidase (HRP)-labeled antibody specific for the proliferating cell nuclear antigen (PCNA) [10] was incubated with 70 biopsies from 24 heart transplant patients. AEC

chromogen (Sigma, St. Louis, MO) was used as the substrate which produced a reddish brown color from the enzymatic reactions in the case of positive antibody binding. Also, a hematoxylin counter stain was applied to the specimens to stain the nuclei blue. In parallel with the sectioned endomyocardial biopsy specimens, paraffin-embedded sections of human tonsil (DAKO, Carpentia, CA) were immunohistochemically stained with the PCNA-specific antibody to provide a positive control as seen in Figure 7a. Also, a negative control of HRP-labeled goat serum (Sigma, St. Louis, MO) was substituted for the primary antibody to confirm the specificity of the PCNA antibody as shown in Figure 7b.

Immunocytochemistry Procedure Using Smooth Muscle α -actin Antibody

The vascular smooth muscle α -actin specific mouse monoclonal antibody 1A4 (Sigma, St. Louis, MO) was incubated with 54 biopsies from 9 heart transplant patients for 1.5 hours at a dilution of 1:500, followed by rhodamine conjugated goat anti-mouse IgG (Hyclone, Logan, UT) for 1.5 hours using a dilution of 1:100. The fluorescently-labeled arterioles were imaged by confocal microscopy (Biorad, Hercules, CA) and subsequently analyzed using Optimas 4.1 image analysis software (Optimas Inc. Edmund, WA). The confocal laser averages a z-series of each vessel at different consecutive focal levels and presents it as a digitized greyscale image. The digitized signal from bound antibody consisted of multiple pixels each with an intensity value

from 0 to 255. A histogram of the pixel intensity values derived from the antibody signal for each vessel was generated by the imaging software along with a mean histogram value. The mean pixel histogram value was denoted as a measurement of smooth muscle α -actin antibody intensity and compared statistically between different arterioles from different patient biopsies.

Variations of the α -actin antibody signal could occur due to variability in staining. The samples were not stained simultaneously due to the prospective design of this study and the numerous amount of slides being processed. However, all of the samples were stained by the same investigator using a regimented protocol. We believe the large number of samples analyzed and the consistent technique should minimize variations in antibody signal.

Computer-automated edge detection defined the boundaries of the fluorescent signal and the enclosed area was calculated (antibody signal area). The antibody signal had a circular cross-sectioned morphology with a central unlabeled region we have termed the lumen. Area measurements of the lumen were calculated and used in the following equation to determine the percentage of antibody signal within the vessel: $\text{Antibody Signal Area} / [\text{Lumen Area} + \text{Antibody Signal Area}] \times 100$. The percentage of antibody signal was then compared between arterioles. Finally, we assigned qualitative values to denote heterogeneity in the patterns of the antibody signal. Each fluorescently

labeled vessel was ranked according to the degree of signal fragmentation observed:

Rank 0 = no fragments, Rank 1 = 1 to 3 fragments, Rank 2 = 4 to 9 fragments, Rank 3 = 10+ fragments.

Results

Histological Analysis

Quantitative morphometric data for small intramyocardial vessels are presented in Table 3. The percent stenosis was similar in the normal and transplant vessels. In addition, there was no change in the degree of stenosis between Early, Middle and Late post-transplant groups. The ratio of the intimal area to the tunica media and total vessel area also was similar to the normals and unchanged throughout the study period.

Comparison of Biopsies with Corresponding Angiograms

Percent stenosis for the 51 arterioles analyzed were as follows: mean $71.33 \pm 14.6\%$, range 40.5 - 94.2%, coefficient of variation .204 Vessels were compared based on the presence of epicardial coronary disease classified as none, proximal, distal or mixed and the percent stenosis of the endomyocardial arterioles. No relationship or trends were observed when comparing the epicardial coronary arteries and the respective

endomyocardial arterioles. Because the percent stenosis was rather homogeneous and there was no variation over time, it is not surprising that no relationships were identified.

Immunohistochemical Analysis Using PCNA Antibody

The PCNA antibody reacted strongly with human tonsil tissue that contains actively dividing cells as evidenced in Figure 7a. However, among 70 biopsies removed at various time intervals following transplant (1 week to 3 years), and placed into 3 groups: Early (n=25), Middle (n=22) and Late (n=23), no PCNA antibody binding was observed in the intramyocardial arterioles. A representative arteriole from an endomyocardial biopsy following reaction with a PCNA-specific antibody is shown in Figure 8.

Immunocytochemical Analysis Using α -Actin Antibody

We analyzed 101 arterioles from transplanted heart biopsies immunocytochemically labeled with a monoclonal antibody specific for vascular smooth muscle α -actin. No significant difference in the mean size of the vessels between Early, Middle and Late groups was observed as summarized in Table 4. A varying degree of fragmentation of the fluorescent antibody signal in the arterioles also was observed. An

example of a rank 0 vessel (no fragmentation) and a rank 3 vessel (extreme fragmentation) is shown in Figure 9. However, as shown in Table 4, no significant difference was observed in fragmentation scores among the 3 groups.

The percentage of α -actin occupying the vessel wall was compared between the 3 groups. There was a significant difference between the Early and Late group as well as between the Middle and Late group (Table 4). The Late group had a significantly greater percentage of α -actin compared to the other two groups. Likewise, the mean antibody signal intensity was significantly higher in the Late group as compared to the Early and Middle groups (Table 4).

Discussion

Our prospective analysis of arterioles found in endomyocardial biopsy specimens from heart transplant recipients did not support the hypothesis that CAV is a diffuse process, at least as judged by histologic criteria. A quantitative, morphometric analysis showed no change in the intimal characteristics exhibited by the arterioles in heart biopsies measured over time post-transplantation. Furthermore, there were no significant differences in the morphometric data when the experimental group was compared to the normal control group. Based on our results we conclude that histological disease is not apparent in human cardiac allograft coronary arterioles.

PCNA analysis failed to indicate active proliferation of smooth muscle cells within the arterioles implying that a myointimal proliferative response had not developed or not yet emerged in the small caliber vessels. Proliferating smooth muscle cells in intimal hyperplasia of vascular injury have been well established in animal models [11,12]. However, direct evidence for smooth muscle cell proliferation in human vascular lesions is not as prevalent as in animal models. Katsuda et al. used PCNA antibodies to characterize proliferating cells within early human atherosclerotic lesions from young adults [13]. Only 2% of the cells in the lesions were PCNA-positive and of those only a small fraction were identified as smooth muscle cells. O'Brien et al. also found that PCNA-positive cells occurred infrequently and at low levels in human primary and restenotic coronary atherectomy specimens [14]. In addition to these studies in human epicardial atherosclerotic lesions, we now report that smooth muscle cell proliferation does not occur in the microvasculature of transplanted human hearts up to 3 years post-transplant. Alternatively, it is possible that smooth muscle cell proliferation did occur in the arterioles and we missed the mitotic event. However, missing the event is unlikely due to the multiple biopsy samples taken at different time points following transplantation.

Even though the PCNA analysis showed that cellular proliferation was not occurring, the analysis of vascular smooth muscle α -actin levels in adjacent sections removed from the same series of biopsies appeared to provide a different view of the disease process. Studies on isolated smooth muscle cell cultures and vascular injury

models in animals have revealed characteristic changes in smooth muscle cell phenotype as a response to proliferation signals [15,16]. Whereas vascular smooth muscle α -actin is the major cytoskeletal component of quiescent smooth muscle cells, proliferative cells exhibit decreased expression of α -actin and elevated levels of β -actin. Our results showed that the α -actin-antibody signal intensity and the area it occupied actually increased in the coronary arterioles in the Late (18 mo.-36 mo.) group of biopsies taken from transplant recipients. The increase in α -actin was consistent with the finding that the smooth muscle cells were not in a proliferative phenotype as assessed by PCNA binding studies.

We propose that the smooth muscle α -actin immunocytochemical analyses may provide evidence for vascular remodeling of the coronary microvasculature in the transplanted heart. While the fragmentation of the antibody signal may be considered an approximate measure of remodeling, the mean fragmentation score between Early, Middle and Late biopsy groups did not differ significantly. However, the significant increase in α -actin-antibody signal intensity as well as the area it occupied in the late group of biopsies could be interpreted as a vascular remodeling event. Arteriolar smooth muscle cells may be remodeling in response to circulating growth factors that accompany vascular injury after transplantation. For example, serum growth factors such as transforming growth factor- β have a transient inducible effect on vascular smooth muscle α -actin gene expression in cultured smooth muscle cells [17] and myofibroblasts [18] that appears to be based on direct activation of the α -actin gene promoter [19]. In this

context, serum growth factor-induced activation of the vascular smooth muscle α -actin gene in coronary microvessels could reflect the developing process of CAV involving actin cytoskeletal remodeling in arteriolar smooth muscle cells.

Study Limitations

Potential limitations in the analysis of the microvasculature contained within endomyocardial biopsy specimens include artifactual representations of vessel size and shape. Inherent problems with the interpretation of small vessels (<100 μ m in diameter) include shrinkage from fixation, sectioning planes, and the clarity of borders defining the vascular compartments. Endomyocardial biopsies are obtained from living patients and due to their small size, perfusion fixation is not feasible to maintain vessel architecture during processing. We addressed this limitation by “circularizing” the vascular compartments of a small sample of 50 vessels by mathematically converting their perimeter values into the area of a perfect circle.²⁰ The percent stenosis was calculated from these circularized vessels and compared with the percent stenosis of the same vessels when not circularized. We found that the percent stenosis of the vessel areas not circularized was overestimated by 12% when compared to the circularized vessel areas ($p < .001$). In general, the greater a vessel deviated from a perfect circle, the greater the overestimation of the percent stenosis. However, our conclusions were not influenced by the artifact because we reported trends in vessel morphology. Overestimation of the %

stenosis due to artifact helps to explain the unexpectedly high 66% stenosis we discovered in normal arterioles found in endomyocardial biopsy specimens from normal humans using conventional formulae. We thought that an animal model would address this limitation involving vessel collapse. However, as will be discussed in Chapter 4, perfusion of mouse coronary arteries gave no difference to their cross-sectional morphology.

We have observed examples of diseased arterioles within biopsies from heart transplant recipients as have been previously noted by other researchers [7]. Although these isolated incidents of disease occur, our study which combines data from an entire population of arterioles over time shows no changes in intimal growth. In addition, we compared the arterioles from transplanted hearts with those from normal hearts which should better elucidate the presence of arteriolar graft disease. A comparison with normal biopsies has not to our knowledge been done prior to this study.

Conclusion

The coronary arterioles from biopsies of transplanted heart recipients do not show the intimal hyperplasia characteristics associated with epicardial CAV. Therefore, the histologic assessment of endomyocardial biopsy arterioles cannot be used to predict Cardiac Allograft Vasculopathy within the epicardial coronary arteries. Intravascular ultrasound has taught us that epicardial coronary remodeling may occur in the cardiac

allograft. As the vessel diameter increases over time and the intima thickens, the absolute luminal area may be unchanged. Artery enlargement may be a reaction to increased flow and/or atherosclerotic plaque formation as described by Glagov [21]. Our results confirm the absence of histologically evident disease within small vessels (<100 μ m in diameter) of the cardiac allograft up to 3 years after transplant. We conclude from the results that there is no myointimal proliferative disease occurring in the small vessels, but a vascular remodeling in response to injury may be present.

List of References

1. Hosenpud JD, Shipley GD, Wagner CR. Cardiac allograft vasculopathy: current concepts, recent developments, and future directions. *J Heart Lung Transplant* 1992; 11: 9-23.
2. Lin H, Wilson JE, Kendall TJ, et al. Comparable proximal and distal severity of intimal thickening and size of epicardial coronary arteries in transplant arteriopathy of human cardiac allografts. *J Heart Lung Transplant* 1994; 13: 824-33.
3. Hammond EH, Yowell RL, Nunoda S, et al. Vascular (humoral) rejection in heart transplantation: pathologic observations and clinical implications. *J Heart Lung Transplant* 1989; 8: 430-43.
4. Billingham ME. Cardiac transplant atherosclerosis. *Transplantation Proceedings* 1987; 19: 19-25.
5. Kosek JC, Bieber C, Lower RR. Heart graft arteriosclerosis. *Transplantation Proceedings* 1971; 3: 512-514.
6. Gao SZ, Alderman EL, Schroeder JS, Silverman JF, Hunt SA. Accelerated coronary vascular disease in heart transplant patients: coronary arteriographic findings. *J Am Coll Cardiol* 1988; 12: 334-40.
7. Palmer DC, Tsai CC, Roodman ST, et al. Heart graft arteriosclerosis. *Transplantation* 1985; 39: 385-88.
8. Demetris AJ, Zerbe T, Banner B. Morphology of solid organ allograft arteriopathy: identification of proliferating intimal cell populations. *Transplantation Proceedings* 1989; 21: 3667-3669.
9. Starling RC, VanFossen DB, Hammer DF, Unverferth DV. Morbidity of endomyocardial biopsy in cardiomyopathy. *Am J Cardiol* 1991; 68: 133-136.
10. Waseem NH, Lane DP. Monoclonal antibody analysis of the proliferating cell nuclear antigen. *J Cell Science* 1990; 96: 121-29.

11. Dilley RJ, McGeachie JK, Prendergast FJ. A review of the proliferative behaviour, morphology and phenotypes of vascular smooth muscle. *Atherosclerosis* 1987; 63: 99-107.
12. Ip JH, Fuster V, Badimon L, Badimon J, Taubman MB, Chesebro JH. Syndromes of accelerated atherosclerosis: role of vascular injury and smooth muscle cell proliferation. *J Am Coll Cardiol* 1990; 15: 1667-87.
13. Katsuda S, Coltrera MD, Ross R, Gown AM. Human atherosclerosis IV. immunocytochemical analysis of cell activation and proliferation in lesions of young adults. *Am J Pathol* 1993; 142: 1787-93.
14. O'Brien ER, Alpers CE, Stewart DK, et al. Proliferation in primary and restenotic coronary atherectomy tissue. *Circ Res* 1993; 73: 223-31.
15. Schwartz SM, Campbell GR, Campbell JH. Replication of smooth muscle cells in vascular disease. *Circ Res* 1986; 58: 427-44.
16. Thyberg J, Hedin U, Sjölund M, Palmberg L, Bottger BA. Regulation of differentiated properties and proliferation of arterial smooth muscle cells. *Arteriosclerosis* 1990; 10: 966-990.
17. Björkerud S. Effects of transforming growth factor- β 1 on human arterial smooth muscle cells in vitro. *Arteriosclerosis and Thrombosis* 1991; 11: 892-902.
18. Desmoulière A, Geinoz A, Gabbiani F, Gabbiani G. Transforming growth factor- β 1 induces α -smooth muscle actin expression in granulation tissue myofibroblasts and in quiescent and growing cultured fibroblasts. *J Cell Biol* 1993; 122: 103-111.
19. Lee SH, Yan H, Reeser JC, Dillman JM, Strauch AR. Proteoglycan biosynthesis is required in BC3H1 myogenic cells for modulation of vascular smooth muscle α -actin gene expression in response to microenvironmental signals. *J Cell Physiol* 1995; 164: 1-15.
20. Eich DM, Nestler JE, Johnson DE, et al. Inhibition of accelerated coronary atherosclerosis with dehydroepiandrosterone in the heterotopic rabbit model of cardiac transplantation. *Circ* 1993; 87: 261-269.
21. Glagov S. Intimal hyperplasia, vascular modeling, and the restenosis problem. *Circ* 1994; 89: 1888-91.

Group	n	% Stenosis			Ratio of Intimal Area/ Tunica Media Area			Ratio of Intimal Area/ Vessel Area		
		Mean	Std. Dev	ANOVA (F/P Value)	Mean	Std. Dev.	ANOVA (F/P Value)	Mean	Std. Dev.	ANOVA (F/P Value)
Early	82	68.72	17.08	.585 / .6254	.52	.42	.688 / .5604	.28	.21	1.100 / .3509
Middle	42	66.67	16.54		.53	.42		.29	.20	
Late	40	71.38	16.46		.55	.37		.31	.19	
NonTx	11	66.28	23.87		.70	.31		.39	.11	

Note. In each analysis there was no significant difference in mean values between the 4 groups.
NonTx = Normal control hearts from nontransplant patients.

Table 3: Mean percent stenosis and area ratios compared between the three time groups of coronary arterioles and non-transplanted control arterioles using analysis of variance.

Groups	n	Vessel Area (μm^2)		Fragmentation Rank		% of Vessel Wall Occupied by Actin		Antibody Signal Intensity	
		Mean	Std. Dev.	Mean	Std. Dev.	Mean	Std. Dev.	Mean	Std. Dev.
Early	41	1813.39	2533.47	1.73	0.93	45.93 _a	9.71	183.06 _a	36.67
Middle	31	1259.93	659.44	1.32	0.83	49.00 _a	11.99	184.54 _a	36.69
Late	29	1344.02	749.25	1.43	0.85	59.68 _b	13.99	211.27 _b	23.39
ANOVA (F / p Values)		1.118	/ .3312	2.121	/.1254	12.149	/ <.0001*	7.048	/.0014*

Note. Means with different subscripts differ significantly at *p < .05 by ANOVA.

Table 4: Immunocytochemical analyses of arterioles labeled specifically for vascular smooth muscle α -actin.

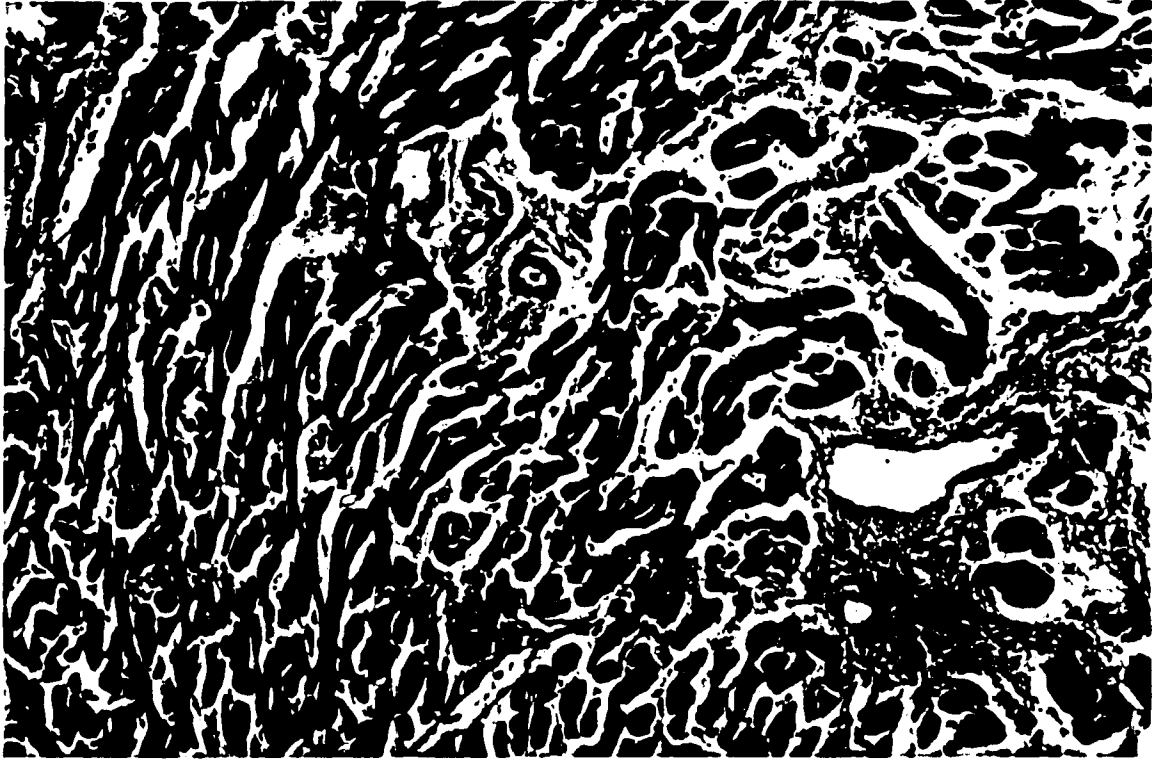


Figure 6: Tissue section from an endomyocardial biopsy specimen from a human transplanted heart. An arrow indicates a measurable arteriole that is 50 μ m in diameter. (Masson's Trichrome, x80.)

Figure 7: (A) represents a PCNA positive control of human tonsil. Arrows indicate positively stained lymphocytes. (B) represents a negative control of human tonsil substituting goat serum for the primary antibody. (AEC chromagen, Hematoxylin, x100.)

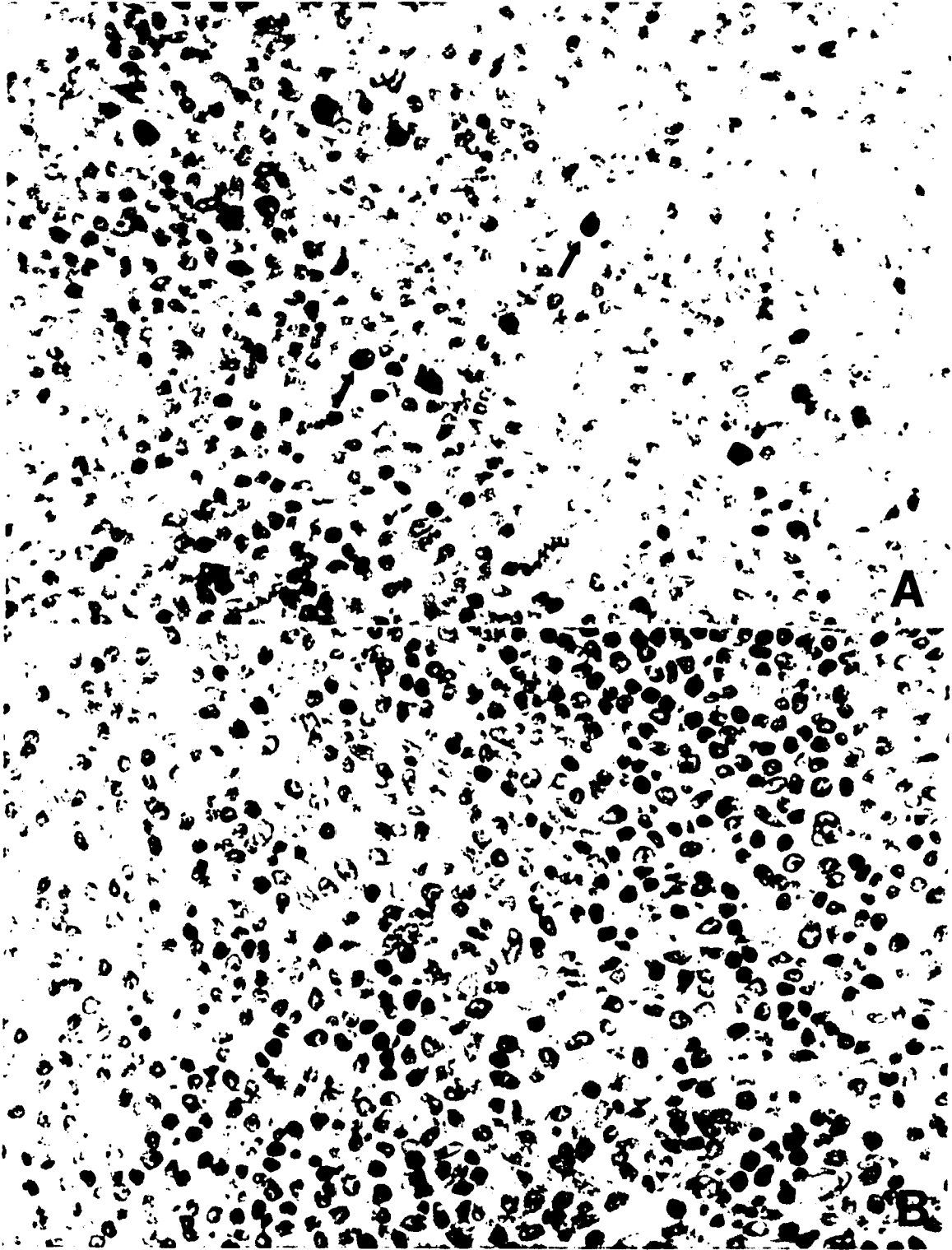


Figure 7A and B

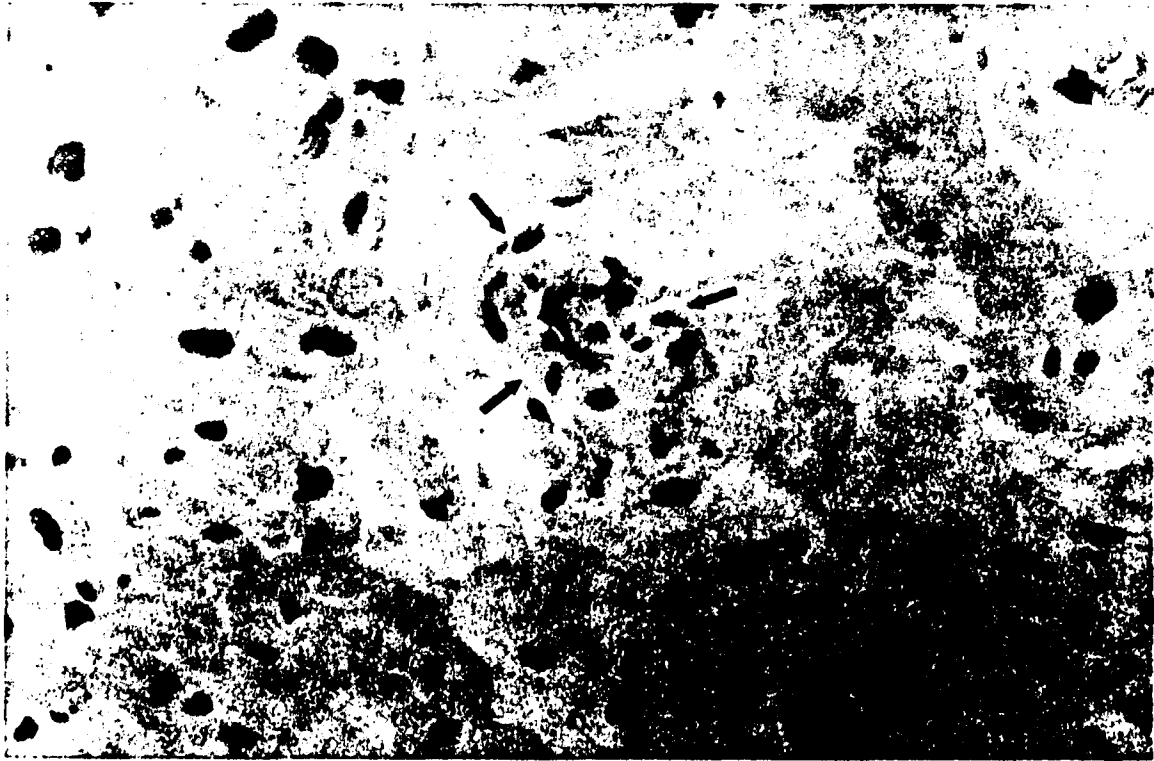


Figure 8: This figure represents an intramyocardial arteriole (circumscribed by arrows) after reaction with a PCNA-specific antibody. The lack of antibody staining is reflective of all arterioles studied within each time interval. (AEC chromagen, Hematoxylin, x100.)

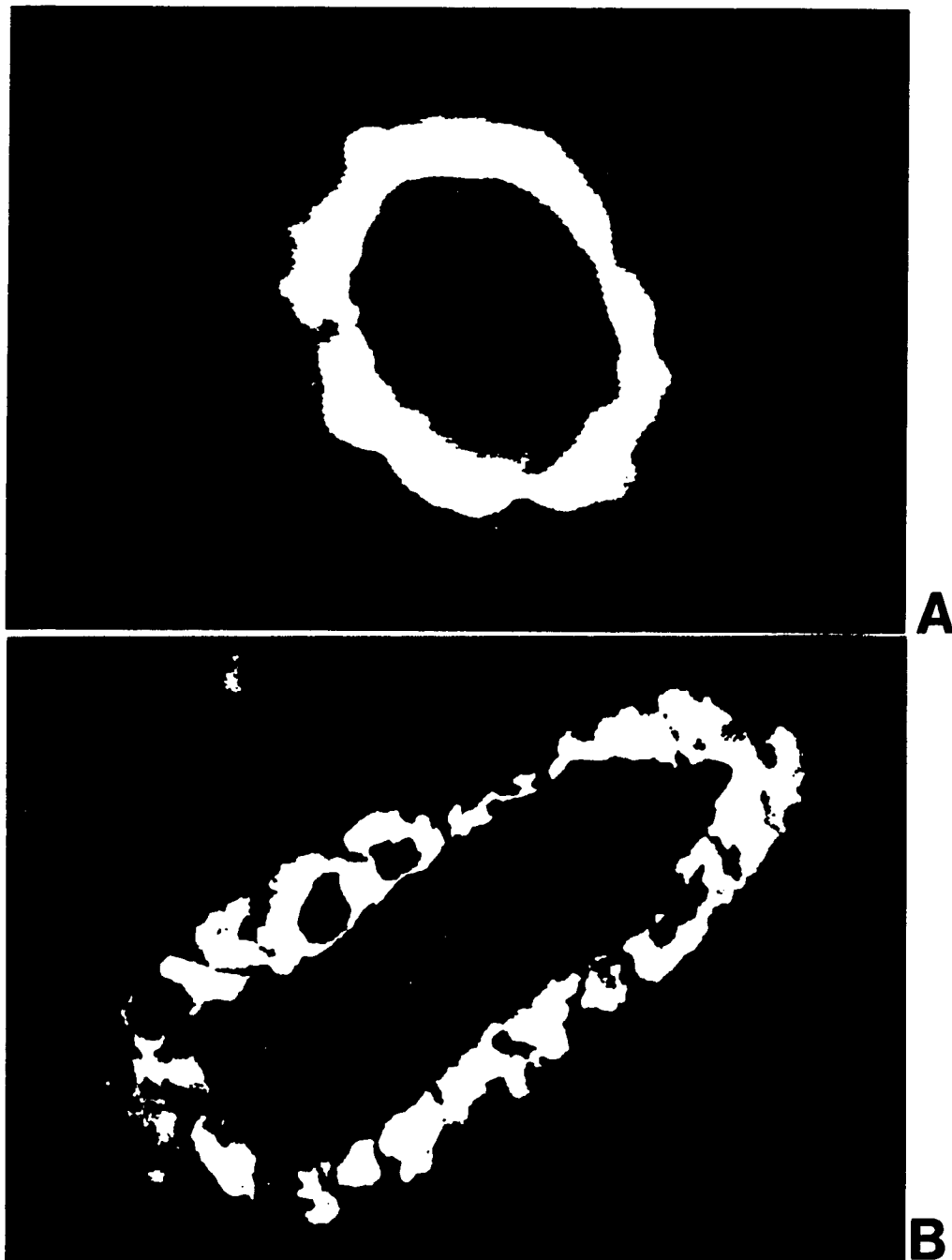


Figure 9: Immunocytochemically labeled arterioles from different human transplanted heart biopsies. Vessels are fluorescently labeled with a monoclonal antibody specific for vascular smooth muscle α -actin. Note the varying degree of signal fragmentation. Vessel A has a rank of 0 and Vessel B has a lower rank of 3.

CHAPTER 4

MOUSE HEART ALLOGRAFT MODEL

Introduction

Cardiac allograft vasculopathy (CAV) has been studied for many years in several small and large animal experimental models. In fact, CAV was noted in transplanted dog hearts well before it was appreciated as a major limitation to long term survival of human transplanted hearts [1]. From the basic science standpoint, animal studies of CAV provide many advantages. Hearts can be harvested at any time after transplant and the entire vascular system studied. *In vivo* studies of human allografts are limited to specific regions of the heart that are analyzed through less than optimal methods as discussed in the previous chapter. In addition, experimental therapies can be used in animal allograft models to determine effects on CAV.

Another advantage to using animal models is that inbred strains can be used to isolate the immunologic compatibility factors needed to produce CAV. Major histocompatibility complex (MHC) Class I and Class II antigens as well as non-MHC antigens are the factors most generally compared between strains. Heart transplants have

been performed in rabbits which produced coronary intimal thickening between weakly RLA-mismatched rabbits [2]. Transplants in rat strains that differ in MHC Class I antigens also produced vascular lesions [3-5]. Mouse allografts are a superior model compared to rats and rabbits for studies of CAV because the genetic background and immunocompatibility of various mouse strains are better defined [6]. Studies by Russell et al. [7] have shown that vascular lesions can be produced when the donor murine heart differs from the recipient with respect to MHC antigens (Class I and Class II) and non-MHC antigens. They found that lesions developed progressively over time and with more severity when there was a MHC Class I difference between strains. The Russell group found that immunosuppressant therapy of anti-CD4 and anti-CD8 monoclonal antibodies helped the grafts to survive longer so as to see these advanced lesions [7]. Ardehali et al. [8] used the same strain combination which differed in MHC Class I antigens, but without using immunosuppression, and also observed the development of vascular lesions. Both groups of investigators characterized the lesions as being fibrocellular, concentric lesions of varying severity. A subjective grading system was used to indicate the amount of luminal occlusion and mononuclear infiltration. However, anatomical differences throughout the heart in terms of the frequency and/or severity of vascular lesions were not investigated. Moreover, the anatomy of the mouse coronary system was not discussed nor were individual coronary vessels followed along their length to assess possible regional variation in the development of CAV. In short, while previous studies using the mouse allograft model have shown the strain

combinations required to produce CAV lesions, they have not clearly documented the severity of such lesions, the cellular components, and the overall susceptibility of heart allografts to CAV. In addition, the anatomical basis of murine CAV and its temporal development have not been explored in any detail.

The greater the immunogenic incompatibility between mouse strains, the more rapid the onset of disease as well as severity. For this reason we found it advantageous to use a mouse transplant model which would give optimal lesions within a convenient time frame. In the mouse allograft model utilized in this study, the histocompatibility of the donor and recipient strains differed markedly from one another in both MHC Class I and II antigens requiring immunosuppression therapy be provided for survival greater than one week post transplant. An experimental immunosuppressant therapy, gallium nitrate (GN), was used to keep the allografts viable for a period of time sufficient to allow the development and analysis of CAV. Originally, GN was used in cancer research to prevent hypercalcaemia in malignant tumors [10]. At present, GN is considered a new immunosuppressant therapy shown to be useful in heart transplantation [11]. The immunosuppressive activity of GN was shown by Whitacre et al. in an autoimmune encephalomyelitis-rat model [12]. Matkovic et al. discovered that GN interfered with the macrophage and T cell functions involved with arthritis development in rats [13]. Further studies were performed by Huang et al. to determine the effects of GN on T cell activation [14]. GN was found to inhibit T cell proliferation when stimulated by allogeneic endothelial cells or allogeneic monocytes. GN also blocked the induction of

MHC Class II expression on gonadal vein endothelial cells by activated T cells. Orosz et al. compared GN with anti-CD4 monoclonal antibodies in prevention of mouse cardiac allograft rejection [11]. It was found that GN, like anti-CD4, promoted long-term graft survival >60 days and that the treated grafts expressed vascular lesions.

Following our study of CAV in humans using endomyocardial biopsies, we reasoned that a murine allograft model would help to overcome limitations and extend our findings in the human transplant patient as discussed in Chapter 3. There were two major limitations with the human biopsy study that the mouse model can address. First there was the possibility of artifactual arteriolar thickening produced by vessel collapse in the non-perfused biopsy specimen. Perfusion of the mouse hearts prior to histological analysis should show the possible effect of vessel collapse on quantitative measurements of percent stenosis. The second limitation seen in the human study was related to regional location of the tissue being sampled. The endomyocardial biopsies were always taken from the same general area of the interventricular septal region of the heart. This limited view of the heart cannot tell us the effects of CAV throughout the allograft epicardium. However, analyzing the entire mouse heart allograft can address whether CAV occurs globally or regionally. Based on the immunologic injury occurring in our mismatched mouse allografts, we hypothesized that a uniform and global disease would occur throughout these hearts. The following objectives were addressed to demonstrate the feasibility of the mouse allograft model for studies of CAV.

1. Determine whether perfusion of the mouse coronary vasculature was necessary for accurate measurement of intimal thickening.
2. Determine which coronary arteries consistently presented lesions within the mouse allograft.
3. Observe the lesions prospectively over time following transplantation to determine if they progressively enlarge to occlude the lumen.
4. Observe possible evidence for smooth muscle cell phenotypic modulation and proliferation within lesioned vessels and its effect on the surrounding myocardium.

We initially hypothesized that CAV lesions within the mouse coronary arteries would be similar to humans and therefore would present themselves as uniform intimal thickenings throughout the entire length of the vessel, which would of course occlude the distal, smaller caliber vessels first. In humans, a variability existed regarding which coronary arteries were affected, but we expected that arteries in mouse allografts should be similarly affected between individual mice of the same inbred strain. Thus, we hypothesized that mice from the same strain would exhibit the same lesions within the same coronary arteries. As will be described in this chapter, our experimental results differed considerably from this hypothesis.

Methods

Mouse Strains used for the Transplant Procedures

Five to six-week old, 20g, female DBA/2 (H-2^d) and C57BL/6 (H-2^b) mice were used in the study and were obtained from Harlan Sprague Dawley (Indianapolis, IN). The mice were housed at the Ohio State University vivarium in accordance with NIH guidelines for care and use of laboratory animals.

Surgical Procedures

DBA/2 mouse hearts were heterotopically transplanted into the abdomens of C57BL/6 recipient mice using an adapted version of the method described by Correy et al. [9]. The following is a brief description of the technique. The thoracic cavity of the donor was opened and 1.5 ml of heparin was injected into the inferior vena cava of the heart to arrest it. Both the inferior and superior vena cavae were ligated and the aorta and pulmonary artery were transected. The pulmonary veins were ligated en bloc. The harvested donor heart was then placed in cold Ringer's lactate solution while the recipient was prepared by exposing and clamping the abdominal aorta and inferior vena cava. Within the abdominal cavity of the recipient mouse, the infrarenal abdominal aorta and vena cava were incised and end-to-side anastomoses were performed with the donor

aorta and pulmonary artery respectively. Blood flow was re-established and contraction resumed in the grafted heart. The total ischemic time required to anastomose the vessels was 20-25 minutes and the heart was covered in gauze soaked with cold Ringer's solution while sutures were placed. Oxygenated blood entered the graft aorta as back flow to reach the coronary arteries and supply the myocardium. Following the surgical procedure, the allograft was palpated through the abdomen once a week and given a subjective grade corresponding to the strength of cardiac impulse. All surgeries were performed by Elaine Wakely, M.S. in collaboration with Charles G. Orosz, Ph.D., Professor of Surgery, Division of Transplantation at the Ohio State University.

Immunosuppression

Recipient mice were treated with gallium nitrate (GN) which was manufactured by Ben Venue Laboratories, Inc. (Bedford, Ohio) and provided to us by the National Cancer Institute. Recipients were treated the day prior to transplantation with 88 μ l of undiluted GN subcutaneously injected into the nape of the neck. Osmotic gallium pumps were implanted immediately following the transplant that released 0.5 μ l of GN per hour. After 14 days the pump was replaced and finally removed after an additional 28 days after which time the recipient did not receive any additional therapy.

Histological Procedures

Mouse heart allografts were harvested from the abdomen of recipient mice at specified time points following transplantation, fixed in formalin for 4-6 hours, and dehydrated and stored in 70% ethanol until processed for sectioning. The time-dependent study of cardiac allograft vasculopathy within the mouse model entailed harvesting allografts at different times after transplant. Three hearts were explanted at 30, 60, and 90 day post-transplant intervals giving a total of 9 allografts analyzed. A control group was analyzed as well and compared with the allografts. The control group consisted of two non-transplanted hearts which were obtained from the DBA/2 donor strain.

In some experiments, the mouse hearts were perfused prior to harvest. The perfusion technique involved inserting a 20 gauge needle into the abdominal aorta just below the grafted organ. The perfusate consisted of a warmed gelatin and saline mixture (49% gelatin). An aliquot of KCl and heparin (0.5cc) was injected into the aorta to arrest the beating hearts just prior to a 1.5cc injection of perfusate. Perfusion was assessed to be complete upon noting blanching of the liver. Perfused hearts were harvested and processed as described above.

The fixed heart tissue was processed and embedded in paraffin with the apex of the heart positioned at the bottom of the embedding well. Sections (4 μ m thick) were removed sequentially at intervals of 150 μ m from the apex toward the aorta of the heart.

Slides containing two to three sections each were collected from 14-21 intervals per heart and used for histological evaluation. The tissue sections were stained with Weigart's elastin stain. Additional unstained tissue sections, corresponding to the same anatomical regions as the elastin-stained slides, were processed for immunohistochemical staining.

Morphometric Analysis of Allografts

The histologically stained vessels were digitized and morphometrically measured using the methods discussed in detail in Chapters 2 and 3. Vessels selected for the analysis were $\geq 85\mu\text{m}$ in diameter. The vessel diameter was an average taken from 2 measures on both a vertical and horizontal plane spanning the distance between the outer wall edges of the vessels. The percent stenosis (%ST) was calculated for cross-sectioned vessels that were not obliquely cut or at a point of branching. A baseline %ST for vessels with no intimal thickening was observed to be $\sim 10\%$. This value was dependent on the thickness of the IEL which was affected in part by the angle of vessel transection. A mean %ST value and histogram for each allograft was derived from the total number of vessels analyzed and compared with other allografts and controls. Vessels smaller than $85\mu\text{m}$ in diameter were not analyzed due to the larger baseline %ST values inherent to their size. Also, there were fewer small vessels that were perfectly cut and therefore only a small population of small vessels could be analyzed per heart.

In addition to the morphometric analysis of the intimal thickening within each vessel, a regional analysis of the mouse heart tissue sections was performed to assess the anatomical prevalence of lesions. Figure 10 shows a representative cross-section of the mouse heart allograft. Based on observations of vessel prevalence, each cross-section was divided into three regions: a left/anterior region, an interventricular septal (IVS) region that included vessels with the IVS separating left and right ventricular chambers, and a right/posterior region. These anatomical regions are illustrated in Figure 10. Each coronary vessel ($>85\ \mu\text{m}$ in diameter) was associated with one of the three regions.

In addition to noting the location of each vessel, a numerical rank was assigned to each vessel based on the extent of intimal thickening. A rank of 0 was considered non-lesioned and corresponded to a baseline %ST value of $\leq 10\%$. A rank of 1 was considered a mild lesion and corresponded to $10\% < \%ST \leq 30\%$, a rank of 2 was considered a moderate lesion and corresponded to $30\% < \%ST \leq 60\%$, and a rank of 3 was considered a severe lesion and corresponded to a $\%ST > 60\%$. An example of each type of lesion rank is shown in Figures 11 and 12.

Comparison of Perfused and Non-Perfused Vessels

Ten vessels without lesions were chosen at random from four perfused hearts and compared with another ten vessels from non-perfused hearts. Circularity was determined by the imaging software for each vessel lumen using the circularity index. The circularity index is derived by taking the perimeter length squared and dividing it by the

area. The circular index for a perfect circle is 4π (12.57). The circularity index was compared between the 20 perfused and non-perfused coronary arteries. In addition, percent stenosis was compared between the vessels.

Immunohistochemistry Procedure Using PCNA Antibody

The mouse monoclonal antibody PC10 (DAKO, Carpentry, CA), a horseradish peroxidase (HRP)-labeled antibody specific for the proliferating cell nuclear antigen (PCNA), was incubated with tissue sections from the nine mouse allografts. AEC chromogen (Sigma, St. Louis, MO) was used as the substrate and produced a reddish brown color from the enzymatic reactions in the case of positive antibody binding. Also, a hematoxylin counter stain was applied to the specimens which stained the nuclei blue. In parallel with the sectioned endomyocardial biopsy specimens, paraffin-embedded sections of human tonsil (DAKO, Carpentry, CA) were immunohistochemically stained with the PCNA-specific antibody to provide a positive control. HRP-labeled goat serum (Sigma, St. Louis, MO) was substituted for the primary antibody to confirm the specificity of the PCNA antibody.

Immunohistochemistry Procedure Using Smooth Muscle α -actin Antibody

A monoclonal antibody specific for vascular smooth muscle α -actin (1A4, Sigma, St. Louis, MO) was incubated with the mouse graft sections at 1:400 dilution in PBS buffer containing 1% bovine serum albumin for 1 hour at room temperature. Following a thorough wash in PBS buffer, the slides were processed using a rapid HRP-staining kit (Sigma, St. Louis, MO). The biotinylated secondary polyclonal antibody (goat anti-mouse IgG) was used at a concentration of 1:50. The characteristic reddish-brown precipitate produced by the enzymatic reaction was obtained using AEC chromagen. Hematoxylin was used to counter stain the nuclei blue.

Results

Coronary Vessel Perfusion

A comparison was made between perfused and non-perfused hearts using both normal and grafted mouse hearts. The vessel architecture was not changed by the perfusion technique as shown in Table 5. The circular morphology of cross-sectioned vessels was not compromised when the hearts were not perfused and the %ST was

unchanged. Visual assessment of the small vessels <85 μ m in diameter showed the vessels to be collapsed and less rounded than the large vessels, regardless of whether perfusion was performed or not.

	n	Circularity Index		Percent Stenosis (%)	
		Mean	Std. Dev.	Mean	Std. Dev.
Perfused Vessels	10	18.38	2.13	11.94	1.89
Non-Perfused Vessels	10	16.78	1.22	10.46	1.71
ANOVA (F / P)		4.245 / 0.054		3.376 / 0.083	

Table 5: Comparison of circularity and percent stenosis between perfused and non-perfused coronary arteries using ANOVA.

Morphometric Analysis

Grafts analyzed using morphometric methods were explanted 30, 60, and 90 days after transplant. A comparison of the %ST values from the three grafts harvested at each time point was performed as shown in Table 6, where n is the number of vessels analyzed. The two normal DBA/2 hearts that made up the control group were also compared with each other. Table 6 shows that the %ST values of the vessels within the 30 day group were not significantly different when compared using analysis of variance (ANOVA). Both the 60 and 90 day groups had significantly different mean %ST values within their own group. The control hearts were not significantly different.

Groups	n	Mean %ST	Standard Dev.	ANOVA	
				F	P
30 day Graft-1 Vessels	55	14.39	9.02	0.30	0.74
30 day Graft-2 Vessels	34	14.52	12.35		
30 day Graft-3 Vessels	47	13.17	6.16		
60 day Graft-1 Vessels	27	46.21	35.58	8.51	<0.001*
60 day Graft-2 Vessels	42	26.57	18.89		
60 day Graft-3 Vessels	33	20.63	20.48		
90 day Graft-1 Vessels	30	34.53	25.16	9.68	<0.001*
90 day Graft-2 Vessels	44	22.97	15.50		
90 day Graft-3 Vessels	35	15.33	10.99		
Control-1 Vessels	31	11.81	4.30	0.09	0.77
Control-2 Vessels	27	12.15	3.31		
Total 30 day Graft Vessels	136	14.00	9.12	21.60	<0.001*
Total 60 day Graft Vessels	102	29.84	26.60		
Total 90 day Graft Vessels	109	23.70	18.95		

*p < .05 denotes statistical significance.

Table 6: ANOVA comparing mean percent stenosis (%ST) of coronary arteries within time study groups and normal controls.

Table 6 also provides descriptive statistics for the 30, 60, and 90 day groups when the %ST of their vessels are averaged together. Using ANOVA to compare the three groups shows them to be significantly different. Table 7 shows this difference in more detail through post-ANOVA tests that compare each of the three time-study groups and the normal control hearts. Both the 60 and 90 day grafts demonstrated significantly greater %ST values than the 30 day grafts and control hearts.

Pairs of Groups Compared	ANOVA	
	F	P
30 day Grafts, 60 day Grafts	41.75	<0.001*
30 day Grafts, 90 day Grafts	27.63	<0.001*
60 day Grafts, 90 day Grafts	3.77	0.05
30 day Grafts, Controls	2.62	0.11
60 day Grafts, Controls	25.73	<0.001*
90 day Grafts, Controls	21.54	<0.001*

Note. *p < .05 denotes statistical significance.

Table 7: ANOVA comparing the mean percent stenosis of vessels within graft time-study groups and controls.

Regional Analysis

Each series of allograft sections from the 3 time-study groups was analyzed for regional differences in lesion severity. The most severe lesion present within each region was noted according to the section location along an axial plane extending between the aorta and apex of the heart. The x-axes of the graphs in Figures 13-15 represent the axial plane of the heart from aorta to apex along which sections were analyzed for lesion severity. The distance between these section planes was ~150µm. The grafts varied in size resulting in more sections being analyzed in some hearts relative to the others. Therefore, a comparison only can be made between lesions in each graft with regard to their relative distance from the apex or aorta of the heart. Figure 13A-C shows the distribution of lesions observed within various regions of 30 day allografts. None of the three 30 day allografts had lesions more severe than rank 2 (moderate lesion). The IVS

appears to be more susceptible to CAV than the LT/ANT and RT/POST regions at 30 days. In general, the lesions occurred more distal than proximal. Figure 14A-C shows the lesion severity observed in anatomical regions of 60 day allografts. All three of the grafts at 60 days show the maximum lesion severity of rank 3. With the exception of graft 3, the LT/ANT region has lesions occurring focally at different locations throughout the length of the vessels. The IVS shows predominately distal lesions. The RT/POST region has lesions occurring mostly within in the middle of the heart. Figure 15A-C shows lesion severity observed within regions of 90 day allografts. There are lesions within all three grafts at 90 days that show maximum severity of rank 3. The LT/ANT region has lesions of varying severity throughout the length of the vessels, with the exception of Graft 3. The IVS at 90 days has more distal lesions. The RT/POST region has lesion diversity throughout the length of the vessels. Graft 3 of the 90 day group does not appear to be very affected by CAV.

PCNA Analysis

Sections obtained from all 3 groups of grafts were immunohistochemically labeled for proliferating cell nuclear antigen (PCNA). Generally, all of the vessels examined from the 30, 60, and 90 day grafts were negative for PCNA as shown in Figures 16 and 17. Figure 16 illustrates a representative vessels from a normal donor heart and a 30 day graft treated with the PCNA-specific antibody. Figure 17 shows

representative vessels from 60 and 90 day allografts treated with the PCNA-specific antibody. There was positive staining of one SMC within a coronary artery from a 30 day allograft. Figure 18 shows a single, positively stained SMC from the 30 day graft along with another positively stained cell situated in the myocardium. A few unknown interstitial cells dispersed throughout the myocardium stained positive for the PCNA antibody in all three 30 day grafts and in one 60 day graft as illustrated in Figure 19. The remaining 60 day and 90 day grafts did not show the PCNA marker. The results imply that PCNA-positive interstitial cells are more likely to be detected within the first 30 days after transplant compared to later time points.

Smooth Muscle α -Actin Analysis

The vascular-specific isoform of actin (VSM α -actin) is a widely accepted marker for smooth muscle cells exhibiting the contractile phenotype. Positive labeling for VSM α -actin is demonstrated in Figure 20 which shows coronary arteries from a normal control heart. In the graft hearts, however, the α -actin signal varies in intensity between vessels and is dependent on lesion severity. The 30 day grafts showed a wide range of labeling variance. Many non-lesioned coronary arteries in 30 day allografts were stained positive with the 1A4 antibody throughout the media as shown in Figure 21. This positive staining was specific based on the lack of reaction product seen in sections from a 30 day graft that were processed by substituting normal goat serum for the primary

antibody. Figure 21 shows the negative control which illustrates the lack of staining in a rather normal coronary artery and minimal background staining in the myocardium.

Lesioned vessels within the 30 day grafts typically showed two types of antibody staining as demonstrated in Figure 22. One type consisted of positive reactivity in both the media and the intima along with a partial decrease in the intensity of the medial signal. The other type showed only positive staining of the medial cells and not the intimal cells. Again, the media in these lesioned vessels exhibited a decreased signal intensity compared to non-lesioned vessels.

Both the 60 and 90 day grafts contained lesioned arteries with positively stained medial and intimal lesions or just intimas alone as shown in Figure 23. However, in some lesions involving large amounts of infiltrate, the vessels did not express any α -actin marker in either compartment as shown in Figure 24. Interestingly, cardiomyocytes from late stage grafts appear to accumulate the fetal VSM α -actin isoform. As shown in Figure 25, the periodic pattern of staining suggested that the VSM α -actin was being incorporated into sarcomeric structures during chronic rejection.

Discussion

Both the quantitative and regional analyses for the mouse allografts showed that advanced coronary artery lesions do not occur in 30 day allografts. None of the 30 day allografts examined contained lesions that could be categorized as severe. The 60 and 90

day grafts had advanced lesions that were not significantly different in appearance from each other. This observation implies that a 60 day time period following transplantation is sufficient for advanced lesion development in the mouse allograft model. There was much heterogeneity in the %ST values of vessels in each allograft. The morphometric features of lesions present within each heart would vary as vessels coursed distally away from the aorta. Interestingly, there appeared to be an anatomical component with regard to lesion development in cardiac allografts. Early lesions in the 30 day grafts were localized in the IVS. Perhaps IVS vessels are more prone to develop CAV lesions. However, no correlation was seen between regions within the 60 and 90 day groups. Lesions would develop in discontinuous fashion both proximally and distally within the late-stage grafts. This data conflicts with current beliefs that CAV is a widespread lesion throughout the entire length of the vessel. The mouse allograft model has concentric lesions occurring at different points along the length of the vessel. The differences between the lesion type proposed to be exhibited by CAV and the focal lesion type we observed are illustrated in Figure 4.17. In the mouse model, regions occupied by lesions are separated by seemingly less affected or normal arterial segments.

As in our human study we tried to monitor SMC proliferation in the mouse grafts by using a PCNA monoclonal antibody probe. Again, we did not find strong evidence for SMC proliferation. Perhaps we missed the mitotic event which may occur just prior to 30 days post transplantation. Future studies will obviously focus on days 1 through 45 after transplant to better delineate the temporal features of CAV.

Prior to this study we hypothesized that CAV exhibited within a single inbred strain of mouse should follow the same general pattern of vascular lesion distribution and severity between individual recipients. The histological evaluation of grafts in our study revealed this not to be the case. However, it would stand to reason that the diverse development of vascular lesions may be related to unique combinations of regulatory molecules, e.g. growth factors, cytokines, transcription factors, that may be unequally distributed in the allografts. We found that the marker, smooth muscle α -actin, varied amongst the many vessels within the allografts. The actin marker was present in both the intima and media of developing lesions but seemingly disappears in advanced lesions containing abundant cellular infiltrate. Surprisingly, the allograft myocardium also exhibited localized expression VSM α -actin. This α -actin isoform is a fetal variant which can be expressed by cardiomyocytes under conditions of stress or injury [15,16]. This stress could be from immune injury via infiltrating lymphoid cells or perhaps ischemic injury brought on by occluded coronary vessels. Future studies may show that activators and repressors of the α -actin gene could be used to distinguish between the various early stages of lesion development.

Regardless of the mechanisms involved, the mouse model clearly demonstrates that regional differences are associated with the histopathologic features of CAV. In contrast, our study of human biopsies focused on only a small localized region of the IVS. The large and small coronary branches within other regions of those transplanted human hearts could contain CAV lesions but clearly were not available for experimental

study. Moreover, if allografts placed in an inbred mouse line vary significantly with regard lesion development, then it is quite likely that individual human allografts will also demonstrate a significantly high variance of lesion development. Future studies with the mouse model will focus on characterizing the various cellular and molecular mechanisms involved in the etiology of CAV and perhaps explain its heterogeneous nature.

List of References

1. Kosek JC, Hurley EJ, and Lower RR. Histopathology of orthotopic canine cardiac homografts. *Lab Invest* 1968;19: 97-112.
2. Alonso DR, Stark PK, and Minnick CR. Studies on the pathogenesis of atherosclerosis induced in rabbit cardiac allografts by the synergy of graft rejection and hypercholesterolemia. *Am J Pathol* 1977; 87: 415-35.
3. Lurie KG, Billingham ME, Jamieson SW, et al. Pathogenesis and prevention of graft arteriosclerosis in an experimental heart transplant mode. *Transplantation* 1981; 31: 41-47.
4. Adams DH, Russell ME, Hancock WW, et al. Chronic rejection in experimental cardiac transplantation: studies in the Lewis - F344 model. *Immunological Reviews* 1993; 134: 5-19.
5. Ewel CH and Foegh ML. Chronic graft rejection: accelerated transplant arteriosclerosis. *Immunological Reviews* 1993; 134: 20-32.
6. Fundamental Immunology. Paul WE. Raven Press, NY, NY. 1984.
7. Russell PS, Chase CM, Winn HJ, and Colvin RB. Coronary atherosclerosis in transplanted mouse hearts. *Am J Pathol* 1994; 144: 260-274.
8. Ardehali A, Billingsly A, Laks H, et al. Experimental cardiac allograft vasculopathy in mice. *J Heart Lung Transplant* 1990; 12: 730-5.
9. Corry R, Winn H, Russell P. Primary vascularized allografts of hearts in mice. *Transplantation* 1973; 16: 343-50.
10. Warrell RP, Israel R, Frisone M, et al. Gallium nitrate for acute treatment of cancer related hypercalcaemia. *Ann Intern Med* 1988; 108: 669-74.
11. Orosz CG, Wakely E, Bergese S, et al. Prevention of murine cardiac allograft rejection with gallium nitrate: comparison with anti-CD4 mAb. In Press.

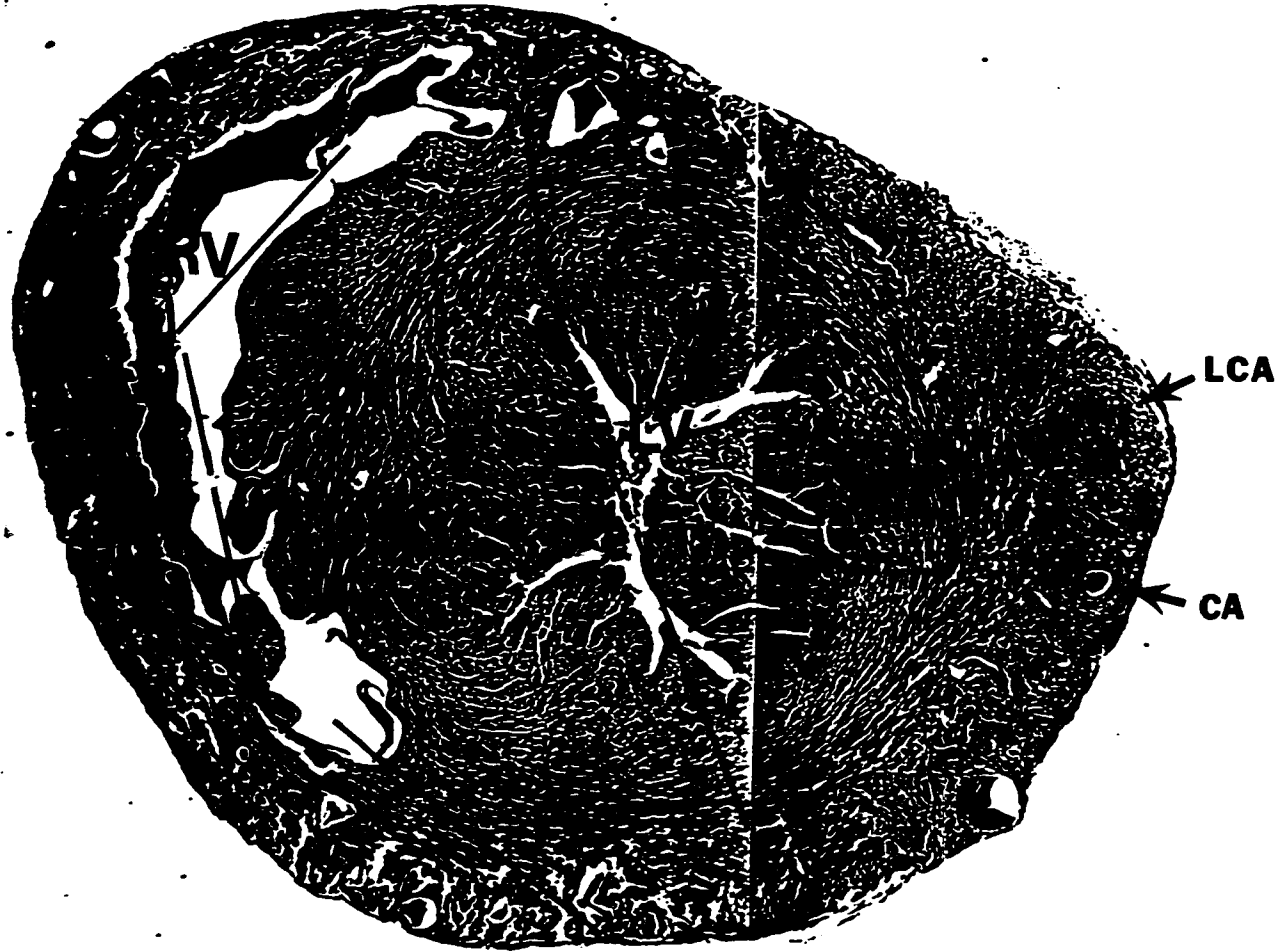
12. Whitacre C, Apseloff G, Cox K, et al. Suppression of experimental autoimmune encephalomyelitis by gallium nitrate. *J of Neuroimmunology* 1992; 39: 175-182.
13. Matkovic V, Balboa A, Clinchat D, et al. Gallium prevents adjuvant arthritis in rats and interfere with macrophage/T cell function in the immune response *Curr Ther Res* 1991; 50 (2): 255-267.
14. Huang EH, Gabler DM, Krecic ME, et al. Differential effects of gallium nitrate on T lymphocyte and endothelial cell activation. *Transplantation* 1994; 58:1216-1222.
15. Black FM, Packer SE, Parker TG, et al. The vascular smooth muscle α -actin gene is reactivated during cardiac hypertrophy provoked by load. *J Clin Invest* 1991; 88: 1581-1588.
16. Parker TG, Packer SE, and Schneider MD. Peptide growth factors can provoke fetal contractile protein gene expression in rat cardiac myocytes. *J Clin Invest* 1990; 85: 507-514.

Figure 10: Histological cross-section of a mouse heart allograft. The tissue section is representative of the lower half of the heart, closer to the apex. The left ventricle (LV) and right ventricle (RV) are labeled. An epicardial coronary artery (CA) is indicated by an arrow. An example of a lesioned coronary artery (LCA) is also labeled. Lines divide the section into anatomical regions that include the Left/Anterior (L/A), the interventricular septal (IVS), and the Right/Posterior (R/P) regions. (Weigart's Elastin, x80.)

101

RIGHT

ANTERIOR



LCA

CA

LEFT

POSTERIOR

Figure 10



Figure 11: Vessel (A) has no vascular lesion and yielded a value for percent stenosis of 9.4 (rank 0 lesion). Vessel (B) has a mild vascular lesion with a percent stenosis equal to 24.9 (rank 1 lesion). (Weigart's Elastin, x640.)

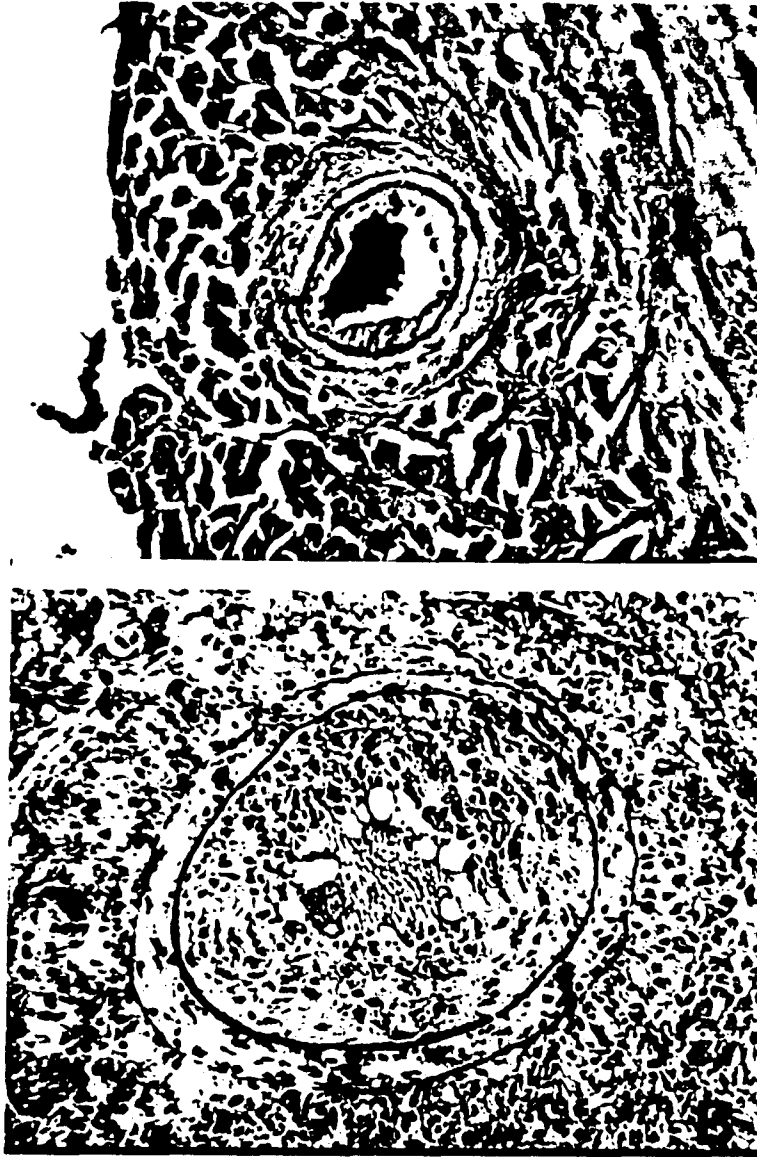


Figure 12: Vessel (A) has a moderate lesion with a percent stenosis value of 47.4 (rank 2 lesion). Vessel (B) has a severe vascular lesion with a percent stenosis equal to 80.9 (rank 3 lesion). (Weigart's Elastin, x640.)

Figure 13A-C: The most severe lesions within each anatomical region of the three 30 day allografts is shown in this graph. The x-axis represents the histological section being analyzed between the heart apex and aorta. (A) illustrates the lesions observed in the left/anterior region of the heart. (B) illustrates the lesions located within the interventricular septum (IVS). (C) illustrates the lesions found within the right/posterior region of the heart.

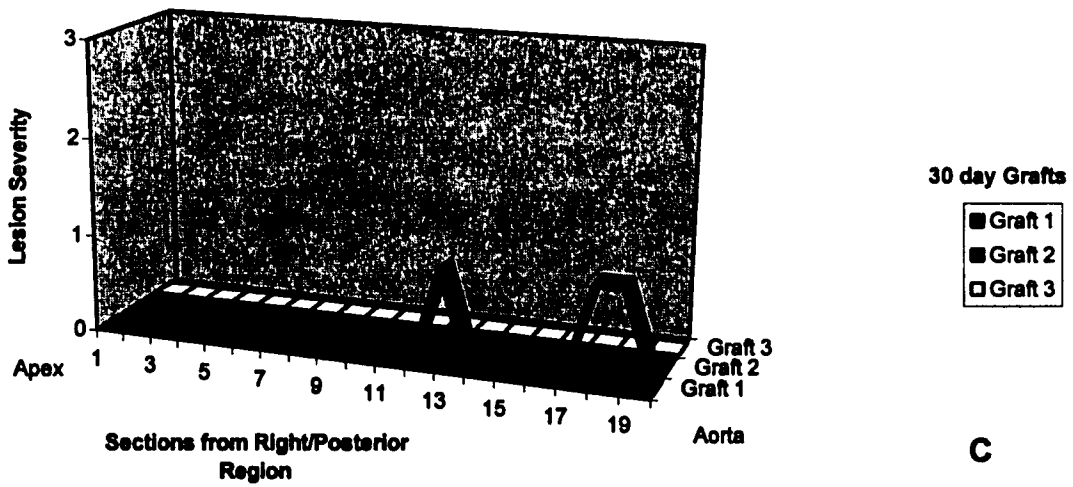
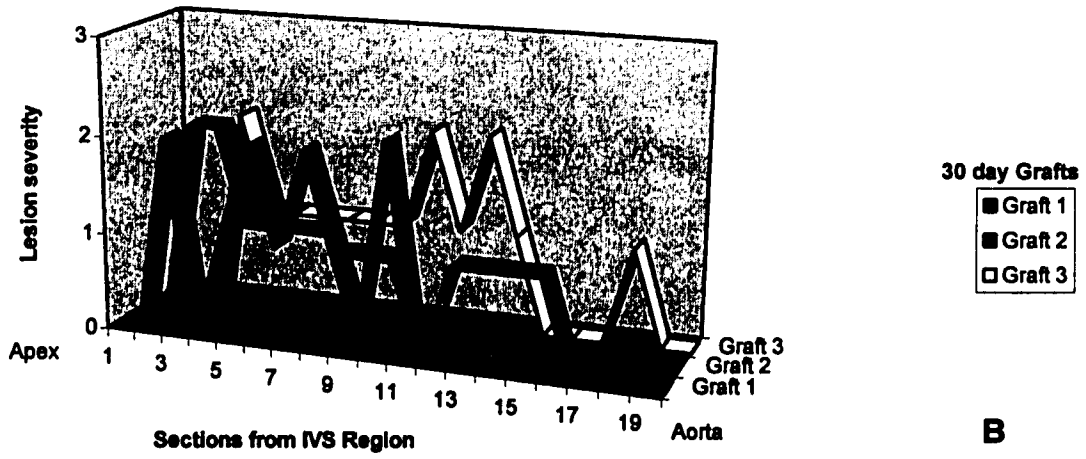
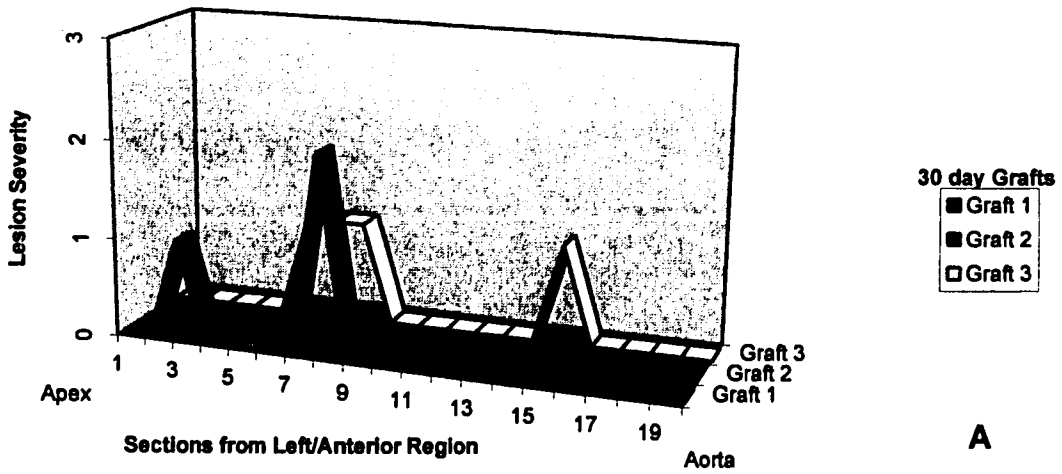


Figure 13A-C

Figure 14A-C: The most severe lesions within each anatomical region of the three 60 day allografts is shown in this graph. The x-axis represents the histological section being analyzed between the heart apex and aorta. (A) illustrates the lesions observed in the left/anterior region of the heart. (B) illustrates the lesions located within the interventricular septum (IVS). (C) illustrates the lesions found within the right/posterior region of the heart.

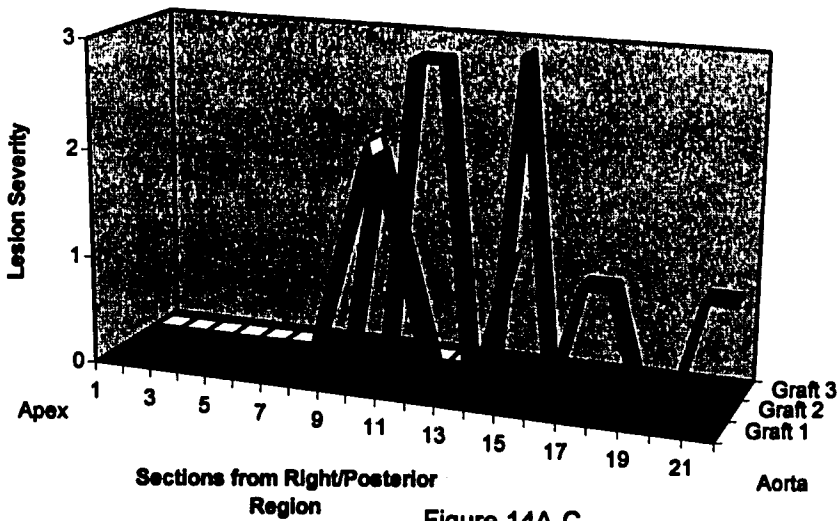
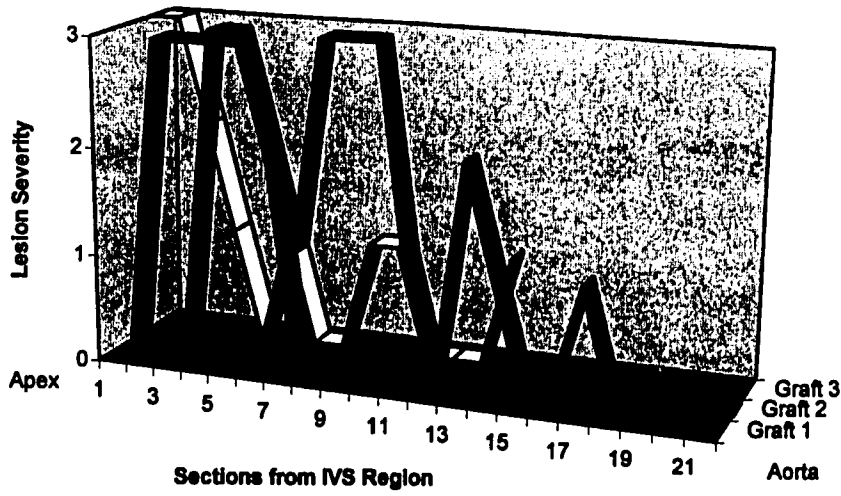
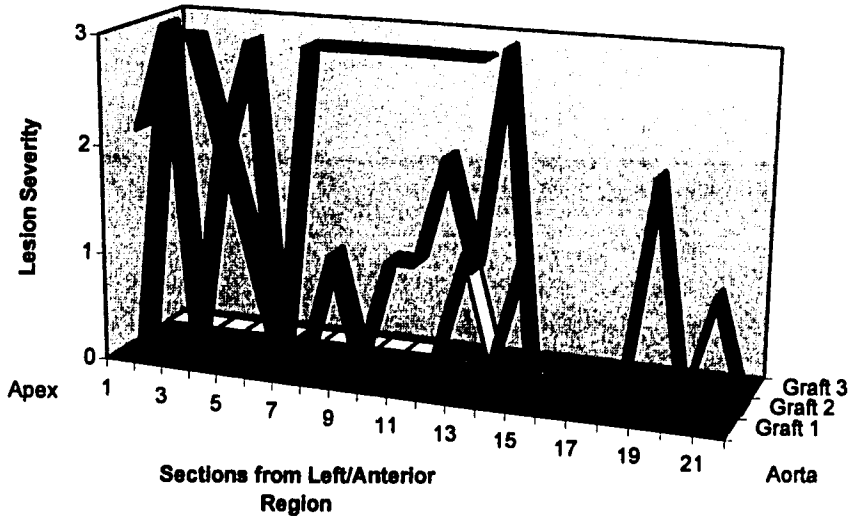


Figure 14A-C
107

Figure 15A-C: The most severe lesions within each anatomical region of the three 90 day allografts is shown in this graph. The x-axis represents the histological section being analyzed between the heart apex and aorta. (A) illustrates the lesions observed in the left/anterior region of the heart. (B) illustrates the lesions located within the interventricular septum (IVS). (C) illustrates the lesions found within the right/posterior region of the heart.

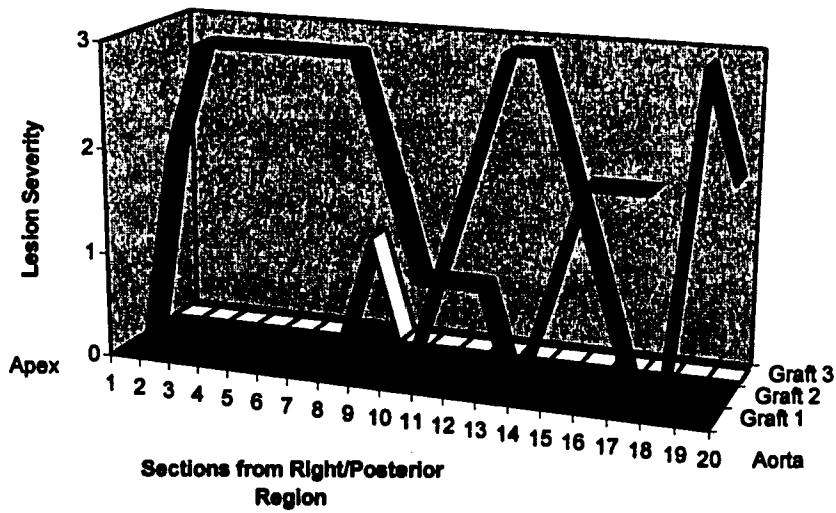
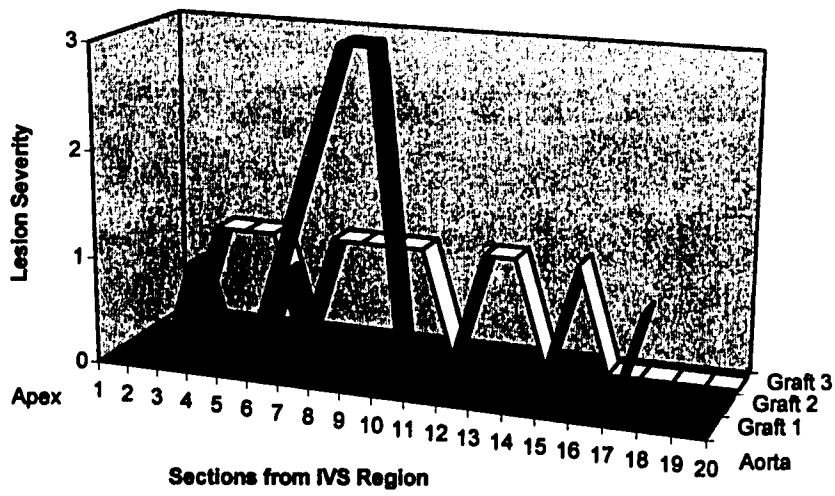
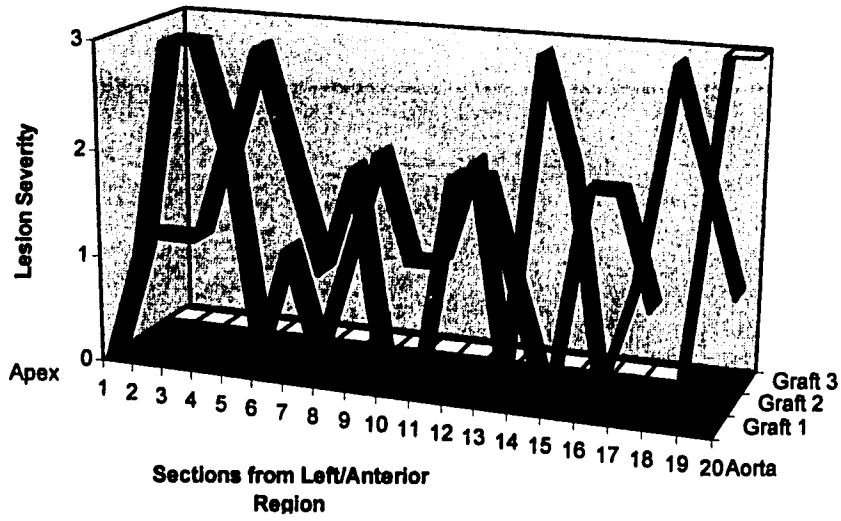


Figure 15A-C
109

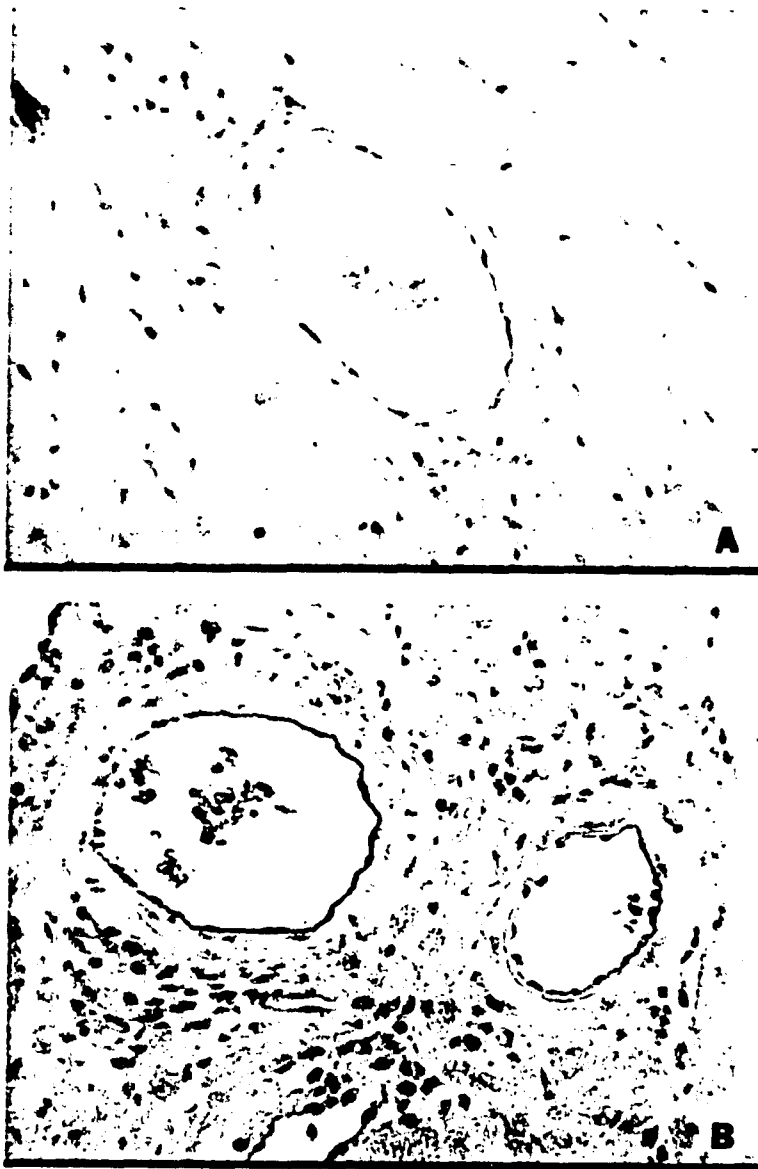


Figure 16A and B: (A) illustrates a vessel from a normal (control) heart that is negative for PCNA. Vessels in (B) are from a 30 day graft and also lack the PCNA antigen. (AEC Chromagen, Hematoxylin, x640.)

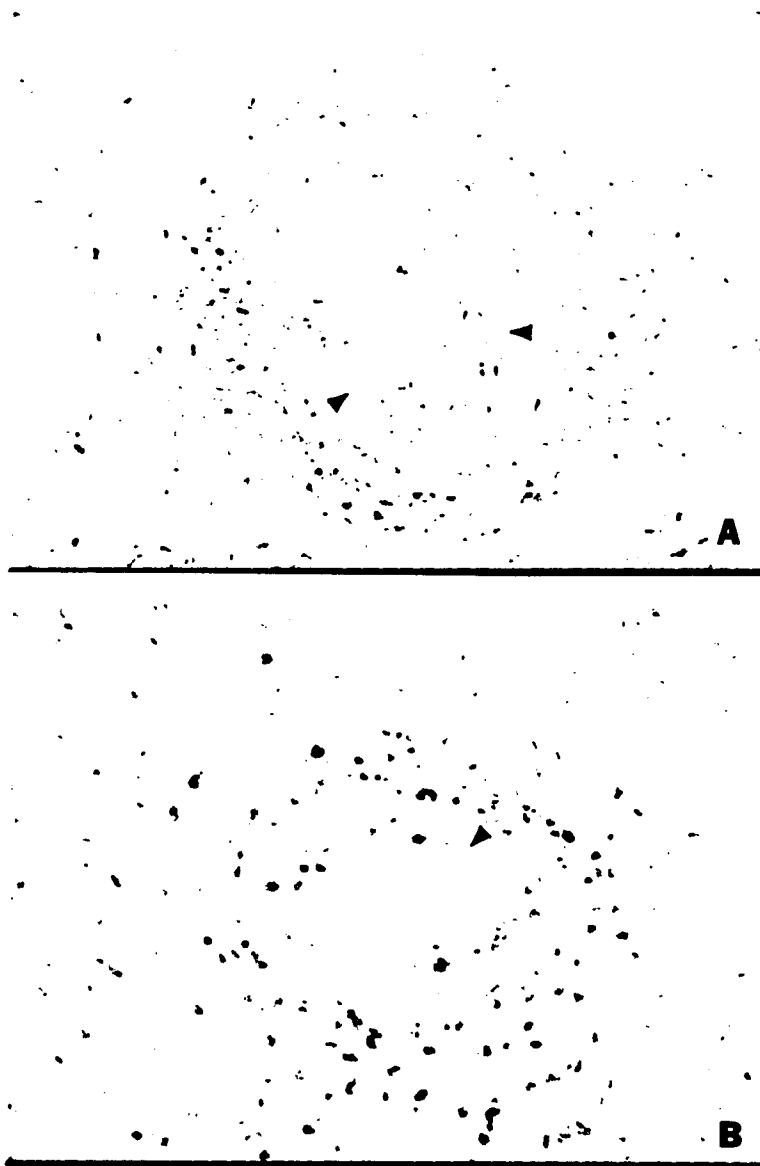


Figure 17A and B: (A) depicts a vessel from a 60 day graft (B) shows a vessel from a 90 day graft. Neither vessel stained positive for PCNA. The IEL is indicated by arrowheads. (AEC Chromagen, Hematoxylin, x640.)

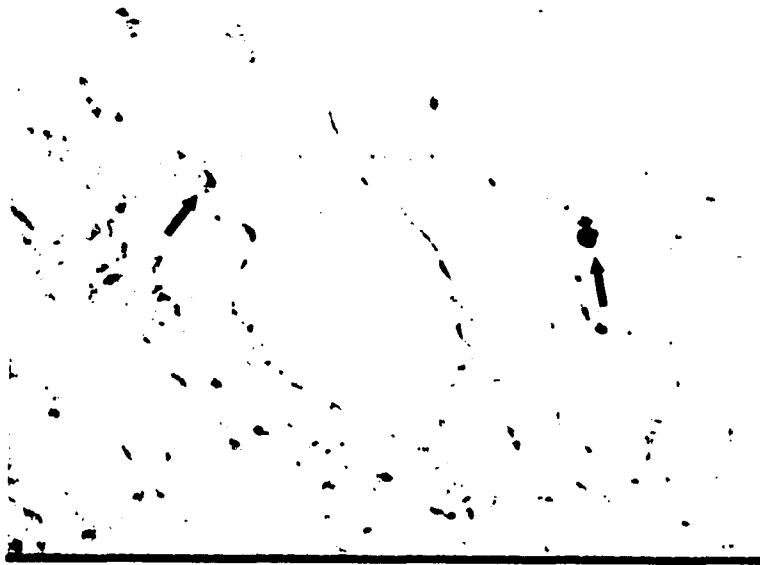


Figure 18: A vessel from a 30 day graft contains a darkly-stained nucleus (arrow) within the vessel wall. This was the only PCNA positive entity observed in the coronary vasculature. Another positive cell nucleus also was seen within the myocardium (arrow). (AEC Chromagen, Hematoxylin, x640.)

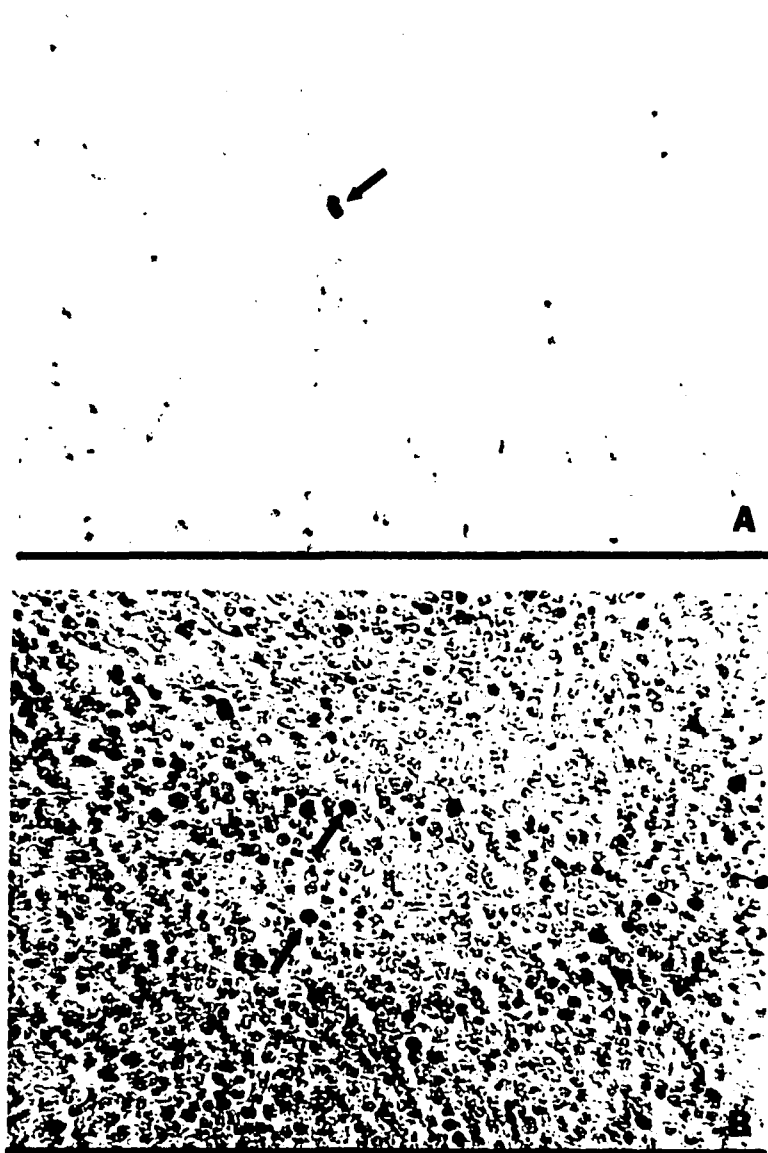


Figure 19A and B: (A) depicts a section from a 60 day mouse graft containing PCNA positive nuclei within the myocardium (arrow). (B) is a section through human tonsil tissue that was used as a control to show positive PCNA staining. Arrows denote some of the many PCNA positive nuclei in tonsil tissue. (AEC Chromagen, Hematoxylin, x640.)



Figure 20A and B: (A) and (B) show positive staining for smooth muscle α -actin in the tunica media of coronary arteries from a normal donor mouse heart. (AEC Chromagen, Hematoxylin, x1520 and x640.)

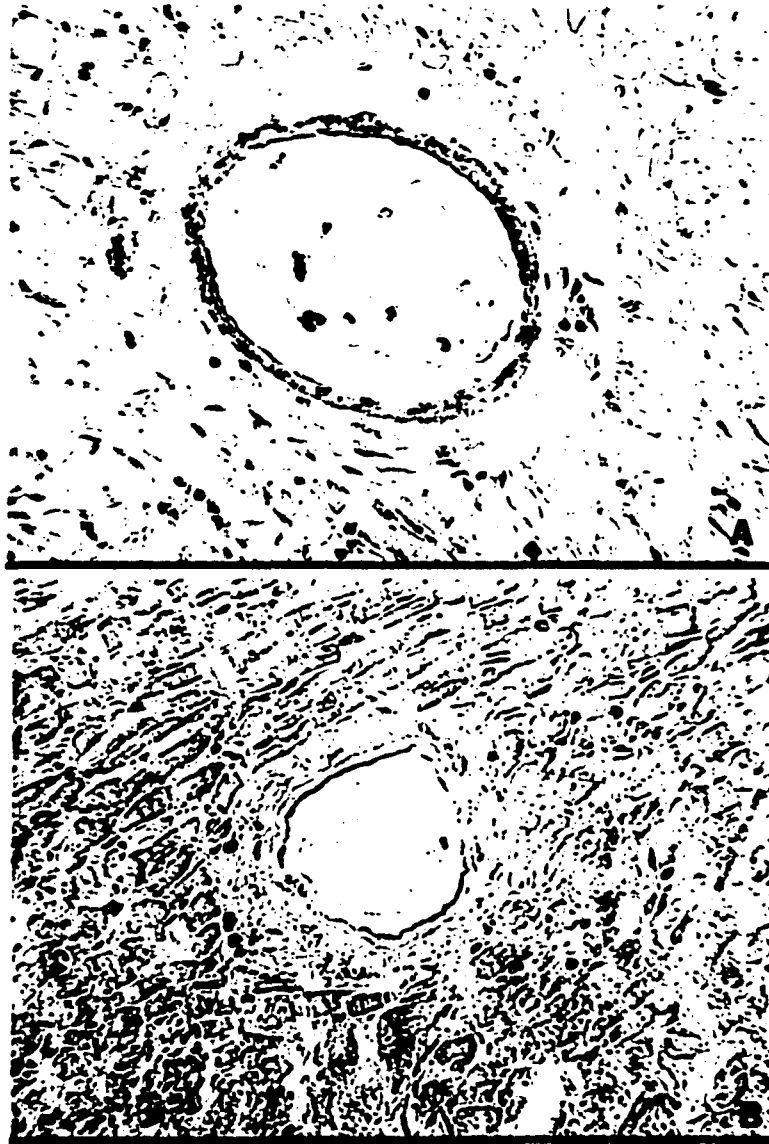


Figure 21A and B: The vessel in panel (A) represents a non-lesioned vessel within a 30 day graft. Note the α -actin signal is relatively strong in the tunica media. (B) is from the same graft but the α -actin antibody was left out to serve as a negative control. Note the media lacks the antibody signal and there is only minimal background signal. (AEC Chromagen, hematoxylin, x640.)

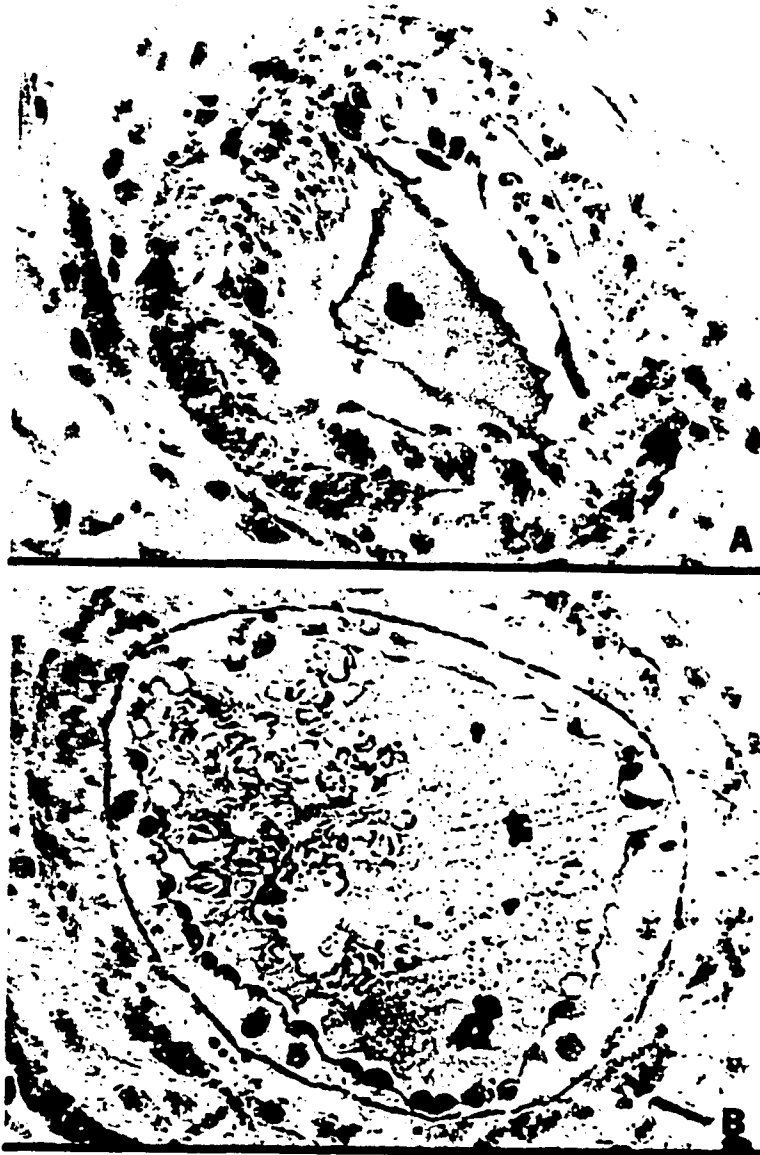


Figure 22A and B: Both images (A and B) were from 30 day grafts. The vessel in (A) shows α -actin within both the media and intima. The vessel in (B) shows α -actin within the media but not the intima. (AEC Chromagen, Hematoxylin, x1520.)

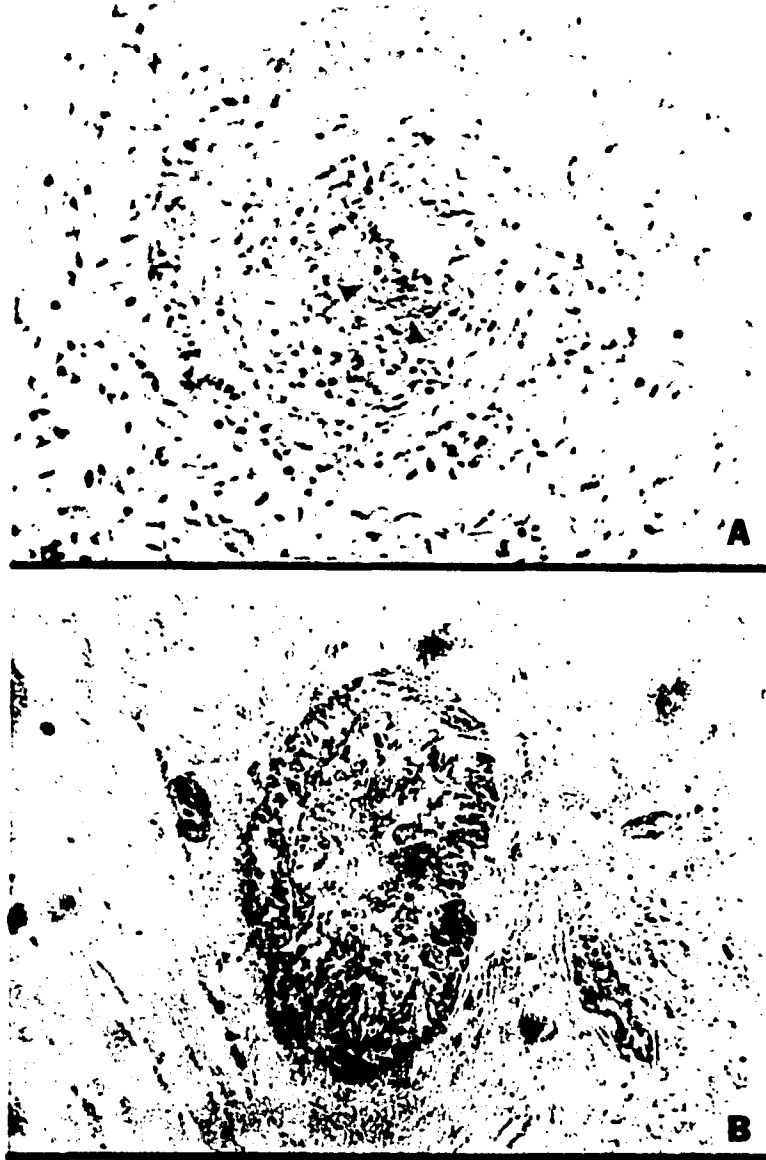


Figure 23A and B: The vessel in panel (A) shows a coronary vessel from a 60 day graft. Note that a small amount of α -actin is seen only in the intima (proximal to the lumen, arrowheads) and not in the media. The vessel in panel (B) is from a 90 day graft and shows seemingly fragmented deposits of α -actin within both the media and the intima. (AEC Chromagen, Hematoxylin, x640.)

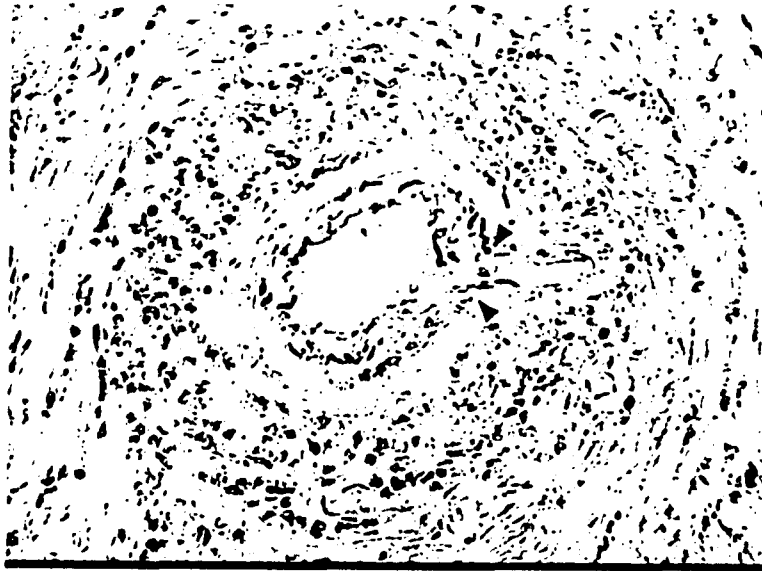


Figure 24: This vessel was from a 60 day graft. The α -actin signal is absent from both the media and intima, perhaps due to the large accumulation of cellular infiltrate. Note that the IEL in this advanced lesion appears disrupted (arrowheads). (AEC Chromagen, Hematoxylin, x640.)

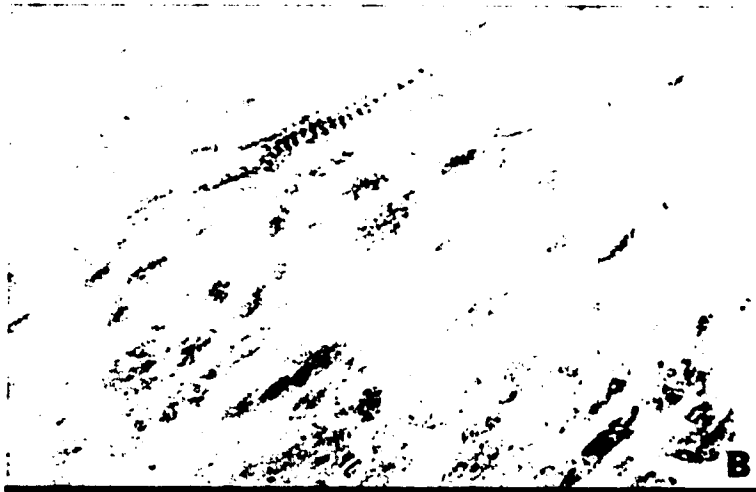


Figure 25A and B: Cardiomyocytes from 60 day allografts can be seen in these images (A and B) that express the smooth muscle α -actin isoform. (AEC Chromagen, Hematoxylin, x1520.)

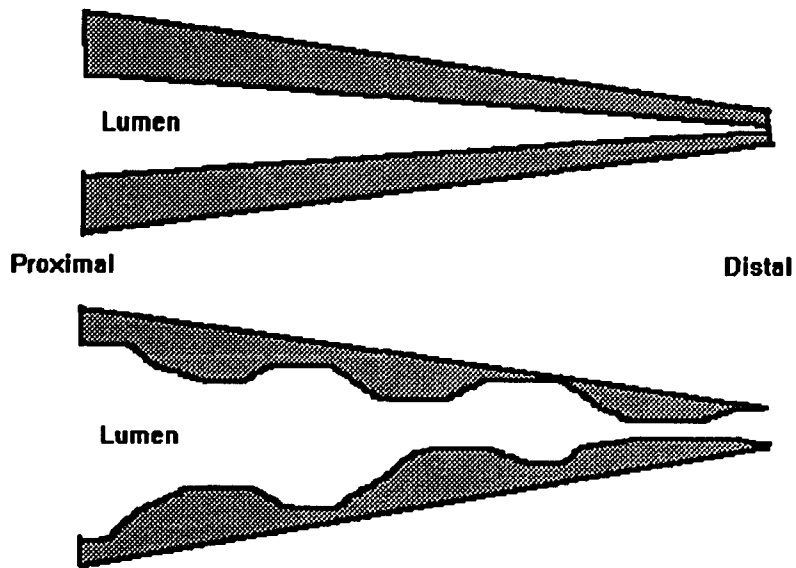


Figure 26: Models of CAV. These are mid-sagittal sections of coronary arteries. Intimal growth is shaded in grey representing CAV. The upper vessel shows the type of lesion suggested by many to be occurring in CAV. The lesion is concentric and diffuse throughout the length of the artery. The lower vessel represents what we have generally found in the mouse allograft model. The lesion is concentric but only occurs at certain points along its length.

BIBLIOGRAPY

- Adams DH, Russell ME, Hancock WW, et al. Chronic rejection in experimental cardiac transplantation: studies in the Lewis - F344 model. *Immunological Reviews* 1993; 134: 5-19.
- Allen MD, McDonald T, Carlos T, et al. Endothelial adhesion molecules in heart transplantation. *J Heart Lung Transplant* 1992; 11: s8-s13.
- Alonso DR, Stark PK, and Minnick CR. Studies on the pathogenesis of atherosclerosis induced in rabbit cardiac allografts by the synergy of graft rejection and hypercholesterolemia. *Am J Pathol* 1977; 87: 415-35.
- Ardehali A, Billingsly A, Laks H, et al. Experimental cardiac allograft vasculopathy in mice. *J Heart Lung Transplant* 1990; 12: 730-5.
- Barnard CN. The operation: a human cardiac TX: an interim report of a successful operation performed at Groote Schuss Hospital, Cape Town. *South African Med Journal* 1967; 41: 1271-1274.
- Bieber CP, Stinson EB, Shumway NE, et al. Cardiac transplantation in man:VII:cardiac allograft pathology. *Circ* 1970; 41; 753-762.
- Billingham ME. Diagnosis of cardiac rejection by endomyocardial biopsy. *Heart Transplant* 1:25-30; 1981.
- Billingham ME. Cardiac transplant atherosclerosis. *Transplantation Proc* 1987; 19(4): 19-25.
- Billingham ME. Histopathology of graft coronary disease. *J Heart Lung Transplant* 1992; 11: 538-44.
- Björkuud S. Effects of TGF- β on human arterial smooth muscle cells in vitro. *Arteriosclerosis and Thrombosis* 1991; 11: 892-902.

- Black FM, Packer SE, Parker TG, et al. The vascular smooth muscle α -actin gene is reactivated during cardiac hypertrophy provoked by load. *J Clin Invest* 1991; 88: 1581-1588
- Bland JM, Altman DG. Statistical methods for assessing agreement between two methods of clinical measurement. *The Lancet* Feb 8:307-310; 1986.
- Cao W, Mohacsi P, Shorthouse R, et al. Effects of rapamycin on growth factor-stimulated vascular smooth muscle cell DNA synthesis. *Transplantation* 1995; 59: 390-5.
- Clowes AW, Clowes MM, Kocher O, et al. Arterial smooth muscle cells in vivo: relationship between actin isoform expression and mitogenesis and their modulation by heparin. *J Cell Biol* 1988; 107: 1939-45.
- Clowes AW, Clowes MM, Fingerle J, et al. Kinetics of cellular proliferation after arterial injury versus role of acute distension in the induction of smooth muscle proliferation. *Laboratory Investigation* 1989; 60: 360-364.
- Clowes AW. Control of intimal hyperplasia by heparin. *J Heart Lung Transplant* 1992; 11: s21.
- Cogan J. Vascular alpha actin gene sequence and transcription factor binding site. Thesis. 1995.
- Corry R, Winn H, Russell P. Primary vascularized allografts of hearts in mice. *Transplantation* 1973; 16: 343-50.
- Costanzo-Nordin MR. Cardiac allograft vasculopathy: relationship with acute cellular rejection and histocompatibility. *J Heart Lung Transplant* 1992; 11: s90-s103.
- Demetis AJ, Zerbe T and Banner B. Morphology of solid organ allograft arteriopathy: identification of proliferating intimal cell population. *Transplantation Proceedings* 1989; 21: 3667-69.
- Dilley RJ, McGeachi JK, and Prendergast FJ, A review of the proliferative behavior, morphology and phenotypes of vascular smooth muscle. *Atherosclerosis* 1987; 63: 99-107.
- Eich DM, Nestler JE, Johnson DE, et al. Inhibition of accelerated coronary atherosclerosis with dehydroepiandrosterone of cardiac transplantation. *Circulation* 87:261-269; 1993.

- Ewel CH and Foegh ML. Chronic graft rejection: accelerated transplant arteriosclerosis. *Immunological Reviews* 1993; 134: 20-32.
- Fermin CD, Gerber MA and Torre-Bueno. Colour thresholding and objective quantification in bioimaging. *J of Microscopy* 1992;44:114-24.
- Gao SZ, Schroeder JS, Alderman EL, et al. Clinical and laboratory correlation of accelerated coronary artery disease in the cardiac transplant patient. *Circ* 1987; 76(Supp V): v56-v61.
- Gao SZ, Schroeder JS, Alderman EL, et al. Clinical and laboratory correlation of accelerated coronary artery disease in the cardiac transplant patient. *Circ* 1987; 76(Suppl. V): v56-v61.
- Gaudin PB, Rayburn BK, Hutchins GM. Peritransplant injury to the myocardium associated with the development of accelerated arteriosclerosis in heart transplant recipients. *Am J Surg Pathol* 1994; 18: 338-46.
- Glagov S. Intimal hyperplasia, vascular modeling and the restenosis problem. *Circ* 1994; 89: 2888-91.
- Geer JC, Bishop SP, and James TN. Pathology of small intramural coronary arteries. *Pathol. Ann.* 14:125-154; 1979.
- Grady KL, Costanzo-Nordin MR, Herold LS, et al. Obesity and hyperlipidemia after heart transplantation. *J Heart Lung Transplant* 1991; 10: 449-54.
- Gregory CR, Huang X, Pratt RE, et al. Treatment with rapamycin and mycophenolic acid reduces arterial intimal thickening produced by mechanical injury and allows endothelial replacement. *Transplantation* 1995; 59: 655-61.
- Halle III AA, DiSciascio G, Massin EK, et al. Coronary angioplasty, atherectomy and bypass surgery in cardiac transplant recipients. *J Am Coll Cardiol* 1995; 26(1): 120-8.
- Hammond EH, Yowell RL, Price GD, et al. Vascular rejection and its relationship to allograft coronary artery disease. *J Heart Lung Transplant* 1992; 11: 5111-9.
- Hosenpud JD, Shipley GD, and Wagner CR. Cardiac allograft vasculopathy: current concepts, recent developments, and future directions. *J Heart Lung Transplant* 1992;11: 9-23

- Huang EH, Gabler DM, Krecic ME, et al. Differential effects of gallium nitrate on T lymphocyte and endothelial cell activation. *Transplantation* 1994; 58:1216-1222.
- Ip JH, Fuster V, Badimon L, et al. Syndromes of accelerated atherosclerosis: role of vascular injury and smooth muscle cell proliferation. *J Am Coll Cardiol* 1990; 15: 1667-87.
- Izutani H, Shirakura R, Miyagawa S, et al. Essential immune attack in graft coronary arteriosclerosis induction detected by return transplantation technique in rat. *Transplant Proceed* 1995; 27: 579-81.
- James TN. Small arteries of the heart. *Circulation* 56:2-14; 1977.
- Jamieson SW. Investigation of heart transplantation coronary atherosclerosis. *Circ* 1992; 85(3): 1211-1213.
- Johnson DE, Alderman EL, Schroeder JS, et al. Transplant coronary artery disease: histopathologic correlations with angiographic morphology. *J Am Coll Cardiol* 1991; 17: 449-57.
- Johnson MR. Transplant coronary disease: Nonimmunologic risk factors. *J Heart Lung Transplant* 1992; 11: s124-s132.
- Kendall TJ, Wilson JE, Radio SJ, et al. Cytomegalovirus and other herpes viruses: do they have a role in the development of accelerated coronary arterial disease in human heart allografts. *J Heart Lung Transplant* 1992; 11: s14-s20.
- Kosek JC, Hurley EJ, and Lower RW. Histopathology of orthotopic canine cardiac homografts. *Lab Invest* 1968; 19: 97-103.
- Kosek JC, Bieber C, and Lower RR. Heart graft arteriosclerosis. *Transplantation Proc* 1971; 3(1): 512-514.
- Libby P. Immunopathology of coronary arteriosclerosis in transplanted hearts. *J Heart Lung Transplant* 1992; 11(3): s32-s37.
- Lin H, Wilson JE, Kendall TJ, et al. Comparable Proximal and distal severity of intimal thickening and size of epicardial coronary arteries in transplant arteriopathy of human cardiac allograft. *J Heart Lung Transplant* 1994; 13: 824-33.

- Lurie KG, Billingham ME, Jamieson SW, et al. Pathogenesis and prevention of graft arteriosclerosis in an experimental heart transplant model. *Transplantation* 1981; 31: 41-47.
- Marx SO, Jayaraman T, Go LO, et al. Rapamycin-FKBP inhibits cell cycle regulation of proliferation in vascular smooth muscle cells. *Circ Research* 1995; 76(3): 412-7.
- Matkovic V, Balboa A, Clinchat D, et al. Gallium prevents adjuvant arthritis in rats and interfere with macrophage/T cell function in the immune response *Curr Ther Res* 1991; 50 (2): 255-267.
- Miller LW. Allograft vascular disease: a disease not limited to hearts. *J Heart Lung Transplant* 1992; 11(3): s32-s37.
- Mosseri M, Schaper J, Yaron R, et al. Coronary capillaries in patients with congestive cardiomyopathy or angina pectoris with patent main coronary arteries. *Circulation* 84:203-210; 1991.
- Neish AS, Loh E, and Schoen FJ. Myocardial changes in cardiac transplant-associated coronary arteriosclerosis: Potential for timely diagnosis. *J Am Coll Cardiol* 1992; 19: 586-92.
- Orosz CG, Wakely E, Bergese S, et al. Prevention of murine cardiac allograft rejection with gallium nitrate: comparison with anti-CD4 mAb. *In Press*.
- Palmer DC, Tsai CC, Roodman ST, et al. Heart graft arteriosclerosis. *Transplantation* 1985; 39: 385-88.
- Parker TG, Packer SE, and Schneider MD. Peptide growth factors can provoke fetal contractile protein gene expression in rat cardiac myocytes. *J Clin Invest* 1990; 85: 507-514.
- Qu G. Modulation of vascular alpha actin. Thesis. 1995.
- Rickenbacher PR, Pinto FJ, Chenybrawn A, et al. Incidence and severity of transplant coronary artery disease early and up to 15 years after transplantation as detected by intravascular ultrasound. *J Am Coll Cardiol* 1995; 25: 171-7.
- Ross R. Atherosclerosis: a defense mechanism gone awry. *Am J Path* 1993; 143(4): 987-1002.

- Rowan RA and Billingham ME. Pathologic changes in the long-term transplant heart: a morphometric study of myocardial hypertrophy, vascularity, and fibrosis. *Human Pathol* 1990; 21: 767-772.
- Ross R. The pathogenesis of atherosclerosis. *New England J Med* 1986; 314(8): 488-497.
- Russel ME, Fujita M, Masek M, et al. Cardiac graft vascular disease. *Transplantation* 1993; 56: 1599-1601.
- Russell PS, Chase CM, Winn HJ, and Colvin RB. Coronary atherosclerosis in transplanted mouse hearts. *Am J Pathol* 1994; 144: 260-274.
- Segal SS, Kurjiaka DT and Caston A.L. Endurance training increases arterial wall thickness in rats. *J. Appl. Physiol.* 74(2):722-726; 1993.
- Schmid C, Heeman U, Azuma H, et al. Rapamycin inhibits transplant vasculopathy in long-surviving rat heart allografts. *Transplantation* 1995; 60: 729-33.
- Schwartz S, Campbell GR, and Campbell SH. Replication of smooth muscle cells in vascular disease. *Circ Res* 1986; 58: 427-444.
- Schwartz RS, Murphy JG, Edwards WD, et al. Restenosis after balloon angioplasty. *Circ* 1990; 82: 2190-2200.
- Schwartzkopff B, Motz W, Frenzel H, et al. Structural and functional alterations of the intramyocardial coronary arterioles in patients with arterial hypertension. *Circulation* 88:993-1003; 1993.
- Smith JA, Ribakove GH, Hunt SA, et al. Heart retransplantation: The 25 year experience at a single institution. *J Heart Lung Transplant* 1995; 26(1): 120-8.
- Starling RC, VanFossen DB, Hammer DF, et al. Morbidity of endomyocardial biopsy in cardiomyopathy. *Am. J. Cardio.* 68:133-136; 1991.
- Tanaka M, Fujiwara H, Onodera T, et al. Quantitative analysis of narrowing of intramyocardial small arteries in normal hearts, hypertensive hearts, and hearts with hypertrophic cardiomyopathy. *Circulation* 75(6):1130-1139; 1987.
- Thyberg J, Hedin U, Sjölund M, et al. Regulation of differentiated properties and proliferation of arterial smooth muscle cells. *Arteriosclerosis* 1990; 10: 966-990.

- Tuzcu E, Hobbs RE, Rincon G, et al. Occult and frequent transmission of atherosclerotic coronary disease with cardiac transplantation. *Circ* 1995; 91: 1706-1713.
- Uys CJ and Rose AC. Pathologic findings in long-term cardiac transplants. *Arch Pathol Lab Med* 1984; 108: 112-16.
- Valentine H, Pinto FJ, St.Goar FG, et al. Cytomegalovirus and other herpes viruses: do they have a role in the development of accelerated coronary arterial disease in human heart allografts. *J Heart Lung Transplant* 1992; 11: s14-s20.
- van Hoeven KH and Factor SM. Endomyocardial biopsy diagnosis of small vessel disease: a clinicopathologic study. *Int. J. Cardiol.* 26:103-110; 1990.
- Ventura HO, Mehra MR, Smart RW. Cardiac allograft vasculopathy: current concepts. *American Heart J* 1995; 129: 791-99.
- Warrell RP, Israel R, Frisone M, et al. Gallium nitrate for acute treatment of cancer related hypercalcaemia. *Ann Intern Med* 1988; 108: 669-74.
- Whitacre C, Apseloff G, Cox K, et al. Suppression of experimental autoimmune encephalomyelitis by gallium nitrate. *J of Neuroimmunology* 1992; 39: 175-182.
- Winters GL, Kendall TS, Radio SJ, et al. Post transplant obesity and hyperlipidemia: major predictors of severity of coronary arteriopathy in failed human heart allografts. *J Heart Lung Transplant* 1992; 11: s69-s72.
- Yeung AC, Anderson T, Meredith I, et al. Endothelial dysfunction in the development and detection of transplant coronary disease. *J Heart Lung Transplant* 1992; 11: s69-s72.
- Young JB. Cardiac allograft arteriopathy: an ischemic burden of a different sort. *Am J Cardiol* 1992; 70: 9F-13F.